Finite Element Analysis of the Seismic Behavior of Guyed Masts

by

Gregory Martin Hensley

Thesis submitted to the faculty of the
Virginia Polytechnic Institute and State University
in partial fulfillment of the requirements for the degree of

MASTER OF SCIENCE
IN
CIVIL ENGINEERING

APPROVED:

_____

Raymond H. Plaut, Chairman

_____ _____

Carin L. Roberts-Wollmann Elisa D. Sotelino

June 2005
Blacksburg, Virginia

Keywords: Synthetic Fiber Ropes, Finite Element, Mast, Guy Wires, Seismic Response

Finite Element Analysis of the Seismic Behavior of Guyed Masts

by

Gregory Martin Hensley

Raymond H. Plaut, Committee Chairman

Civil Engineering

(ABSTRACT)

Seismic design of guyed masts, commonly used in the broadcasting and telecommunications industries, has not been fully addressed in the United States. There is no specific design code, and only a limited amount of research has been reported on the subject. This research investigates the behavior of guyed masts incorporating synthetic ropes as guys, with a particular focus on the effect of snap loads on the mast behavior. This is the third phase of a multi-stage project aimed at analyzing the potential for Snapping-Cable Energy Dissipators (SCEDs) to minimize lateral response in structures.

A finite element model of a 120-m-tall guyed mast was developed with the commercial program ABAQUS. The three-dimensional behavior of the mast was observed when subjected to two ground motion records: Northridge and El Centro. Three orthogonal earthquake components were input, two horizontal and one vertical. A series of parametric studies was conducted to determine the sensitivity of the response to guy pretension, which is a measure of the potential slackness in the guys during response. Additionally, the studies examined the effects of guy stiffness, mast properties, and directionality of input motion.

Deflections, bending moments, guy tensions, and base shears were examined. The results were used to characterize the trends in the structural response of guyed masts. The level of slackness in the guys changed the behavior, and the lessons learned will be used to continue research on the application of SCEDs in structures.

Acknowledgements

I would first like to express my appreciation to the faculty members at Virginia Tech for the knowledge they have shared during my studies here. In particular, I would like to express my sincere thanks for the guidance provided by my advisor and committee chairman, Dr. Ray Plaut. I would also like to thank my committee members, Dr. Carin Roberts-Wollmann and Dr. Elisa Sotelino, for their support and assistance on this research project. Many thanks go to Gregor Wollmann for reviewing the text and sitting on the committee for the defense.

I would further like to thank all of the people who assisted me in this research, especially three of the graduate students involved in this project: John Ryan, Mike Motley, and Paul Taylor. Their help with learning the finite element program was greatly appreciated.

I want to thank all of my friends and family who have supported me along this journey. A special thank you goes to Paul and Lou for all the good times and late nights together, and to Elizabeth who has been beside me from start to finish. To my family, thank you for your endless love and support. Lastly, I want to thank my best friend, Rebekah.

This research was generously supported by the National Science Foundation under Grant No. CMS-0114709.

Table of Contents

List of Figures

List of Tables

Chapter 1
Introduction and Literature Review

1.1 Introduction

Earthquakes can cause considerable damage to structures, especially among older structures that were built to less stringent seismic design codes. An increasing amount of money is being spent on energy dissipation devices to mitigate structural response due to large ground motions during earthquakes. While some of this comes as the result of lessons learned in recent seismic events, it is partly due to the recent shift to performance based design. Some popular energy dissipation devices include base isolation systems, tuned mass dampers, and fluid inertial dampers, among many other passive and active control systems. The majority of available systems are fairly expensive, and the additional cost to install them in an existing structure can be excessive.

New research has shown that, in addition to the West Coast, significant seismic risk exists in the Central and Eastern United States, a region where there are many older structures and historically less focus on seismic design. Thus, seismic retrofitting in older structures, as well as implementation of these devices in new structures, is essential throughout the country. Because of the heightened demand and lack of cost-effective alternatives, a new-found research focus has been the development of inexpensive passive control devices to mitigate structural damage due to earthquakes.

This investigation is part of a multiple-stage research project designed to examine the behavior of synthetic fiber ropes and their application as passive earthquake dampers known as SCEDs, Snapping-Cable Energy Dissipators. When ropes transition from a slack to taut state, they build up large tensile forces, known as a snap load, over a very short time period. Synthetic ropes tend to dissipate a significant amount of energy due to friction during these snap loads, and thus may be well suited for use as cost-effective passive control devices. While the primary setup envisioned involves synthetic ropes

installed diagonally across the vertical bay of a building frame, these ropes have potential for other applications such as cable restrainers to prevent bridge deck unseating.

The purpose of this research is to examine the behavior of guyed masts utilizing synthetic ropes when subjected to seismic loading. The majority of the lateral stiffness is provided by the guys, and thus structural response is dependent on their dynamic properties. A typical guyed mast was modeled using the dynamic properties of the synthetic ropes as the guy elements and subsequently the response was investigated. The structural behavior due to snap forces and the response of towers subjected to three-dimensional ground motions were of specific interest.

The previous work of Pearson (2002) and Hennessey (2003) involved testing and characterizing the dynamic behavior of synthetic ropes. In parallel with the current research, another graduate student at Virginia Tech, John Ryan, performed field tests to expand on and validate the earlier model developed by Hennessey (2003). These rope properties were then included in the three-dimensional finite element guyed mast models that were used to examine the dynamic behavior. One standard model, based on previous studies, was designed for use in this research: a 120-m-tall mast with 4 guy levels. A series of parameter studies was then performed on this model by varying the seismic input, the geometry of the structure, the stiffness and pretension of the guys, and the mast properties. The results of these studies were used to characterize how the ropes affect the dynamic behavior of guyed masts, with the goal of supporting continued research towards the application and utilization of SCEDs.

1.2 Literature Review

1.2.1 Previous Research

The initial work to examine the dynamic behavior of high-modulus synthetic ropes was performed by Pearson (2002). In that research, 19 different rope types were tested, involving several diameters, to see which ropes would exhibit dynamic characteristics beneficial for energy dissipation. Both static and dynamic tests were performed with the use of a 3.7-m-tall drop tower. This assembly utilized a load cell and an accelerometer to record the behavior of the rope while a weight was dropped from the free end. Multiple combinations of drop heights and weights were used to test the ropes dynamically. One of the most important trends found in this research was that the majority of the permanent set occurs in the first loading cycle. Additionally, ropes with smaller diameters, higher moduli of elasticity, and tighter braids were shown to displace less. Finally, it was also established that significant energy was dissipated during the dynamic tests, showing potential for their use as passive damping devices.

Hennessey (2003) continued research on the dynamic behavior of high-modulus synthetic ropes. This research consisted of more controlled static and dynamic trials on two of the original rope types tested, Amsteel Blue and Amsteel II. The Amsteel Blue ropes have a lower modulus of elasticity and a looser braid than the Amsteel II ropes. As might be expected, the experiments showed that more displacement, and thus more energy dissipation due to friction between the strands, occurred in the Amsteel Blue ropes.

The results of this initial phase of research were presented in Hennessey et al. (2005). While the Amsteel Blue ropes dissipated more energy, the excessive displacements associated with the dissipation were too large for the ropes to be of practical use. Thus, it was decided that the dynamic characteristics of the Amsteel II ropes would make them better suited for use as SCEDs. Also, by precycling the ropes under static load, a substantial portion of the permanent set can be removed and thus displacements can be reduced by a factor of two. By avoiding these large displacements, the ropes should be

able to act for more than just the first cycle of loading in a structure. Using the large amount of data from these drop tower tests, a mathematical model was developed for determining the dynamic force in a snapping rope as a function of relative displacement and relative velocity.

Current research is investigating the potential use of these ropes in building frames. Ryan, a graduate researcher at Virginia Tech, has run several additional dynamic trials on the Amsteel II ropes involving forced harmonic loading. These experiments specifically utilized smaller velocities, such as those that might be seen when a slightly slack rope pulls taut inside of a building frame under lateral loading. As a result of these trials, it has been established that the dynamic behavior of the rope is mostly dependent on relative displacement and the highest load previously experienced by the rope, with the small magnitude of the relative velocity having little effect on the dynamic behavior.

1.2.2 Cable Behavior and Modeling

For most applications, fully modeling the behavior of cables is a fairly complex task. The self-weight and the lack of flexural rigidity of the cable dictates that a cable is never straight except in a vertical position. Additionally, dynamic excitation of cable modes can cause highly nonlinear response. A considerable amount of research has gone into the development of simplified cable models that still maintain adequate accuracy for dynamic analyses.

Irvine (1981) offered a comprehensive treatment of classic and contemporary examples of cable structures and analytical techniques to solve these problems. The basic concepts regarding the catenary shape were covered, as well as response to static and dynamic loads. Guyed towers were briefly addressed - an example was presented illustrating an analytical method to find the static and dynamic stiffnesses of guy clusters.

Desai and Punde (2001) proposed a simple, nine-degree-of-freedom finite element for accurately describing vibrations in an inclined cable, as opposed to the common method

of discretizing the cable into small elements. Cable vibrations can be very important in guyed masts, especially tall masts with extremely long guys. Their research validated the cable model proposed by analyzing the response of full-scale guyed masts incorporating their model compared to other finite element models.

In order to model guyed masts, Kahla (1994) utilized cable elements that were perfectly flexible and had linear viscous dampers in parallel with each element. These dampers were included to account for the energy dissipation associated with the material and the friction between strands.

There have not been many studies of cable models that examine the slack to taut transition and its effect on the behavior of structures. While most analyses with guyed structures use a tension-only formulation of the guy element, the specific consequences of this modeling decision are rarely examined. The snap loads associated with the transition phases in tension-only elements are generally accepted as significant, and this should warrant a closer look at their impact on structural response.

A particular area of research that deals with the alternating slack and taut modes of cables is that of marine applications. Plaut et al. (2000) conducted a study on snap loads in the mooring lines of an underwater cylinder. It was found that with large motions the mooring lines could go slack, and when they returned to the taut state a spike in tension occurred that was short-lived but often much larger than would be modeled with a linear spring.

One such study that looked at the results of slack cables during seismic motion was conducted by Filiatrault and Stearns (2004). While this particular study looked at the potential benefits of connecting electrical substation equipment with slightly slack cables, it has particular relevance to all types of structures that might be affected by snapping cable behavior. This research looked at several types of equipment, with varying levels of initial rope slackness. The experimental results showed two very distinct types of response. For the less slack cases, a significant amount of interaction between the

equipment occurred, changing the fundamental frequencies of the equipment, and at times the dynamic response was amplified by the presence of the cables. The cases with more initial slack exhibited no significant changes in fundamental frequencies and the dynamic response was generally reduced. However, in all cases, the use of cables increased the damping ratios associated with the equipment. Thus, damping benefits may be seen with the use of slack cables, but care must be taken to avoid instances where the dynamic response is amplified.

Active control of tension cables was used to damp a guyed truss by Preumont et al. (2000). Each guy was fitted with a sensor to measure cable tension and an actuator to manipulate the cable tension. Certain control laws exist that can be used to determine how to change the tension in the cables. This form of active control was shown to increase stiffness and dissipate energy for all of the instances under investigation. Also included in the findings was the discovery that the more lightweight the cables are, the less of a negative effect the cable vibrations have on the structure.

The use of tendons supplementing a rocking shear wall was examined by Ajrab et al. (2004). The purpose of that investigation was to examine cost-effective ways to minimize interstory drifts and control structural damage during seismic events. In previous studies, it was shown that rocking shear wall response only provided minimal damping, with a damping ratio less than 2%. However, the results of this study showed that utilizing supplemental tendon systems in conjunction with the rocking shear wall has the potential for significant damping with damping ratios in the general range of 20%. The tendons were draped in an “x” pattern through the shear wall, and each tendon included a damper. Structural performance was found to be relatively distinct and unrelated to the amount of pretension in the tendons. However, the pretensions involved in the study were always large enough to prevent the tendon from going slack during the reverse cycle. The outcome of these experiments shows potential for the damping inherent to the synthetic rope behavior to be a significant factor in the response of a structure.

1.2.3 Design of Guyed Masts

The current research is intended to be a general investigation without being design oriented. While some sense of the practical design and nature of guyed masts is needed in order to instill a measure of reasonableness in the results, the purpose is not to fully design a specific guyed mast and then test the structure under a myriad of conditions. The purpose is to investigate the general behavior of guyed masts incorporating synthetic ropes and conduct sensitivity studies. Therefore, there is no desire to include individual member buckling, specific limit states, or material failure in the model of the structure. For this reason, only basic research into the design of guyed masts was conducted so that the studies would have relevance to everyday applications.

Guyed towers are used for a number of structural purposes, the two most common being electrical transmission lines and communication towers. There are many different setups and structural configurations with which these guyed towers can be constructed, all with distinct advantages for certain situations. For this research, the simple nature of a guyed mast, used prevalently for communication towers, was used. These consist of a vertical mast with guy wires usually extending from multiple levels to the ground. However, some of the design guidelines involving electrical transmission towers are still applicable and were reviewed as well.

The American Society of Civil Engineers (ASCE) maintains a series of Manuals and Reports on Engineering Practice. Several of these are devoted to the design of transmission towers and proved helpful for design criteria.

In Manual 72 (ASCE 1990), it is noted that wire strand is usually the material of choice for guys, and the measure of strength most commonly used is minimum rated breaking strength. If the specific guy properties are not known, 23,000 ksi is used as a general estimate for the modulus of elasticity of these wire strands. Pertaining to the design of guys, tension under design loads is kept below 65% of the breaking strength in order to keep the deformation from becoming nonlinear at the point of yielding. Some of the

recommending modeling practices specify that guyed masts should not be treated as axial struts, and that guys can be modeled as tension-only truss element members. As an additional note, in mountainous terrain, guys can be twice as long as compared to a structure on flat ground, and this can cause considerable changes to the structural performance.

Manual 52 (ASCE 1988) offers some insight into the pretensioning of guys. While the initial tension required is dependent on several factors (length and size of the guy, allowable deflection of the structure), a pretension of 10% of the rated breaking strength is generally adequate to prevent slack guys. Sometimes these guys are provided prestressed and cut to length, but for the majority of cases they are cut in the field and an adjustment device such as a turnbuckle is used. Also of interest is the fact that columns of guyed masts almost always have tension-compression bracing systems.

All real structures have some inherent damping, and this has the potential to significantly alter the structural behavior. Manual 74 (ASCE 1991) gives the average damping values for structural vibrations in transmission towers. These damping ratios cover the range from 4 to 8%.

The most recent and relevant of these manuals is No. 91 (ASCE 1997), which is entitled *Design of Guyed Electrical Transmission Structures*. As previously noted, guys are usually wire strands, and this manual gives a table of the breaking strengths for typical diameters of wire strands. This is useful for evaluating the effectiveness of wire strand versus high-modulus synthetic ropes, which offer comparable strength for the same diameter with much less weight. For a normal transmission line structure, the pretension in the guys ranges from 5 to 10% of the breaking strength. However, guys in electric transmission line structures are almost always taut, which is not the case for tall communication structures. Common and efficient guy slopes range from 45 to 60 degrees from the horizontal.

Among other general design considerations, most mast to footing connections are theoretically pinned. For multi-guy level latticed masts, a simple column model (not including bending) is not acceptable for modeling steel masts, even when hinged at the base, due to significant stiffness in the mast. Also, in order to take into account the effects of possible large deflections in addition to large axial compression, it is recommended to use nonlinear computer analysis for design of guyed structures in electrical transmission lines (ASCE 1997).

Mulherin (1998) has conducted a study involving failures of communication towers due to atmospheric icing. While icing failures are not the focus of the current investigation, the research was used to characterize the trends observed in these towers. Of the 77 cases researched and investigated, all but one involved guyed towers. Research showed that the majority of these guyed communication towers were triangular in cross section, with legs and bracing made of solid rod, tubular, or angular steel. Depending on the tower height, the guys were attached to anywhere from one to four sets of anchors on the ground. Mulherin also commented that most masts had a uniform cross section, but it was not uncommon to have a tapered mast or tapered sections of the mast.

The Telecommunications Industry Association publishes a standard (TIA 1996) for the design of antenna supporting towers. In this industry standard, the recommended range for initial tension in guys is from 8 to 15% of published breaking strength. These suggestions are an attempt to avoid galloping and slack guy behavior for low tension cases and to avoid aeolian vibrations for high tension cases.

Madugula (2002) provides perhaps the most complete treatment available regarding the design of guyed masts and lattice towers. While seismic design of guyed masts is generally neglected or performed improperly using building code rules, Madugula offers a rigorous outline of many static and dynamic procedures applicable to guyed masts. Many topics of interest are covered in this resource, however only the most pertinent ideas are covered here.

One distinction in the height of communication towers is that most telecommunication towers measure up to 100 m tall, while broadcasting towers generally range from 120 to 600 m tall. Those that are constructed as guyed masts can have 20 or more active vibration modes, and earthquakes generally have the ability to excite modes from 0.1 to 10 Hz. When modeling guyed masts for analysis of earthquake effects, it is appropriate to use a bare tower, devoid of any extra mass due to antennas, receivers, or other equipment. Additionally, Madugula notes that while guyed masts are usually pinned at their base, the short and usually stiff guys near the base can sometimes result in a boundary condition that approaches fixed-end behavior (Madugula 2002).

In guyed masts, the guys provide resistance to lateral motion through both elastic stretching and change in sag. If there is a moderate amount of sag in the guys, the energy required to lessen the sag, i.e., raise the mass of the cable, can substantially affect to the stiffness of the guy. Thus, the dynamic stiffness and response of guys can become extremely nonlinear due to curvature of the guy profile and additional tension due to vibration. Also, due to the relative lightness of typical masts and the long cumulative lengths of multiple guys in such structures, guys can account for a significant portion of the total mass of the structure (Madugula 2002).

Madugula writes that nonlinear effects must be taken into account when modeling guyed masts, as well as strong vertical ground motion, such as that seen in the Northridge earthquake. There are inherent means of energy dissipation in the system due to structural, aerodynamic, and soil damping. However, in order to control the dynamic response to wind and large ground motions, there are also many options for supplemental energy dissipation, using both passive and active dampers, and both displacement- and velocity-dependent dampers (Madugula 2002).

1.2.4 Research Involving Guyed Masts

There have been several previous studies regarding the dynamic behavior of guyed masts and telecommunication towers. The vast majority of these analyses involve the dynamic response of guyed masts due to wind loads. Although the current research is specifically focused on seismic response, the methods used to model the masts for wind loads are still applicable and provide a launching point for developing the finite element models that will be used throughout the current research.

Field experiments were conducted by Harikrishna et al. (2003) on the dynamic excitation under normal wind speeds of a 50-m-tall guyed mast in India. The test structure had a constant, square cross-section with steel angles used for the vertical members. It had four guy levels, and four guys at each level. The mast itself was instrumented with anemometers and accelerometers in order to record the wind forces as well as the structural response. Large amounts of data were taken over an extended period of time, and the measured response showed the presence of closely spaced modes and significant multimode excitation. Damping ratios in the structure were found to vary between 1 and 3% with an average of 1.6%, as compared to an accepted value of 2% for bolted steel structures. This was smaller than the referenced value of 4 to 8% associated with electrical transmission towers (ASCE 1991).

Borri and Zahlten (1991) analyzed a 130-m-tall guyed mast with four guy levels under wind loading. One of the key results was that the dynamic response of the structure can be significantly different if the nonlinear effects due to large displacements are included. Their results showed differences on the order of 25% in the computed displacements and internal forces when a nonlinear analysis was performed.

In research involving the dynamic analysis of guyed masts under wind loads, Kahla (1994) used equivalent beam-columns to model the mast. This provided an easy method to approach the modeling of the mast and drastically reduce the number of elements needed while still achieving reliable results.

Moossavi Nejad (1996) examined the dynamic response of a 327-m-tall guyed mast with five guy levels. The analytical model of the mast was subjected to three-dimensional, artificially generated seismic records. Highly nonlinear structural behavior was observed, and it was shown that strong ground motions can cause significant levels of dynamic tension in the guys.

Two guyed masts were analyzed under seismic loads in a study by Guevara and McClure (1993). Specific information was provided about the geometry and stiffness of the towers, and this was used for developing the models for this current research. When analyzing the masts, the response in terms of axial, lateral, and torsional loads of an equivalent beam model differed by less than 5% from a detailed space truss model. The research concluded that the dynamic interaction between the guys and the mast is important, especially in the vertical direction.

The effect of multiple support excitation in guyed masts was specifically examined by Amiri et al. (2004). This research looked at two masts, 342 m and 607 m tall. Using finite element models, the responses of the structures were measured for different shear wave velocities and compared to those due to uniform ground motion. When the spatial effect of ground distances between guy anchors of large masts is included, it was found that lateral displacement of the tower tip decreased, while base shear and axial force in the mast increased significantly, on the order of 15 to 38%.

Amiri (2002) conducted several full-scale, finite element analysis studies on the seismic response of guyed masts. Previous seismic studies were reviewed in this research, but these were few and only addressed specific issues. Most of the time, wind and ice loads control the design of guyed towers, and this leads to earthquake effects often being "ignored or improperly evaluated". The purpose of the study was to develop some simple indicators of sensitivity to seismic motion so that designers would know when it is advisable to include seismic effects in the design of guyed masts. Eight existing towers ranging in height from 150 m to 607 m were studied, and the in-depth data provided on

tower geometries, weights, and guy tensions was used for developing the finite element models in this current research.

Amiri (2002) described the trends and behaviors for guyed masts 150 to 350 m tall: masts with fundamental natural periods in the range of 0.5 to 3.0 Hz were sensitive to horizontal motion; base shear ranged from 40 to 80% of the tower weight; the dynamic component of axial force in the mast was about 80% of the tower weight; dynamic guy tensions typically varied from 50 to 200% of the initial tension; and guyed masts with relatively slack guys (initial tensions below 5% ultimate tensile strength) were sensitive to the combination of vertical and horizontal ground motion. The study showed that discontinuities in behavior along the mast should be expected due to the differences in lateral stiffness at guy levels and between guy levels. Additionally, the inertial effects of the guys had only a small effect on the lateral response of the mast, but were difficult to predict with regard to response due to vertical accelerations.

1.2.5 Ground Motions

Seismic events are very unpredictable, and consequently choosing a particular ground motion(s) to use in designing a structure is complicated. While many methods exist to search and find records that are appropriate for a particular design, this investigation merely attempts to utilize historical ground records without regard to design motions that would be present at a specific site.

Chen and Scawthorn (2003) offered a comprehensive treatment of historical earthquakes and design practices. Extremely useful information was presented on past earthquakes, their magnitudes, and characteristics. Also, information on the modeling of strong ground motion was thoroughly explained.

Madugula (2003) stated that if correctly used, any of the three types of records (actual, modified, and synthesized) of ground accelerations can be used for the seismic design of guyed masts.

When a detailed seismic design is required by code, the majority of seismic codes call for the structure to be analyzed for an event of a certain magnitude and distance. One of the approaches for generating a ground record for this design event is to take a record of similar magnitude and scale it to match the desired event. The most common method employed is scaling with regard to the peak ground acceleration (PGA), although this is not the only technique (Shome et al. 1998).

1.3 Objective and Scope of Research

The objective of this research is to examine the seismic behavior of guyed masts utilizing synthetic ropes. Energy dissipation associated with the hysteretic loading nature of the synthetic ropes makes them potentially useful as passive control devices. Currently, guyed masts are often used in the communication industry and almost exclusively utilize wire strands for the guys. The alternate use of high-modulus synthetic ropes, which have comparable strength and significantly less weight than steel wire strands, offers a possibility for minimizing the dynamic structural response, as well as reducing the negative effects of vibrations in the guys. Also, the snap loads that occur during the slack to taut transition have the likelihood of significantly affecting the structural system and their effects should be closely examined.

Previous research on the behavior of snap loads in these high-modulus synthetic ropes made it possible to characterize their dynamic behavior. However, this behavior is extremely nonlinear, as well as discontinuous between loading and unloading. In order to efficiently incorporate the rope model into a finite element model, a simplified model was desired. Simple viscoelastic models involving a combination of spring and dashpot elements were investigated to determine an adequate but simple representation of the ropes.

A three-dimensional finite element model of a guyed mast was then be created, based on basic research into the current design practices. Parametric (or sensitivity) studies were

conducted on the standard model while observing the three-dimensional structural behavior and any possible effects due to snap loads.

Many seismic studies only involve ground motions in one direction, but this simplification is far removed from what actually occurs. Also, previous research has shown that vertical ground motions can have significant dynamic impact on the guy tensions, and thus should be included in all seismic analyses of guyed masts. For these reasons, two historical records of three-dimensional ground motions, exhibiting different magnitudes and frequency characteristics, were used for the investigation, and three-dimensional responses was determined.

The information gathered from these studies was used to draw conclusions on the effect of synthetic ropes in guyed masts. The results will serve to increase the general knowledge regarding snap loads and support research directed at investigating the potential application of SCEDs in structures.

1.4 Overview of Thesis

Chapter Two of this thesis presents the basic modeling decisions regarding the finite element program used for this investigation. It also details the development and subsequent testing of two validation studies designed to confirm the accuracy of the aforementioned modeling decisions.

Chapter Three addresses the methods used to develop a rope model in ABAQUS that approaches the behavior seen in previous experiments. The load-displacement relationships of potential spring and dashpot models are presented and compared to the dynamic behavior recorded in the previous research.

Chapter Four discusses the setup of the three-dimensional models that are used in this research. The decisions pertaining to the design and modeling of the towers are

addressed, in addition to the ground motions that will be used. An outline is given to note the parameters of the trials to be performed.

Chapter Five provides a discussion the results of the parametric studies performed on the two guyed masts. Trends in the behavior of these structures are described, as well as the specific effects due to snap loads.

Chapter Six contains a brief summary of the procedures and results, and presents the conclusions that can be drawn from the research. Some possible areas for improvement and extension are also addressed in this chapter.

Appendix A consists of the theoretical formulations and the parameter combinations used in the preliminary trials. Appendix B includes two-dimensional plots of the ground motion records and a sample input file. Appendix C contains graphed results from the parametric studies.

Chapter 2
Methods and Validation Studies

2.1 Preliminary Validation

The quality of this research endeavor is based solely upon the ability to accurately model the dynamic behavior of guyed tower systems and obtain useful results with the finite element analysis program ABAQUS. In order to ensure accurate use of the software, several simple, preliminary models were analyzed and then compared against the theoretical behavior. This validation procedure served to check that the methods of modeling the dynamic behavior of guyed masts were sufficient for the purpose of this research. Since the accuracy of modeling procedures completely dictates how applicable the results of the research will be, this was an essential task to complete before continuing further with the research.

2.2 Overview of the Software

ABAQUS, developed by ABAQUS, Inc., is one of the leading finite element analysis programs in the world and can be used to analyze a comprehensive assortment of physical behavior (ABAQUS 2005). This program can easily solve dynamic, nonlinear, finite element models of guyed masts. In order to capture the nonlinear nature of the synthetic ropes, with a stiffness that varies as a function of relative displacement and relative velocity (Hennessey 2003), ABAQUS was chosen to model the behavior of structures incorporating SCEDs.

2.3 Basic Modeling Decisions

In this preliminary stage of the research, several basic decisions were made regarding how to model the specific materials, structural components, and physical behaviors that would be encountered in this problem. These choices were made by researching the

software documentation, and then running simple trials to observe the impact of manipulating the input variables. A brief treatment of these modeling decisions follows.

One of the main issues associated with the finite element model was the choice of element type. The ABAQUS library contains many elements, and they are all well suited for certain applications. Out of the many options available, the best choice to model the mast for the early models was a three-dimensional beam-column element. A specific element was chosen with three integration points; the program refers to this as a B33 element. This Euler beam element has a cubic interpolation function, which is reasonably accurate for distributed loads and thus is well-suited for dynamic vibrations that involve inertial loads along the length of the beam. This particular element was also used in the full-scale studies.

An arbitrary cross section was utilized which allows the user to input the section properties of a member without actually defining the geometry of the cross section. Additionally, linear elastic material properties for steel were applied to this element. These choices were made because the purpose of this study was to investigate the general trends in the behavior of the structure as opposed to having the limit states of individual mast members control the behavior.

In order to represent the guys, spring and dashpot elements were used. In particular, a SPRINGA element was used, in which the line of action of the force is always directed between the nodes. This matches the behavior of guyed wires in that the angle of the restoring force can change with large displacements. For the preliminary models, a simple, linear spring was used that acted in compression and tension according to a fixed stiffness value. Following these initial models, the arrangement of a spring and a dashpot (the DASHPOTA element, also with the same line of action) between two nodes was examined. Several combinations of spring and dashpot behavior were used to see which would most accurately represent the observed behavior of the synthetic ropes. Nonlinearities were included in both types of elements, with a provision that no force was present if the element was in compression.

In addition to the material nonlinearities of the ropes, it was desirable to include large displacements in the model. Seismic inputs have the potential to generate significant motions in structures, and thus a large-displacement analysis was warranted. This was very easy to perform with the software; the NLGEOM command was simply activated for the analysis and the effects associated changes in the shape of the structure were calculated throughout the analysis.

For rigorous time-history analyses, there are three main options in ABAQUS to solve for the motion of a structure. The simplest of these is a modal approach – a routine within the software solves the eigenvalue problem for the structure, and the user is then given the choice of which modes to include in the dynamic analysis. However, this does not allow for nonlinear elements to model the ropes, as it is based on the modes of a structure in its undeformed state. Dynamic analyses are also available through either an implicit or explicit solver. The computational time is relatively longer for both the implicit and the explicit analyses, but they are able to accommodate the nonlinear elements and large displacements that were being used in this research. While there may be some computational efficiencies when using the explicit solver with highly transient loads at very short time steps, the analysis is limited to using linear shape functions for most of the available elements. Also, the implicit solver has a convergence parameter that makes it easier to control the stability of the solution. For these reasons, the standard dynamic analysis with implicit solver was chosen over the other two options.

Before each general model was evaluated in depth, a convergence study was performed to determine how many elements were needed to fully capture the behavior of the structure. Trials were run with increasing numbers of elements until the solution converged. This was an easy method to ascertain exactly how many elements were needed to accurately represent the structure.

The damping of the structure is also a consideration to evaluate when constructing a model. A general estimate of damping in a steel structure below yield is 2% to 6% of

critical damping, depending on whether the members are welded or bolted, respectively (Chopra 2001). The majority of communication towers are comprised of bolted members, but those with welded members are not uncommon (Madugula 2002). However, for most of the initial analyses, no damping was used under the assumption that this generally leads to larger motions in a structure. When it was necessary to include damping effects, this was done using the Rayleigh damping option in ABAQUS.

In order to develop appropriate factors for use with the Rayleigh damping option, a short procedure by Chopra (2001) was used. Rayleigh damping uses a classical damping matrix which includes mass- and stiffness-proportional damping:

$$\mathbf{c} = a_0\mathbf{m} + a_1\mathbf{k} \tag{2.1}$$

where $\mathbf{c}$ = damping matrix
$\mathbf{m}$ = mass matrix
$\mathbf{k}$ = stiffness matrix
a_0 = mass-proportional damping factor
a_1 = stiffness-proportional damping factor

The damping ratio of any particular mode n is

$$\zeta_n = \frac{a_0}{2}\frac{1}{\omega_n} + \frac{a_1}{2}\omega_n \tag{2.2}$$

where ζ = damping ratio
ω = natural frequency

It may be desired to damp the participating modes of structural response at roughly the same value. To accomplish this, choose modes *i* and *j* near opposite ends of the range of participating modes. If they are assigned the same damping ratio, ζ, then the values of the damping factors are as follows:

$$a_0 = \zeta \frac{2\omega_i \omega_j}{\omega_i + \omega_j} \qquad a_1 = \zeta \frac{2}{\omega_i + \omega_j} \tag{2.3a, 2.3b}$$

The choices presented above represent basic modeling decisions and methods that were constant throughout the research; all were validated in the following preliminary models. Decisions pertaining to a specific model are addressed with the setup of those particular models. Additionally, the standard metric system based on units of kilograms and meters was used for all of the analyses.

2.4 Preliminary Models

The basic models for preliminary validation were chosen with two priorities: application to the geometry, components, and forcing mechanisms that would be involved in the full-scale models, and ease of computing theoretical results for the validation of the models. Their sole purpose was to make sure the modeling procedures were adequate, and they all matched the theoretical behavior with very little error.

2.4.1 First Preliminary Model

A previous study by Virgin and Plaut (1993) investigated the effect of axial load on the behavior of beam-columns subjected to forced vibrations. This series of investigations was purely theoretical and utilized non-dimensional forces and section properties. One part of that research examined how the natural frequency of a beam changed in response to varying magnitudes of axial load. In order to check the accuracy of the beam-column elements in conjunction with the eigensolver methods, this particular setup was modeled and the results were compared to the findings of Virgin and Plaut.

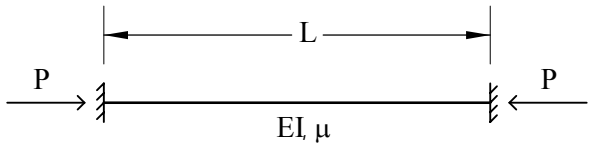

Figure 2.1 Geometry of Fixed-Fixed Beam Used in First Preliminary Model

A finite element model of a fixed-fixed beam, whose geometry is shown in Figure 2.1 above, was generated and the eigensolver routine in ABAQUS was used to find the natural frequencies for different levels of axial load. The results obtained from the analysis were then non-dimensionalized and evaluated against the theoretical results.

In non-dimensional terms, solving Equation 2.4 gives the natural frequencies of the beam subjected to axial load. The lowest solution is thus the fundamental natural frequency. This equation was provided by Plaut and provides a means to establish the exact theoretical frequencies relating to different levels of axial load.

$$(\lambda^2 - \sigma^2)\sin(\sigma)\sinh(\lambda) + 2\sigma\lambda[1 - \cos(\sigma)\cosh(\lambda)] = 0 \tag{2.4}$$

where $\sigma = \sqrt{\dfrac{p + \sqrt{p^2 + 4\omega^2}}{2}}$, $\lambda = \sqrt{\dfrac{-p + \sqrt{p^2 + 4\omega^2}}{2}}$

$p = \dfrac{PL^2}{EI}$, $\omega^2 = \dfrac{\Omega^2 \mu L^4}{EI}$

P = axial force

Ω = frequency

EI = bending stiffness

L = length

μ = mass per length

A beam-column was modeled with 20 elements and trials were run for three different combinations of beam-column length and stiffness:

1) L = 10 m, I = 0.002 m^4

2) L = 10 m, I = 0.004 m^4

3) L = 5 m, I = 0.001 m^4.

The same elastic modulus, E = 209 GPa, was used for each trial. The study was performed up to a non-dimensional axial load of $2\pi^2$, which represents half of the critical buckling load. Axial loads in this research do not approach that magnitude, thus the results are applicable to this investigation. In all three cases the natural frequencies closely matched those presented by Virgin and Plaut (1993). Table 2.1 shows the results for each of the trials.

Table 2.1 Fundamental Frequencies of Fixed-Fixed Beams Under Axial Load

Axial Load,	Fundamental Frequency, ω_0 (rad/s)						
p	Theoretical	Trial 1	% Error	Trial 2	% Error	Trial 3	% Error
$-\pi^2$	24.926	24.921	-0.02	24.916	-0.04	24.907	-0.07
0	22.373	22.373	0.00	22.374	0.00	22.373	0.00
π^2	19.452	19.446	-0.03	19.439	-0.07	19.426	-0.13
$2\pi^2$	15.951	15.920	-0.20	15.888	-0.40	15.822	-0.81

2.4.2 Second Preliminary Model

The second preliminary model involved a basic cantilever beam subjected to a transverse, harmonic displacement at the fixed end. A function in the form $A\sin(\omega t)$ was used to define the forcing displacement, with amplitude A, frequency ω, and time t. Three general cases were examined: A) no springs, B) vertical springs, and C) inclined springs, with spring constant k. The overall geometries of these three cases are shown in Figures 2.2 through 2.4. In effect, these represent a mast subjected to seismic ground excitation with varying degrees of restraint due to guy wires.

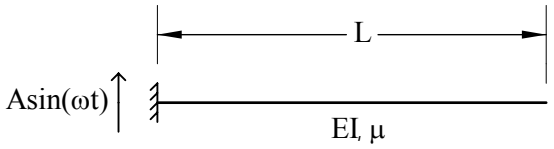

Figure 2.2 Geometry of Cantilever Beam Without Springs (Case A)

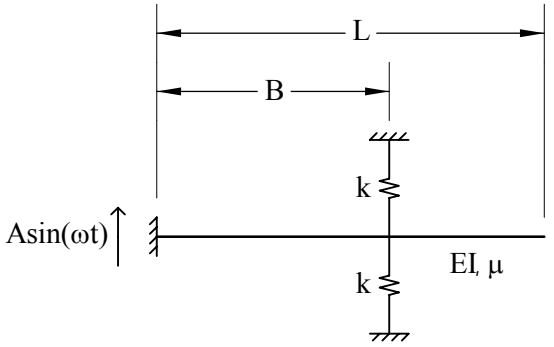

Figure 2.3 Geometry of Cantilever Beam With Vertical Springs (Case B)

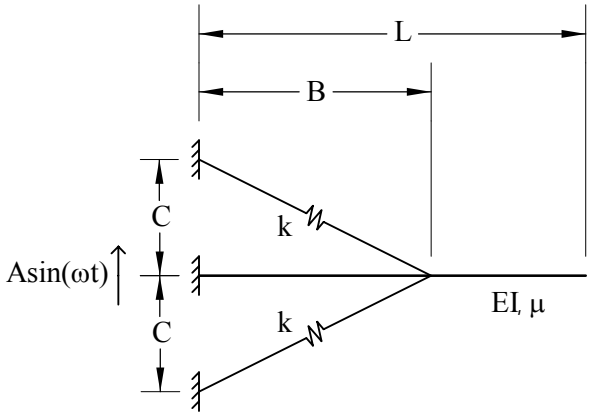

Figure 2.4 Geometry of Cantilever Beam With Inclined Springs (Case C)

Plaut formulated the theoretical motion (damping and self-weight neglected) of the beam for the different cases, and the governing equations are outlined in Appendix A. The steady-state motions of the beams were then found using a standard dynamic analysis with 10 elements for each beam; a small damping value was used in order to damp out transient motions due to initial conditions. These displacement amplitude values were found for eight different variations of each of the three general cases, and then compared to the theoretical motion. The specific parameters involved with each of these trials can also be found in Appendix A.

For Case A, the cantilever model with no springs attached, the amplitude of harmonic displacement, frequency of harmonic displacement, and beam length/stiffness were varied. The amplitude of motion was measured at three-tenths of the beam length from the fixed end and at the free end of the beam. The results are shown in Tables 2.2 and 2.3.

Table 2.2 Amplitude of Motion at x = 0.3L for Cantilever Beam Without Springs

Trial #	Theoretical Displacement Amplitude (mm)	ABAQUS Displacement Amplitude (mm)	% Error
1	202.88	202.88	0.00
2	507.21	507.21	0.00
3	25.16	25.21	0.24
4	62.89	62.91	0.04
5	200.69	200.69	0.00
6	501.72	501.70	0.00
7	20.70	20.66	-0.23
8	51.76	51.64	-0.22

Table 2.3 Amplitude of Motion at x = L for Cantilever Beam Without Springs

Trial #	Theoretical Displacement Amplitude (mm)	ABAQUS Displacement Amplitude (mm)	% Error
1	219.73	219.73	0.00
2	549.33	549.38	0.01
3	56.51	56.94	0.76
4	141.27	142.24	0.69
5	204.71	204.71	0.00
6	511.76	511.75	0.00
7	24.83	24.81	-0.07
8	62.07	62.03	-0.07

The parameters for the model with vertical springs, Case B, were the harmonic displacement function, spring stiffness, and spring location. Results are shown in Table 2.4. For the inclined spring model, Case C, the harmonic displacement function, spring stiffness, and angle of the spring were varied. Table 2.5 shows the results from this model. Amplitudes of steady-state displacements were only compared at the free end of the beam for both of the models involving springs.

Table 2.4 Amplitude of Motion at x = L for Cantilever Beam With Vertical Springs

Trial #	Theoretical Displacement Amplitude (mm)	ABAQUS Displacement Amplitude (mm)	% Error
1	184.62	184.59	-0.01
2	89.24	89.03	-0.24
3	211.80	211.85	0.02
4	104.06	104.27	0.20
5	150.82	150.61	-0.14
6	66.87	66.82	-0.09
7	190.10	190.17	0.04
8	88.38	88.82	0.49

Table 2.5 Amplitude of Motion at x = L for Cantilever Beam With Inclined Springs

Trial #	Theoretical Displacement Amplitude (mm)	ABAQUS Displacement Amplitude (mm)	% Error
1	222.79	222.88	0.04
2	108.57	108.63	0.06
3	205.32	205.41	0.04
4	97.50	97.32	-0.18
5	205.54	205.60	0.03
6	97.63	97.42	-0.21
7	175.47	175.51	0.02
8	80.05	80.45	0.50

All of the cantilever beam models had motions that stayed within one percent of the theoretical motion. For the coarse level of refinement used in these preliminary studies, this level of error is considered acceptable.

2.5 Conclusion of Preliminary Validation

The modeling methods chosen must be validated for simple models in order to have confidence in the results for the complex, three-dimensional analyses that constitute the majority of this research. The preliminary models presented were applicable instances of the behavior to be examined in the following models while utilizing the same elements, and the results closely matched the answers determined by theory. Thus the modeling procedures were validated, and more complex, dynamic analyses could be performed with a significant measure of confidence in the accuracy of the results.

Chapter 3
Rope Models

3.1 Dynamic Rope Behavior

The dynamic behavior of high-modulus synthetic ropes has been thoroughly investigated in the previous stages of this research project. A diverse assortment of rope types was tested under multiple loading sequences in order to determine those ropes with properties suitable for use as SCEDs. It was concluded that Amsteel II ropes had the most desirable characteristics, and these ropes were further examined in concurrent studies by Ryan, a graduate student at Virginia Tech. This specific rope has a double braided configuration, high strength and high modulus of elasticity, and is manufactured by Samson Rope Technologies in Ferndale, Washington.

Ryan has performed several additional trials on Amsteel II ropes having a nominal diameter of 24 mm (1 inch). The particular 24 mm ropes used in these extra studies have a minimum strength of 230 kN , and a weight of 44.2 kg/m (Samson 2005). Two different types of tests have been performed on these ropes to date. Original tests involved measuring the elongation in a single rope under harmonic loads. After these trials were used to identify the stiffness and establish a pretensioning procedure, harmonic forces were applied laterally to a scaled portal frame with pretensioned ropes installed diagonally across the bay.

An example of a rope displacement history in the frame investigations performed by Ryan can be seen in Figure 3.1. There were distinctly different loading and unloading curves, but they remained fairly consistent throughout the experiment. Also, it is evident that energy was being dissipated during each of the cycles.

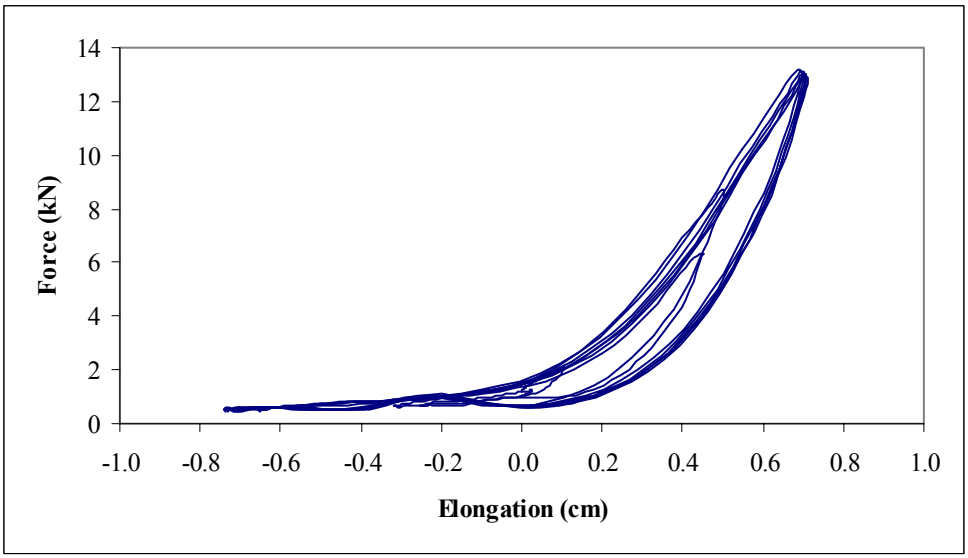

Figure 3.1 Force vs. Displacement Plot of a Typical Experimental Rope Mounted Diagonally in a Frame

In both sets of trials it was seen that the loading portion of the behavior can be approximated by the nonlinear expression

$$F = kx^{1.3} \tag{3.1}$$

where F = force

k = spring stiffness

x = relative displacement

In order to obtain approximately the same stiffness relating to a linear spring for use in comparisons, Motley (2004) showed that the nonlinear spring stiffness should be about 40% of the linear spring stiffness.

While these approximations provided an adequate model for the loading portion of the behavior, once the maximum load was reached the behavior changes and a different curve was followed during unloading. A model was desired that combines both portions of the curve to approach the true behavior of the ropes.

3.2 Rope Model Development

Experiments with different rope models were carried out in an effort to find a model that closely fit the actual behavior of the ropes. Combinations of spring and dashpot elements were used for the basis of these models with the goal of finding a simple and efficient model that could adequately represent the ropes.

The numerical testing of these models consisted of the rope model connecting two nodes and applied displacements in the axial direction. Most of the tests were run at an amplitude of 0.2 m and a frequency of 1 Hz, which results in a maximum acceleration of about 0.8 g. This was on the scale of what might be seen in a structure under seismic loading. All the trials were run for a duration of five seconds to see the behavior during repeated load cycles.

Many variations of the models presented in this chapter were tested. Different combinations of spring stiffnesses and dashpot coefficients were experimented with, as well as different combinations of linear, bilinear, and nonlinear definitions. Also, a point mass was sometimes used at the center node of the model. However, in some cases, this actually added energy to the system and thus is not further addressed. In total, over 50 trials were performed to examine the rope models and determine their applicability to the problem at hand.

3.2.1 Model A

The first rope model considered was a simple spring connecting two nodes, and can be seen in Figure 3.2. This was used as the most basic generalization of slack-taut rope behavior to provide a benchmark for the rest of the trials.

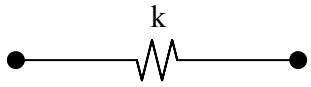

Figure 3.2 Schematic of Rope Model A

A bilinear definition of the spring created a load-displacement behavior like that shown in Figure 3.3. With a nonlinear definition of tension in the spring, the simple model ccould be made to approach the loading curves seen in the experiments. While this is similar to the overall nature of the synthetic ropes under harmonic loading, or any cable for that matter, no energy loss is associated with each loading cycle.

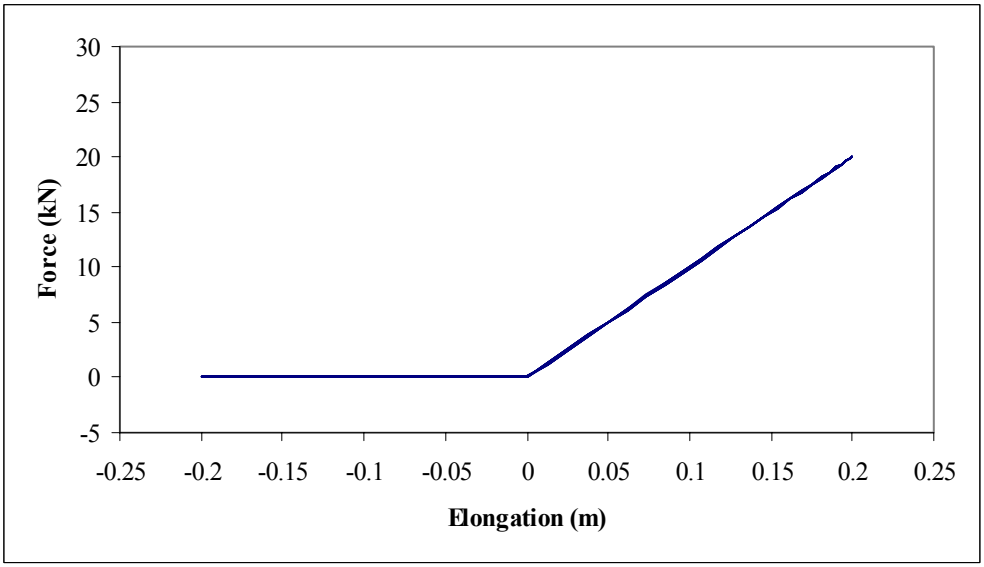

Figure 3.3 Typical Force vs. Displacement Plot of Model A

3.2.2 Model B

The next set of trials looked at the behavior of Model B, which consisted of a spring and dashpot in series, as shown in Figure 3.4. Similar to all of the models excluding the first, this particular model included a dashpot to allow energy to be dissipated during each loading cycle in an effort to match the experimental data.

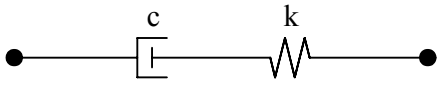

Figure 3.4 Schematic of Rope Model B

The case of a bilinear spring and linear dashpot led to a load-displacement behavior like that shown in Figure 3.5. The first loading cycle dissipated a significant amount of energy like the desired behavior. However, as was often the case, the permanent displacement in the dashpot when the rope becomes slack caused the following load cycles to not generate tensions starting at the same displacement.

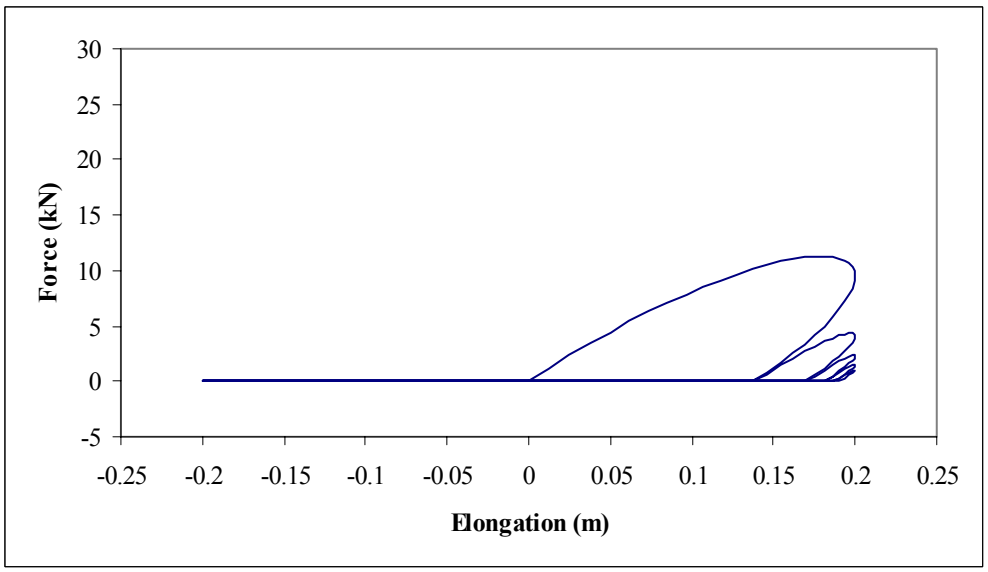

Figure 3.5 Typical Force vs. Displacement Plot of Model B

3.2.3 Model C

Model C consisted of a spring and dashpot in parallel, like the schematic seen in Figure 3.6. This particular model is fairly common and has been used in previous studies to include energy dissipation in the cable, such as in the research by Kahla (1994).

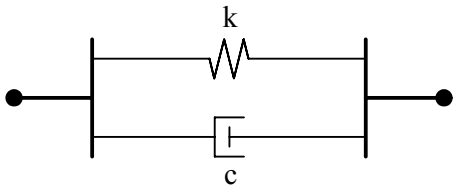

Figure 3.6 Schematic of Rope Model C

Figure 3.7 shows the load-displacement behavior of a bilinear spring and bilinear dashpot. Each cycle dissipated a consistent amount of energy, however there was just as much energy dissipation during negative displacements as there was during positive displacements. Although the shape of the model was fairly good, the dissipative behavior was clearly not accurate.

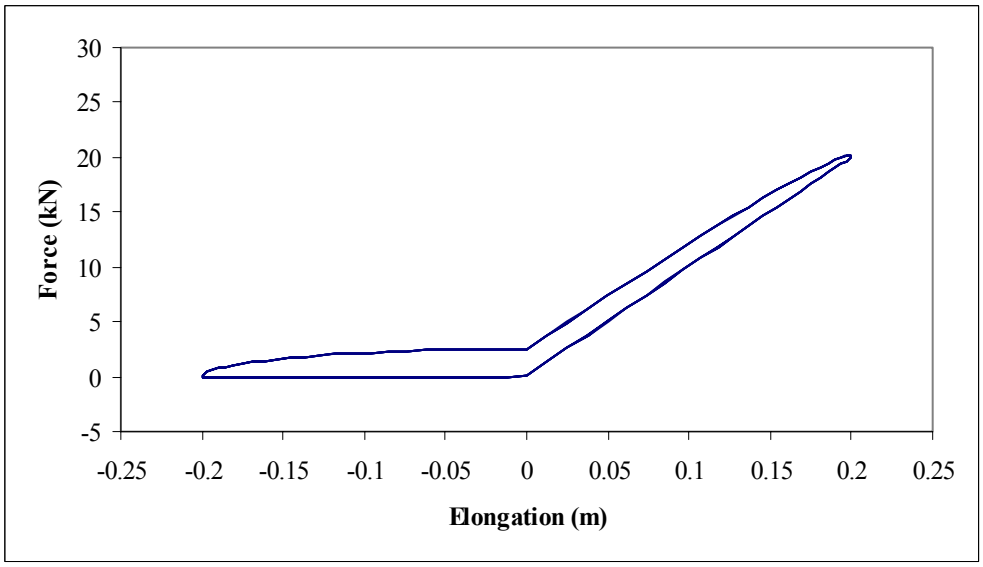

Figure 3.7 Typical Force vs. Displacement Plot of Model C

3.2.4 Model D

The next model examined consisted of two springs and a dashpot; the arrangement is shown in Figure 3.8. This is known as the standard linear viscoelastic model, but these trials did not use only linear definitions for the elements.

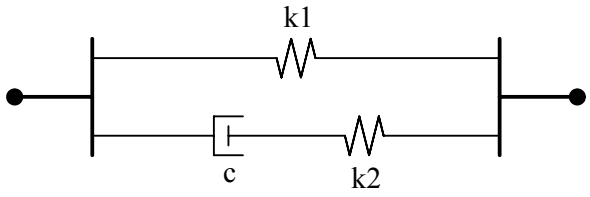

Figure 3.8 Schematic of Rope Model D

The load-displacement behavior of a case where *k1* was nonlinear, *k2* was bilinear, and *c* was bilinear is shown in Figure 3.9. The aforementioned problem of the dashpot having a displacement at the start of a new loading cycle occurred in this model as well, causing the loading behavior to be inconsistent.

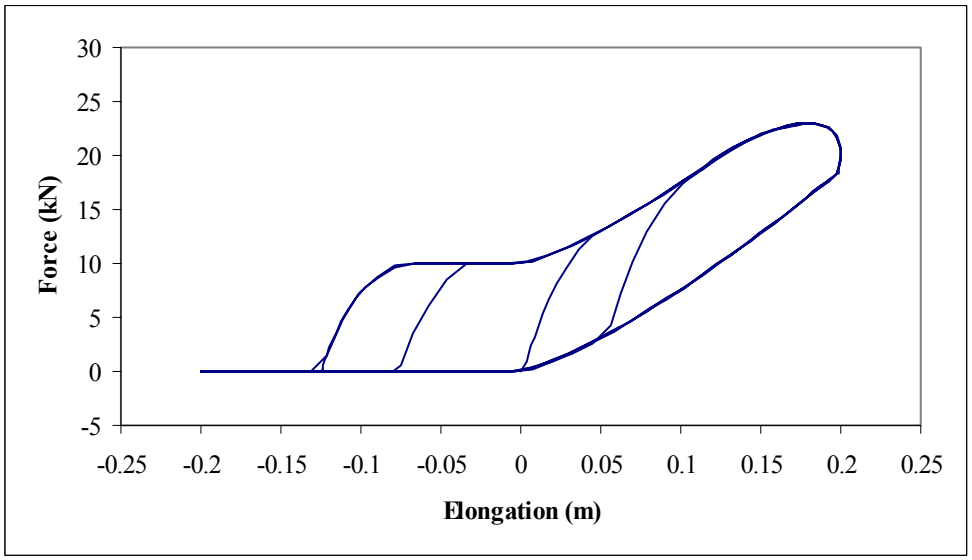

Figure 3.9 Typical Force vs. Displacement Plot of Model D

3.2.5 Model E

Model E also consisted of two springs and a dashpot in a slightly different arrangement that can be seen in Figure 3.10. This model approached the behavior of the synthetic ropes more closely than the other models, mostly due to a spring that would return the dashpot to its original length during the slack portion of the cycle.

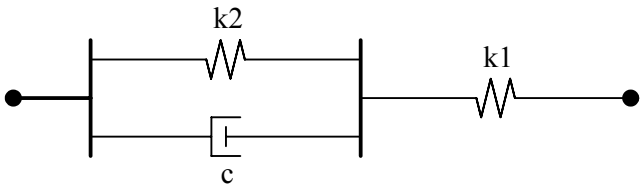

Figure 3.10 Schematic of Rope Model E

The load-displacement behavior of a case where *k1* was nonlinear, *k2* was bilinear, and *c* was bilinear is shown in Figure 3.11. This behavior was very similar to that of the synthetic ropes, and a comparable amount of energy was consistently dissipated in each cycle.

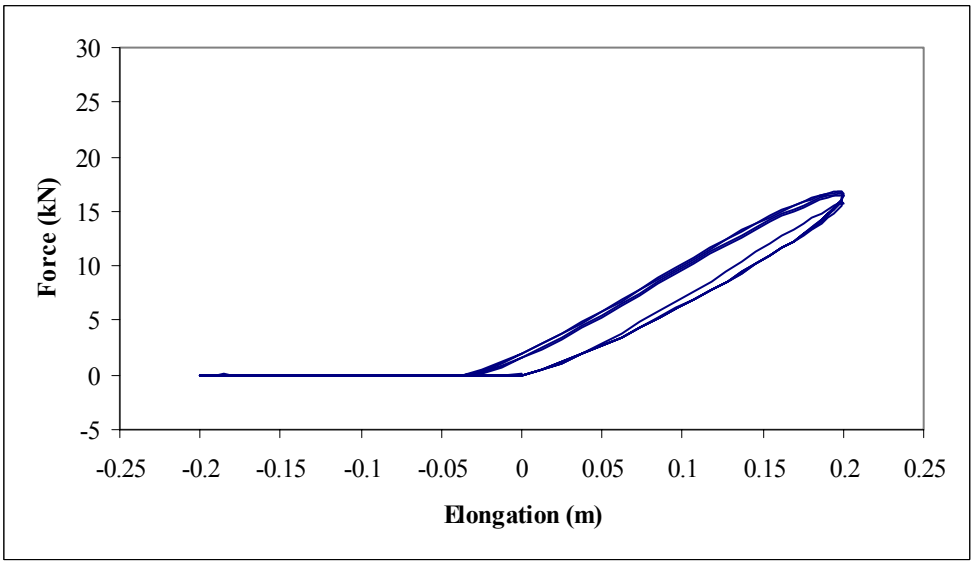

Figure 3.11 Typical Force vs. Displacement Plot of Model E

While this model appeared to be very usable, it still had a significant drawback: the loading behavior was not consistent if the dashpot was not given enough time to return to its original length before the next loading cycle started. The behavior of a model with the same spring and dashpot definitions, but with a frequency of 2 Hz (as opposed to the original trial at 1 Hz), is shown in Figure 3.12.

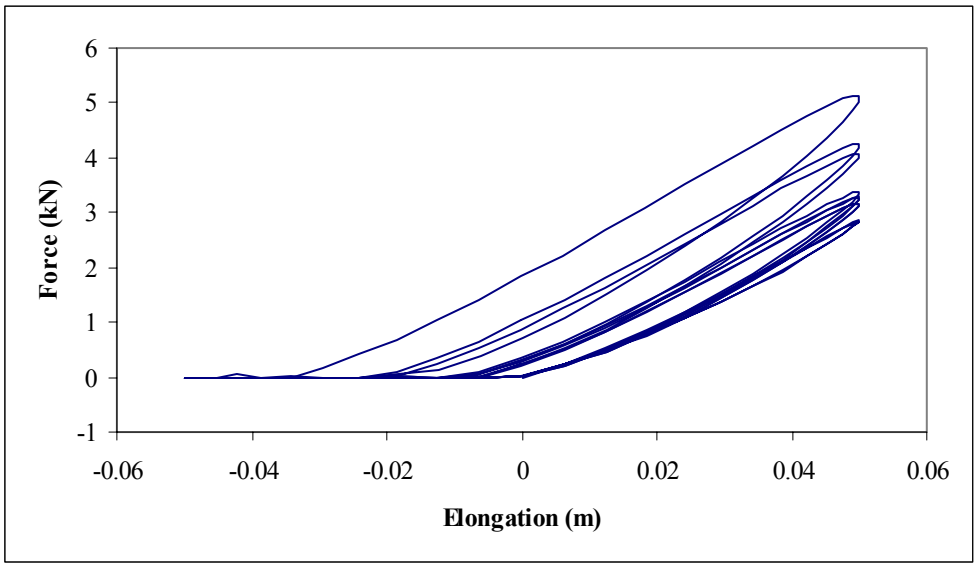

Figure 3.12 Force vs. Displacement Plot of Model E at a Higher Forcing Frequency

3.3 Rope Model Conclusions

Out of the rope models examined, Model E proved to be the most consistent and closest to the true behavior of the synthetic ropes. However, there was still a lack of consistency and no good method to restrict the dashpot to be active only when the spring was active. In order to more accurately model the rope behavior, the use of a more complex element with specific constitutive laws, or a subroutine to return the spring force at each time increment for use in the dashpot definition, is recommended.

The lack of consistency in the behavior of these rope models led to a decision not to include them in the modeling of the guyed masts for this current investigation. This was further supported by trials that showed damping ratios on the order of 0.01 to 0.02 for a guyed mast incorporating Rope Model E. This implied that the measure of damping provided by the ropes was less than the inherent damping in a bolted, steel structure. Therefore neglecting the energy dissipation in the ropes should not drastically change the behavior of the guyed masts investigated in this research.

Chapter 4
Analytical Model

4.1 Overview of Model

A significant amount of time was devoted to the setup of the analytical models that were used for the investigation. As was shown in Chapter 2, many of the basic modeling decisions and elements had already been validated. This chapter presents the details of the specific modeling decisions with regard to the full-scale model, as well as the reasoning behind the selection of values for element properties.

A three-dimensional model of a guyed mast was developed based on a mast used in a previous study by Desai and Punde (2001), and originally examined by Irvine (1981). The mast was 120 m tall, with four guy levels, three guys per level, and two sets of guy anchors as shown in Figures 4.1 and 4.2. In the two previous studies, every cable had the same properties and pretension force, so those characteristics were used in this study. Additionally, convergence studies were performed to determine the necessary number of elements and general Rayleigh damping was included with each model to represent structural damping.

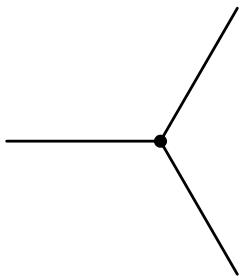

Figure 4.1 Plan View of the Guyed Mast

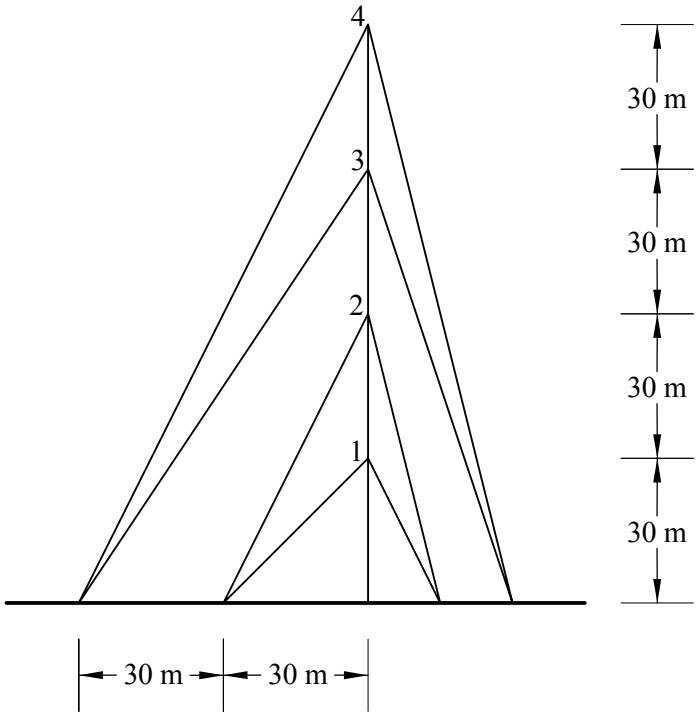

Figure 4.2 Profile View of the Guyed Mast

Once this standard case was developed, parameters were varied to create an array of other similar models. Input files were used to set up the models and define the dynamic analyses, and these were then sent to a University-owned SGI ALTIX 3700 Supercluster for processing with the program ABAQUS. The structural response due to seismic forcing was recorded and later analyzed.

4.2 Strong Ground Motion Records

The focus of this investigation was not the design of a particular mast, or for a particular seismic event, but rather to obtain general response to general seismic motion. For that reason, two historical strong ground motion records were used in the analysis. The El Centro ground motion, also known as the 1940 Imperial Valley event, and the 1994 Northridge ground motion were used. Both these ground motions are commonly used in studies examining structural response to earthquakes.

The time histories of these events were downloaded from the Pacific Engineering and Earthquake Council's website (PEER 2005), where records are maintained from practically all large seismic events that have been recorded. The records are resolved into three orthogonal components, two horizontal and one vertical, and tabular forms of the acceleration, velocity, and displacement time histories are available, as well as the acceleration response spectra at different levels of damping.

For the trials in this investigation, tabular displacement information was used to define the motion and was input as a dynamic boundary condition at the base of the structure and at the guy anchors. The Northridge motion was cropped at 20 seconds after the strong motion ceased, while the full 40-second record of the El Centro motion was used.

All three orthogonal components of ground motion were used. Many studies simply take one record in the direction of the strongest ground motion and apply it to the structure under investigation. However, ground motion is truly a three-dimensional phenomenon, and this study attempted to model it as such. As can be seen in the following figures, there was much more occurring than the simple rectilinear motion that is usually investigated. Figure 4.3 shows the horizontal accelerations for a time period of about 2 seconds of the strongest motion of the Northridge event. Horizontal displacements for the first 15 seconds of the Northridge record are shown in Figure 4.4. The full complement of plots can be found in Appendix B.

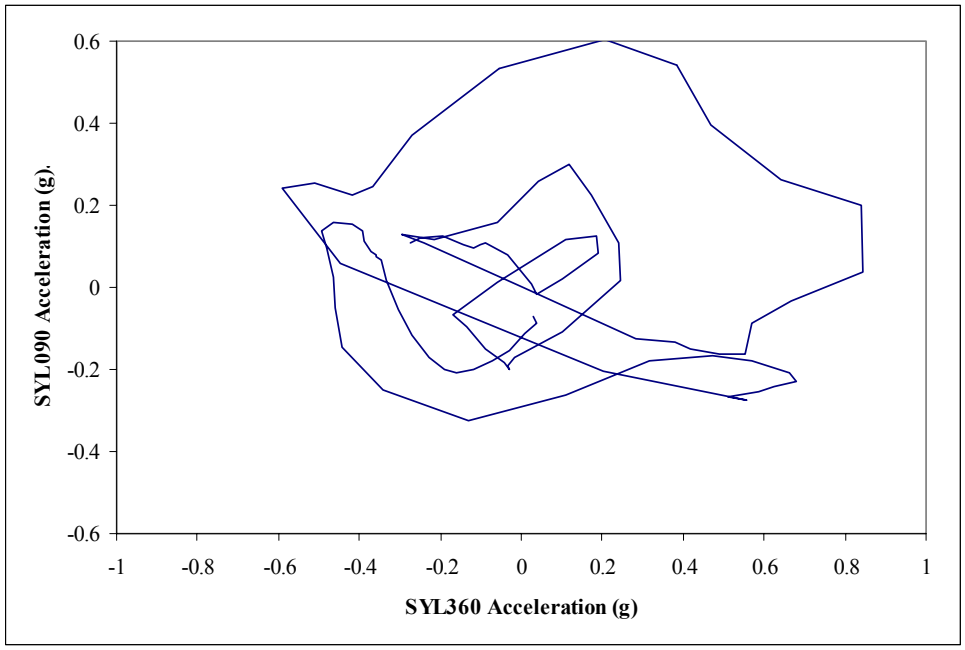

Figure 4.3 Acceleration Time History for Horizontal Northridge Ground Motion

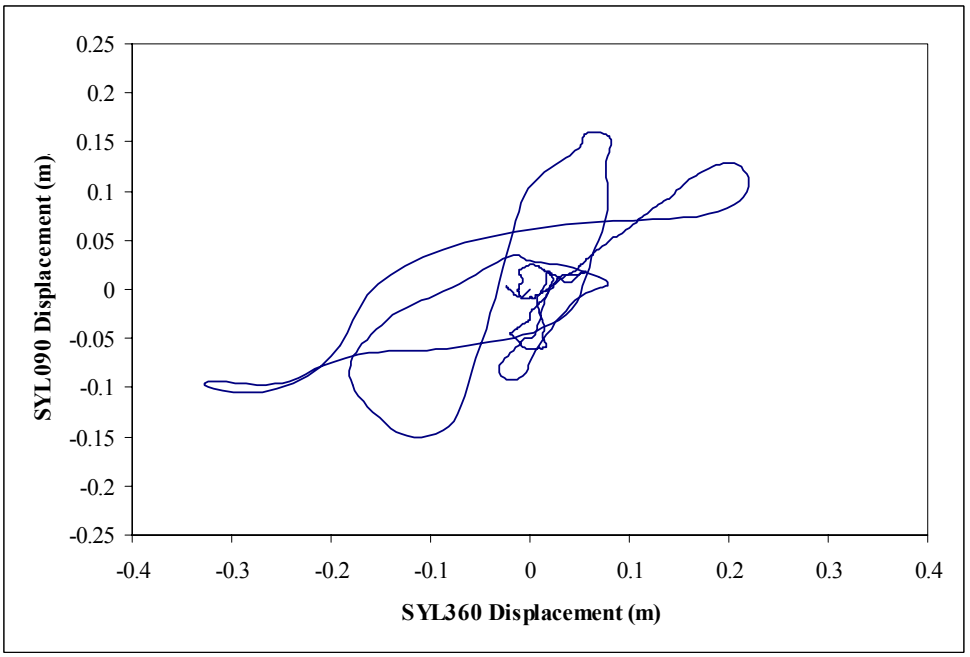

Figure 4.4 Displacement Time History for Horizontal Northridge Ground Motion

One of the objectives of this study was to examine the influence of directionality of input motion on the structural response of guyed masts. Due to the fact that the majority of stiffness is provided by the guys, the angle at which the motion approaches the mast with respect to the guys may change the response of the structure. Three different directions of the strongest ground motion were examined, and a sketch of their relative orientations can be seen in Figure 4.5.

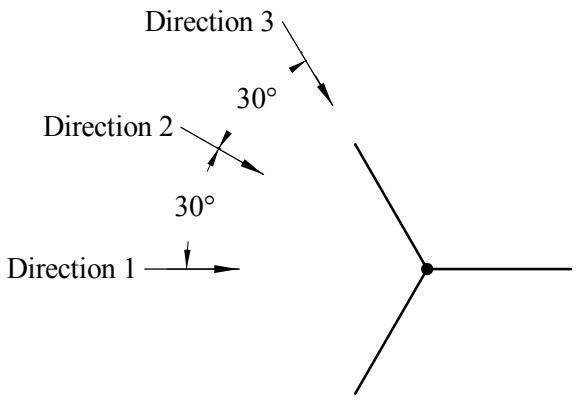

Figure 4.5 Plan View of Directions of Strongest Earthquake Input

4.2.1 Northridge, 1994

The Northridge earthquake occurred just north of Los Angeles on January 17, 1994. It was measured as having a magnitude of 6.7 (Chen and Scawthorn 2003), and many recording stations picked up the ground motion. For the purposes of this investigation, the ground motion used as input was that recorded at the Sylmar County Medical Center, noted as "SYL". This particular recording station was located very near the fault, and the ground motion record exhibits some near-field effects that are not common in other records. The strongest direction of ground motion was SYL360, with a peak ground acceleration (PGA) of 0.843 g. The other horizontal direction, SYL090, had a PGA of 0.604 g, and the vertical SYL-UP record had a PGA measuring 0.535 g. Data was given at time increments of 0.02 sec for this record (PEER 2005).

Figures 4.6, 4.7, and 4.8 show the acceleration time histories of the three ground motion directions, and Figure 4.9 shows the acceleration response spectra of the records.

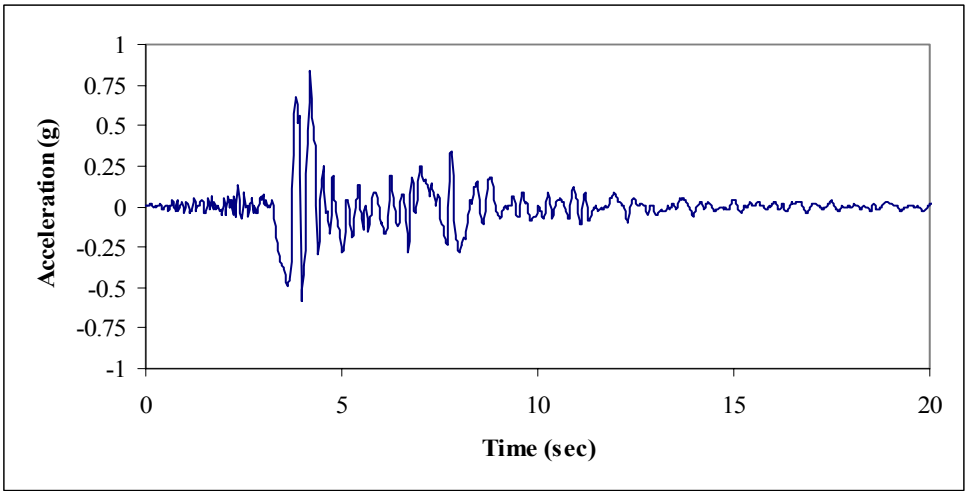

Figure 4.6 Acceleration Time History for SYL360

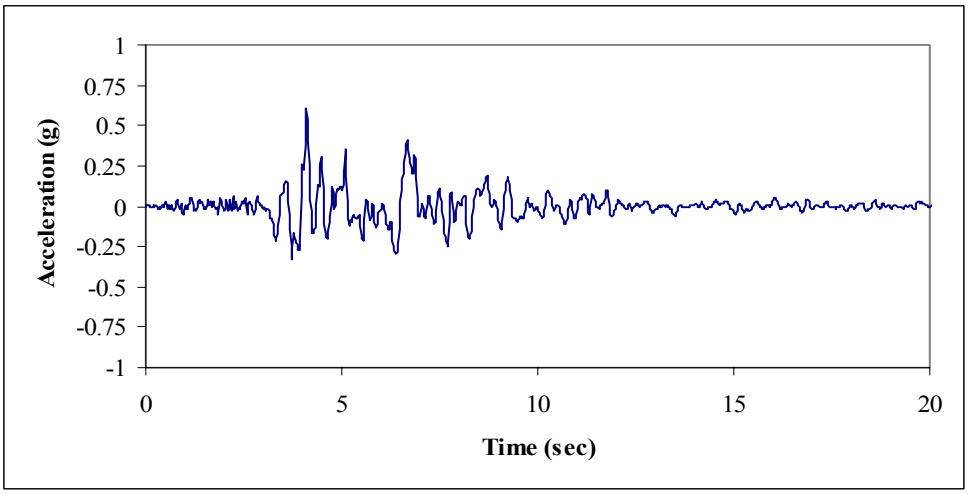

Figure 4.7 Acceleration Time History for SYL090

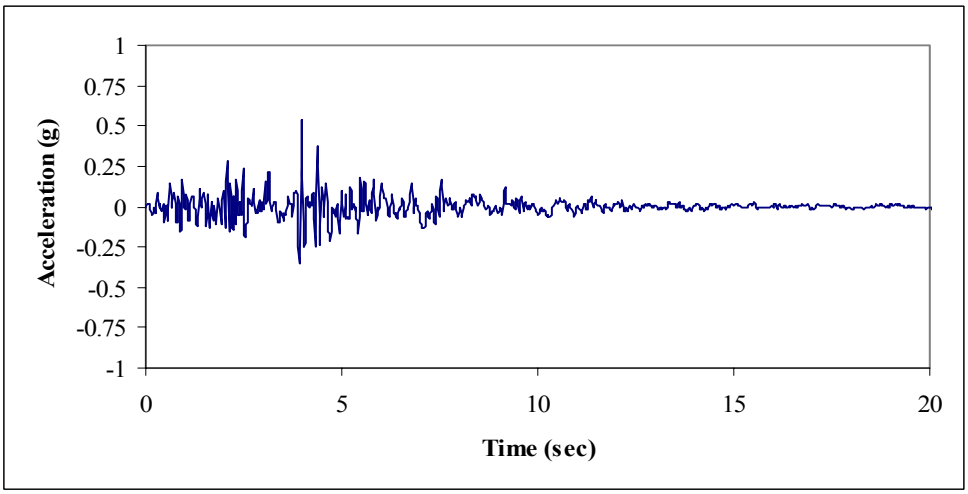

Figure 4.8 Acceleration Time History for SYL-UP

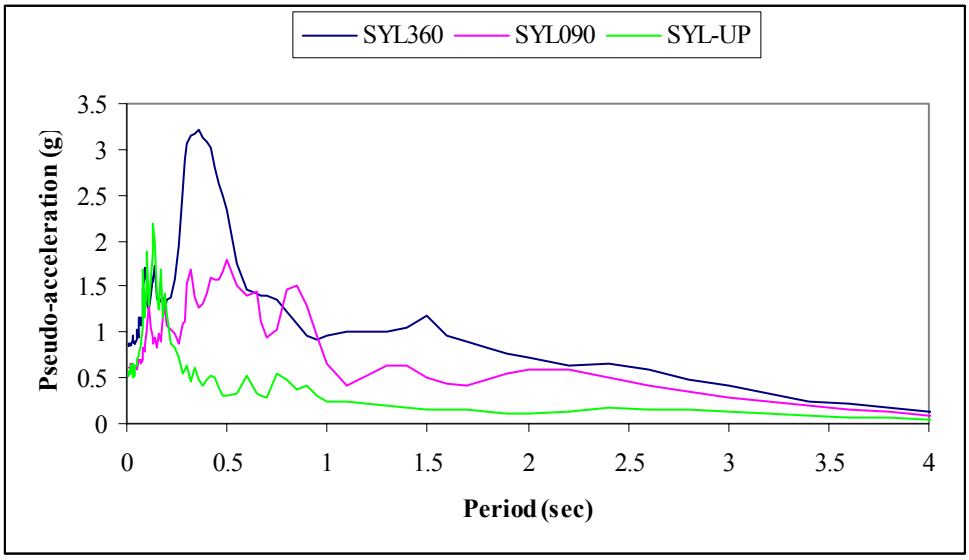

Figure 4.9 Northridge Sylmar Acceleration Response Spectra at 2% Damping

4.2.2 El Centro, 1940

The 1940 El Centro earthquake occurred on May 19. It was characterized as a magnitude 7.0 event, and there was only one recording station in the PEER database, that being the El Centro Array #9. For the purposes of this investigation, the ground motion used as input was that recorded at the El Centro Array, noted as "ELC". The strongest direction of ground motion was ELC180, with a PGA of 0.313 g. The other horizontal direction, ELC270, and the vertical ELC-UP had PGA's measuring 0.215 g and 0.205 g, respectively. Data was given at time increments of 0.01 sec for this record (PEER 2005).

This particular event had more high-frequency content than the Northridge event, but less intensity as measured at this location. In order to see the slack-taut behavior in one particular guyed mast under both earthquake inputs, the El Centro time histories were scaled up 50% with respect to PGA. The scaled versions will be referred to as the amplified El Centro records.

Figures 4.10, 4.11, and 4.12 show the acceleration time histories of the three ground motion directions, and Figure 4.13 shows the acceleration response spectra of the records.

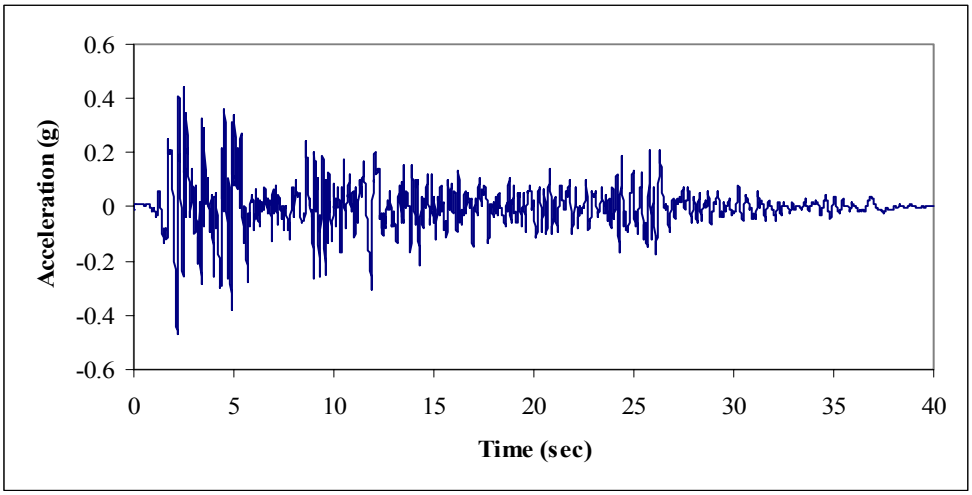

Figure 4.10 Acceleration Time History for Amplified ELC180

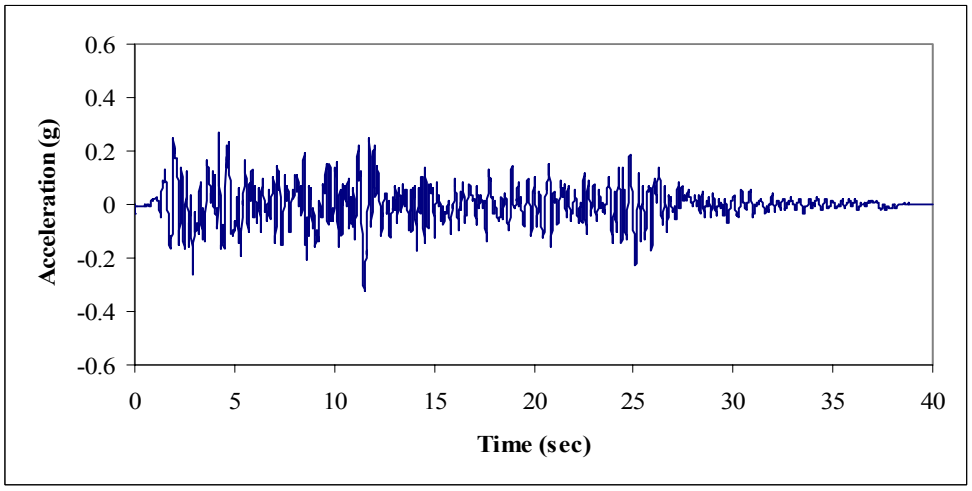

Figure 4.11 Acceleration Time History for Amplified ELC270

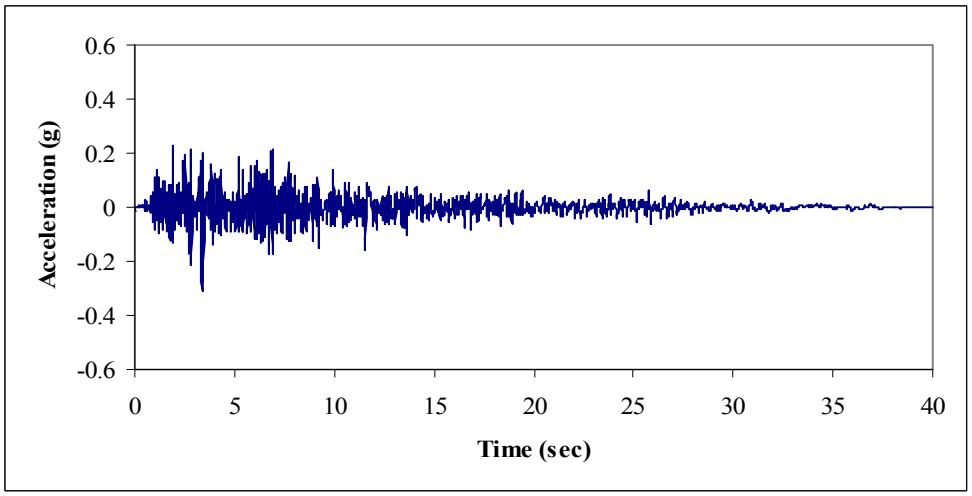

Figure 4.12 Acceleration Time History for Amplified ELC-UP

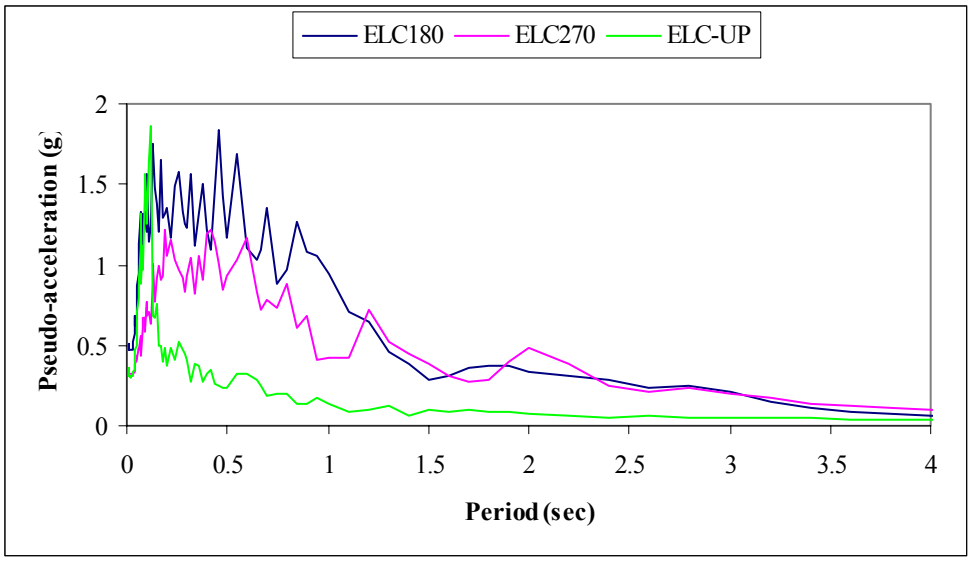

Figure 4.13 Amplified El Centro Acceleration Response Spectra at 2% Damping

4.3 Three-dimensional Model

4.3.1 Guys

As discussed in the previous chapter, a satisfactory spring and dashpot model that included the damping effects of the synthetic ropes was not found. For this reason, a simple spring was used to model the guys – the SPRINGA element that was used in the preliminary validation. It took the form of no stiffness when in compression, and a nonlinear stiffness according to Equation 3.1 when in tension. A sample graph of the spring behavior for the standard case, $EA = 3 \times 10^7$ and 25 kN of pretension, can be seen in Figure 4.14.

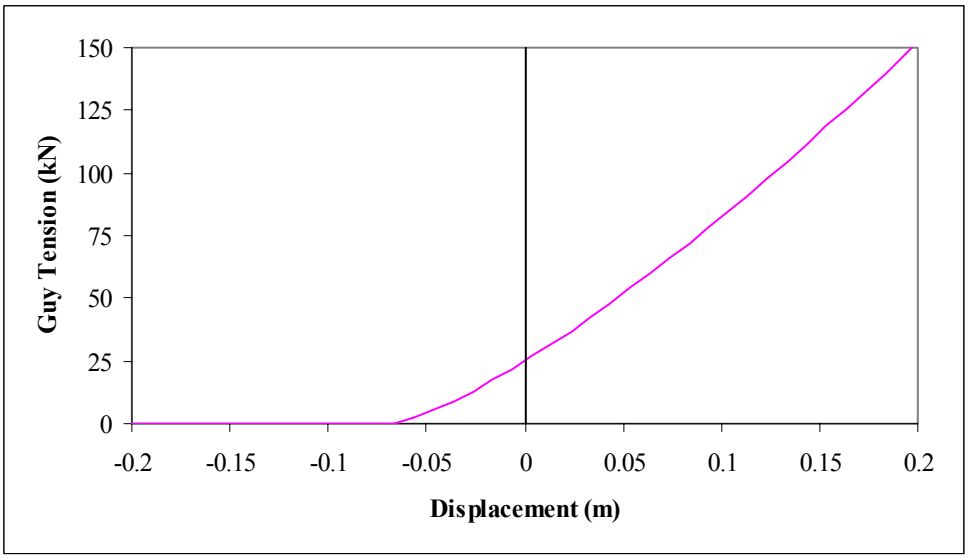

Figure 4.14 Sample Nonlinear Spring Definition

The spring was defined by a linear stiffness and pretension. The current study used the property of *EA*, modulus of elasticity times cross-sectional area, to define the stiffness of the ropes. A definition of this nature allowed this study to be applicable to all types of materials in guy wires, and included hardening effects which are generally present in stranded ropes and cables. The linear stiffness, as defined by a cable cross-section and elastic modulus, was converted into an equivalent nonlinear stiffness based on the factor developed and proven in Motley (2004).

The high-modulus synthetic ropes previously examined are much lighter than steel cables. Due to the significant weight reduction, it was decided not to use a more complex model of the guys because the mass would no longer be a significant portion of the total mass of structure, and additionally, dynamic vibrations in the cables would have much less effect on the dynamic tensions in the ropes than in steel cables.

The anchors of the guys were assumed to be rigid, and their motion was synchronized with the base of the mast. It has been shown that for very tall heights, which result in large distances between guy anchors, multiple support excitations can significantly change the dynamic behavior of guyed masts. However, the tower under investigation

was 120 m tall, which is on the lower end of the spectrum of guyed masts, and thus should not be particularly sensitive to multiple support excitations.

4.3.2 Mast

The mast was modeled as a beam-column using the B33 element with a general beam section, as was validated in the preliminary trials. The general beam section option implies that there is no definition of the shape of the cross-section, merely the necessary properties of the cross-section are defined, such as area, moment of inertia, and modulus of elasticity. This was appropriate for this investigation since the focus was to examine overall mast behavior without focusing on the individual elements that comprise the mast.

In this model, the guys were simply connected to a node at the center of mass of the mast and torsional displacements were neglected. The base of the mast was modeled as a pinned connection, as the literature review showed to be the most common practice.

4.3.3 Analysis Options

The dynamic analysis was performed using the Standard Implicit Solver, verified in the preliminary validation. This analysis included large deflections, vertical loads due to the weight of the mast, and the seismic base motions previously presented. The duration of the analyses was 20 and 40 sec, for the Northridge and El Centro motions, respectively. The tolerance parameter known as the half-step residual was set as 10,000 N and found to be adequate; the maximum time step was taken as 0.01 sec. This implies that frequencies up to 10 Hz were considered in the analyses, and this did not significantly alter the content of the earthquake motions as seen in Figures 4.9 and 4.13.

4.3.4 Output Parameters

In order to examine the structural response, several forms of output were requested from the analysis. This output was written to the output database at every other time increment, which correlates to a maximum of 0.02 sec between readings. Guy tensions and base shears were recorded, as well as axial forces, bending moments, and displacements at each quarter point along the height of the mast. The output generated was converted into an Excel spreadsheet and consolidated and manipulated with that program. Peak values of all the output parameters were calculated. Displacements recorded by the program were absolute, so these recorded values were modified with respect to the base motion to obtain relative displacements which will be exclusively used for the analysis of these trials.

4.4 Convergence Studies, Damping, and Parametric Studies

Convergence studies of the mast model were performed under earthquake loading, specifically the Northridge event, in order to determine an adequate number of beam elements for the modeling of the mast. The results of the convergence studies over a small time period can be seen in Figures 4.15 and 4.16. It was found that 3 beam elements per section between guy levels, for a total of 12 beam elements, provided accurate results. This can be seen as the light blue line lies almost directly over the green line. Both displacements and bending moments were examined in order to make this determination.

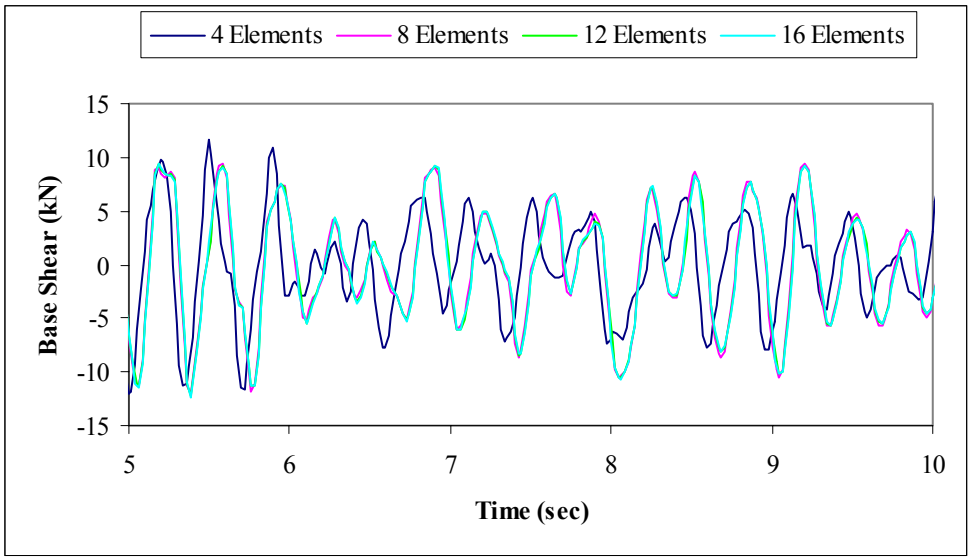

Figure 4.15 Base Shear 1 in Convergence Studies

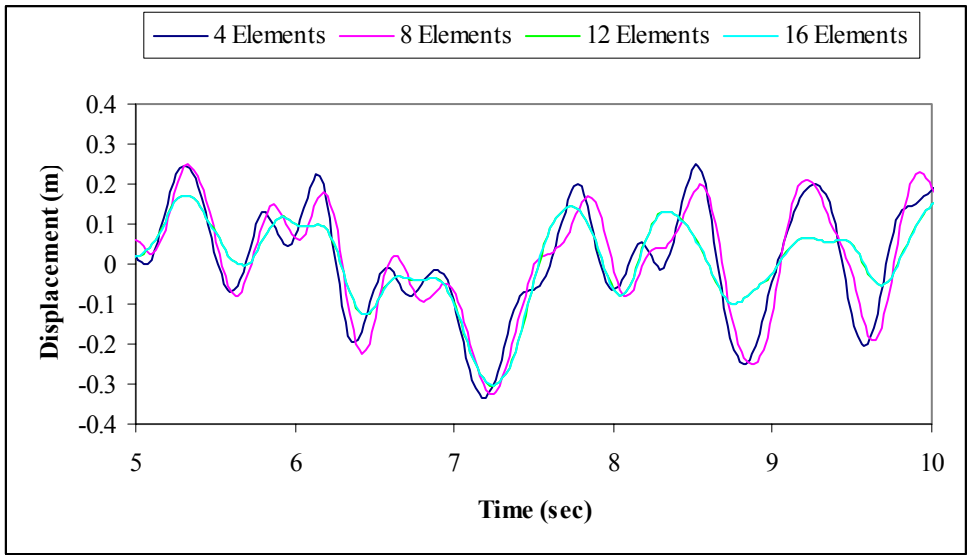

Figure 4.16 Displacement 1 at Top of Mast in Convergence Studies

The eigensolver routine that was validated in the preliminary studies was used to determine the first five bending modes of the general case of the mast. The frequencies, in radians per second, of the first five modes were found to be as follows: 8.37, 10.5, 16.1, 20.3, and 29.3. The frequencies are practically identical to the theoretical values determined by Plaut using beam theory, and the mode shapes using an equivalent spring at each guy level, as can be seen in Figures 4.17, 4.18, and 4.19, closely match those presented on page 149 of Irvine (1981).

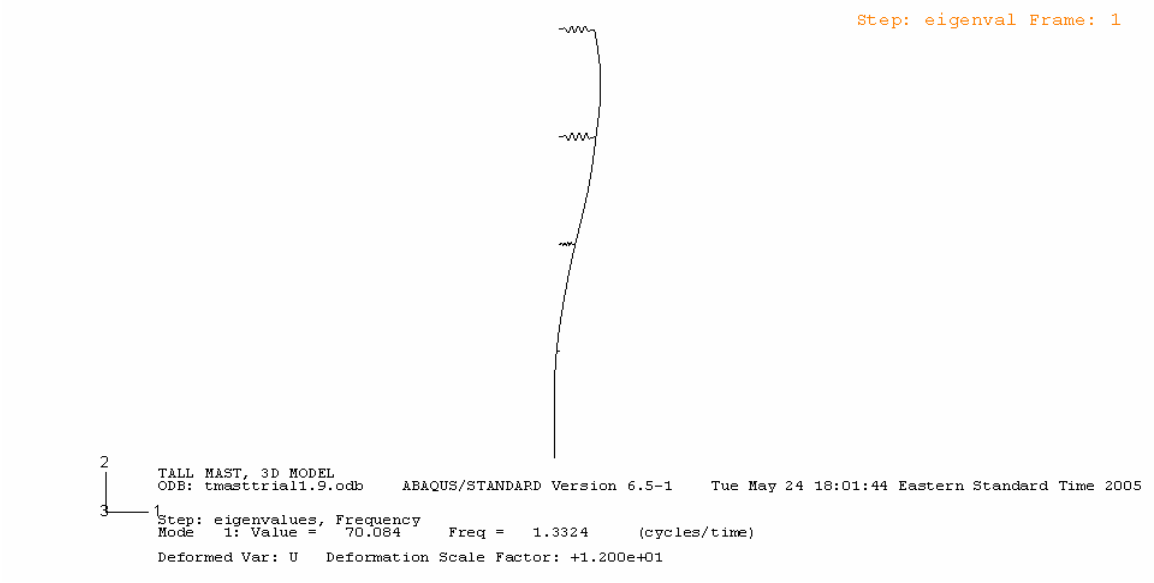

Figure 4.17 First Bending Mode

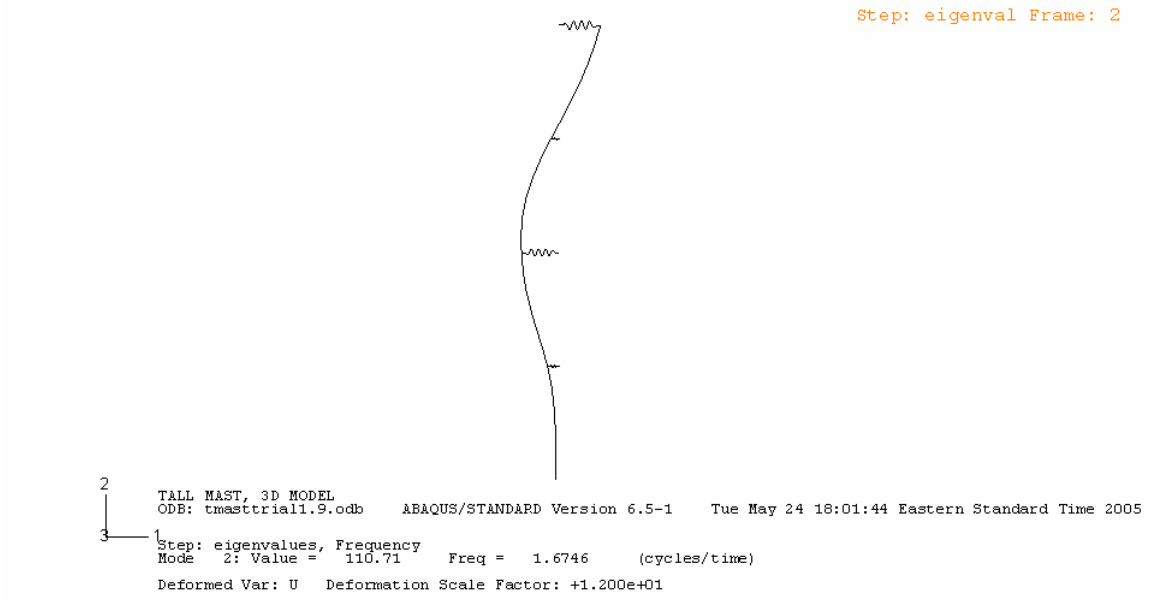

Figure 4.18 Second Bending Mode

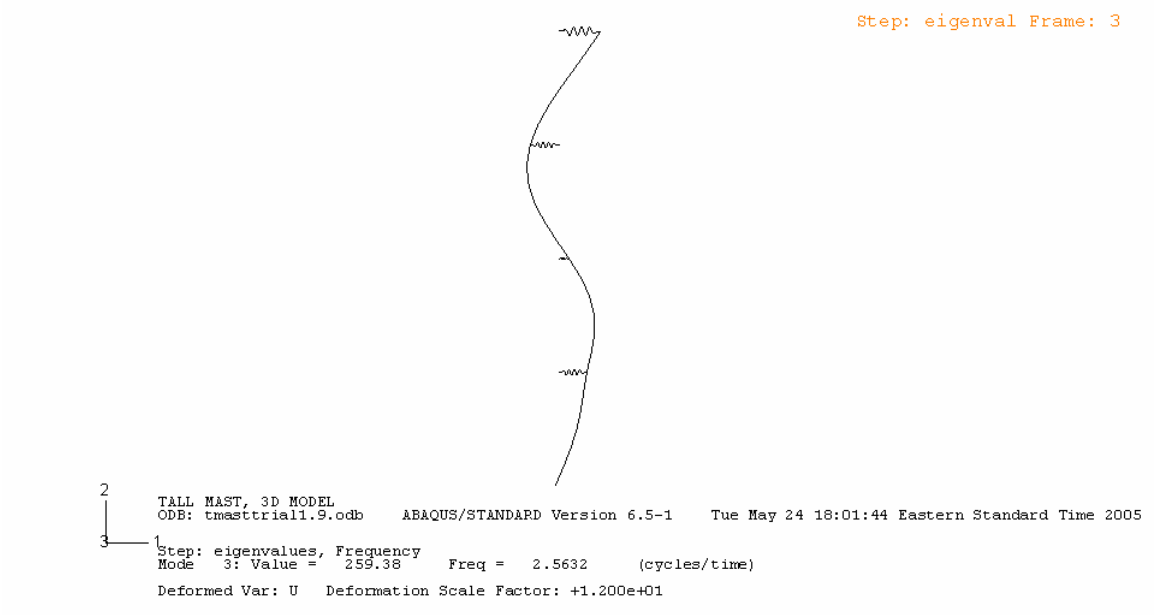

Figure 4.19 Third Bending Mode

The first and fourth modes were then used with Equation 2.3 to determine the parameters for Rayleigh damping that would approach 2% of critical damping in the mast for the first five modes. The values were found to be $\alpha_0 = 0.237$ and $\alpha_1 = 0.00140$. These damping values were held constant and included for all of the three-dimensional trials.

As addressed in the objective and scope of this research, parametric studies were performed on the tower. In addition to the mast presented, another shorter mast was also examined consisting of a 40 m tall mast and two guy levels. However, it did not experience large enough displacements under the seismic motions to exhibit slack behavior in the guys. Therefore this research will focus on the behavior of the 120-m-tall mast. A total of 38 trials was run on this mast model. Rope stiffness, rope pretension, mass and stiffness of the mast, and directionality of the input motion were varied. The cable stiffness, cable pretension, mast weight, and mast bending stiffness used in Desai and Punde (2001) were used as a guideline for developing reasonable structural properties for the parametric studies. Table 4.1 presents the important parameters for each of the trials. A notation with three identifiers separated by a dash is used for the trial names. The first represents the earthquake motion, N for Northridge and E for El Centro; the second represents the value of EA for the guys in N times 10^7; the third represents the

guy pretension in kN. Also, the detail about the values in mast properties and earthquake directions are included. The standard case of the guyed mast design is denoted with an asterisk; all of the trials are variations of the standard case. Also, an example input file is also included in Appendix B.

Table 4.1 Parameter Values for Three-Dimensional Trials

Trial Name	Input Motion	EA (N x 10^7)	Pretension (kN)	Mass (kg/m)	Mast Moment of Inertia (m^4)	Earthquake Direction
N-2-15	Northridge	2	15	60	1.8 x 10^{-3}	1
N-2-20	"	"	20	"	"	"
N-2-25	"	"	25	"	"	"
N-2-30	"	"	30	"	"	"
N-2-35	"	"	35	"	"	"
N-3-15	Northridge	3	15	60	1.8 x 10^{-3}	1
N-3-20	"	"	20	"	"	"
N-3-25 *	"	"	25	"	"	"
N-3-30	"	"	30	"	"	"
N-3-35	"	"	35	"	"	"
N-4-15	Northridge	4	15	60	1.8 x 10^{-3}	1
N-4-20	"	"	20	"	"	"
N-4-25	"	"	25	"	"	"
N-4-30	"	"	30	"	"	"
N-4-35	"	"	35	"	"	"
N-3-25-M1	Northridge	3	25	45	1.6 x 10^{-3}	1
N-3-25-M3	Northridge	3	25	75	2.0 x 10^{-3}	1
N-3-25-D2	Northridge	3	25	60	1.8 x 10^{-3}	2
N-3-25-D3	Northridge	3	25	60	1.8 x 10^{-3}	3
E-2-15	Amp. El Centro	2	15	60	1.8 x 10^{-3}	1
E-2-20	"	"	20	"	"	"
E-2-25	"	"	25	"	"	"
E-2-30	"	"	30	"	"	"
E-2-35	"	"	35	"	"	"
E-3-15	Amp. El Centro	3	15	60	1.8 x 10^{-3}	1
E-3-20	"	"	20	"	"	"
E-3-25 *	"	"	25	"	"	"
E-3-30	"	"	30	"	"	"
E-3-35	"	"	35	"	"	"
E-4-15	Amp. El Centro	4	15	60	1.8 x 10^{-3}	1
E-4-20	"	"	20	"	"	"
E-4-25	"	"	25	"	"	"
E-4-30	"	"	30	"	"	"
E-4-35	"	"	35	"	"	"
E-3-25-M1	Amp. El Centro	3	25	45	1.6 x 10^{-3}	1
E-3-25-M3	Amp. El Centro	3	25	75	2.0 x 10^{-3}	1
E-3-25-D2	Amp. El Centro	3	25	60	1.8 x 10^{-3}	2
E-3-25-D3	Amp. El Centro	3	25	60	1.8 x 10^{-3}	3

Chapter 5
Dynamic Test Results

5.1 Dynamic Tests

The seismic behavior of a 120-m-tall guyed mast was examined using the finite element program ABAQUS. Thirty-eight dynamic trials were performed with varied structural parameters in order to see the effects of those parameters on the dynamic response of the structure. The two ground motions used as input were characteristically different and thus the structure exhibited different responses to the loading; however, the trends in response can be compared in order to make general conclusions about the behavior.

A detailed description of the parameters for each trial was previously presented in Section 4.4. The nomenclature used in that section to denote the different trials was also used in the following presentation of the results. Additionally, N-2 denoted a set of trials under the Northridge input motion with EA = 2 x 10^7 N, whereas N-2-20 denoted the particular trial in that set where the guys were pretensioned to 20 kN. Response values were recorded at the quarter points of the mast (same as the guy levels); these were denoted as base and Points 1 to 4 progressing from the ground level up the mast where Point 4 is at the tip. The different degrees of freedom for response values were related to the direction of input motion: DOF1 was in the direction of the strong horizontal input, DOF2 was in the vertical direction, and DOF3 was in the direction of the other horizontal component.

Detailed dynamic behavior of the mast under the two different ground motions is discussed first. The focus of this research was the effect of the slack-taut behavior of the guys, and the majority of the analytical trials were aimed at examining this. Thus, the overall trends in peak response values are examined for the different levels of pretension (slackness) in Study 1. Finally, the trends regarding changes in mast properties (Study 2) and earthquake direction (Study 3) are presented.

5.2 Detailed Dynamic Behavior

In order to first understand how seismic motion affects the guyed mast, a description of the behavior over time is given for two specific trials. Both trial N-2-25 and trial E-2-25 are examined, the cases where Northridge and amplified El Centro ground motion inputs were applied to the same standard case of the model. The parameters for the models were the same for these two cases, and were in the middle of the ranges investigated. Therefore, while the dynamic behavior was nonlinear and dependent on several variables, these two trials provide a look at the behavior of the average structure in this investigation.

5.2.1 Behavior in Northridge Earthquake

The trials involving the Northridge earthquake were 20 seconds long, and the strongest motion occurred between about 3 and 10 seconds into the record. Input displacements at the Base, and displacements relative to the ground motion at Points 2 and 4, can be seen in Figures 5.1 through 5.6. The input displacements for both horizontal degrees of freedom were fairly similar in shape with different magnitudes. Displacements at Point 4 tended to be larger than those displacements at Point 2. However, there was a larger difference in the two magnitudes relating to DOF1. Of particular interest is the fact that maximum displacements in DOF3 were larger than in DOF1, even though the input motion had less energy. Also, the oscillation of the mast in DOF3 was much more consistent than that of DOF1 and approached almost periodic behavior. This would suggest that the mast response was being dominated by a particular bending mode in DOF3. Overall, the horizontal displacement of the mast was characterized by large motions coinciding with the strongest part of the ground motion and then the remaining oscillations slowly being damped out.

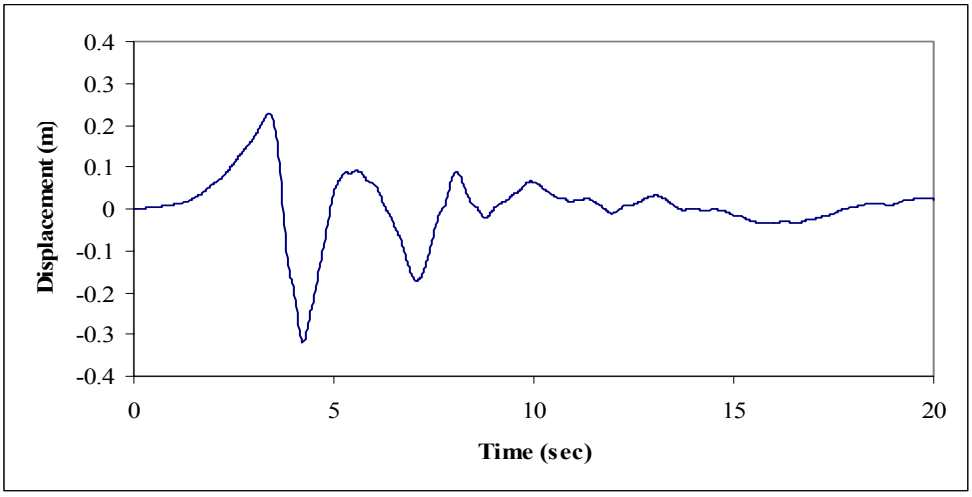

Figure 5.1 Displacement 1 at Base for N-3-25

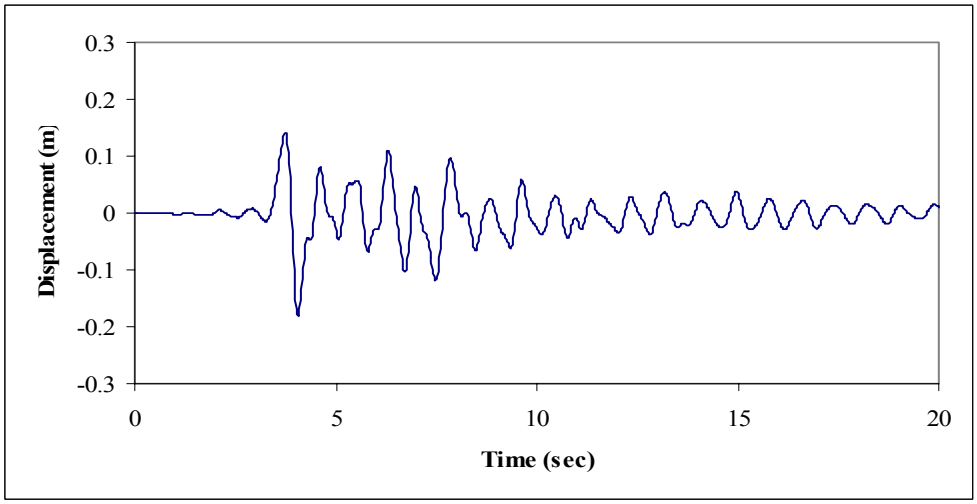

Figure 5.2 Displacement 1 at Point 2 for N-3-25

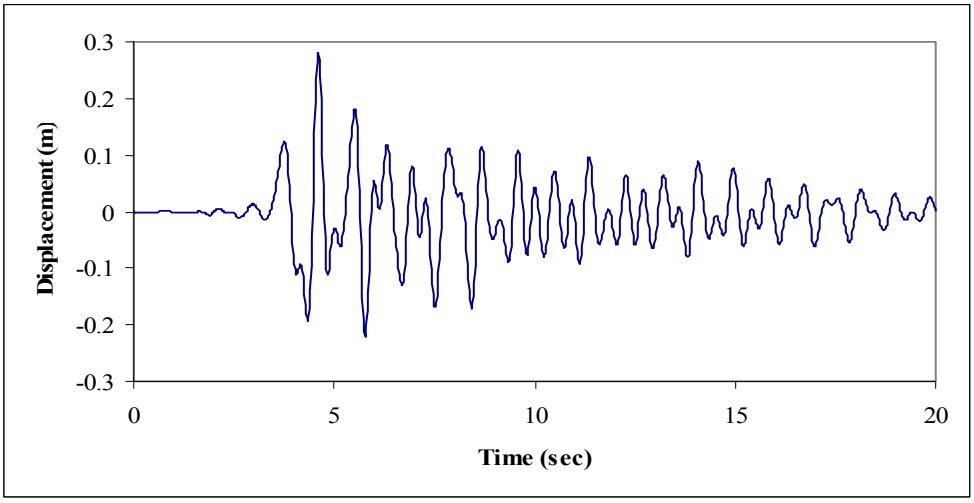

Figure 5.3 Displacement 1 at Point 4 for N-3-25

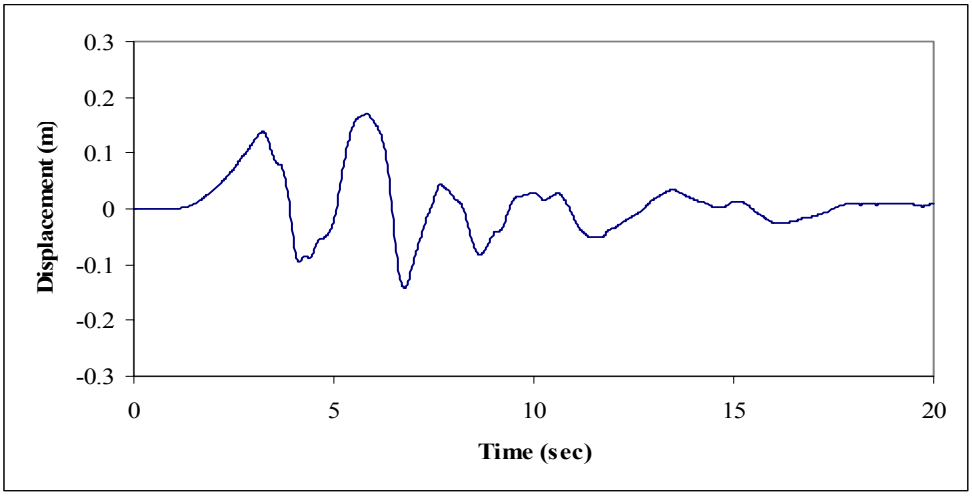

Figure 5.4 Displacement 3 at Base for N-3-25

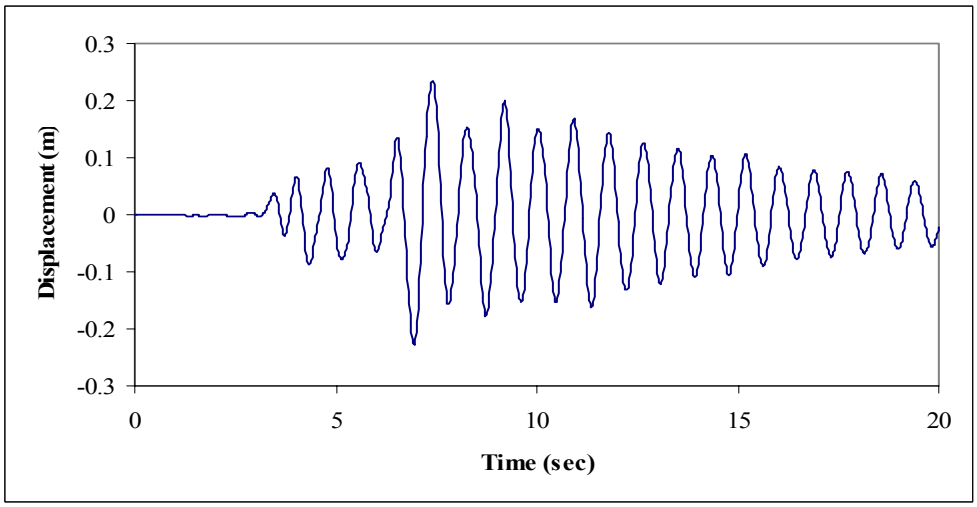

Figure 5.5 Displacement 3 at Point 2 for N-3-25

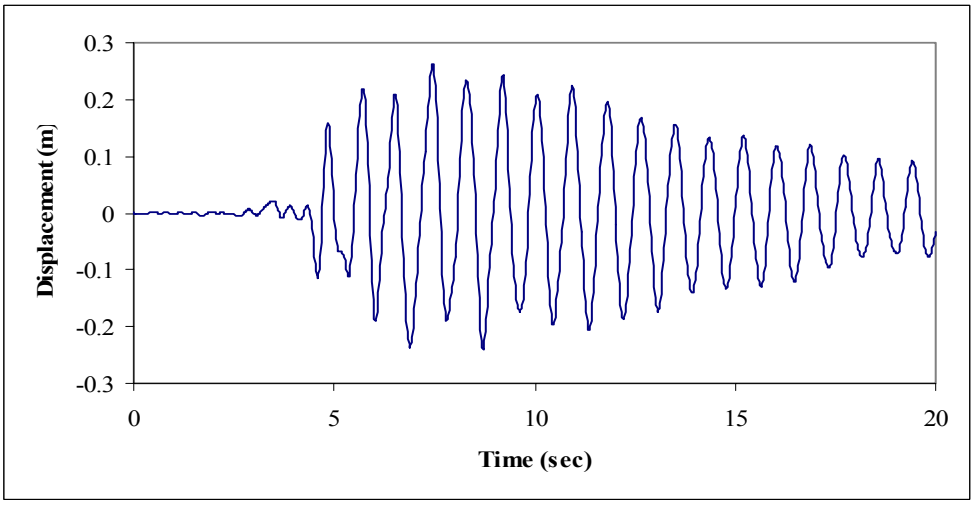

Figure 5.6 Displacement 3 at Point 4 for N-3-25

Since the displacement behavior was somewhat different at each guy level, it is easier to see the relationship between displacements at each guy level when plotted on top of each other. This is shown in Figures 5.7 and 5.8 for the time period of the strongest motion. Both directions were characterized by displacements at each height generally occurring in the same direction. However, there was much more variation in DOF1, which would indicate that some higher modes were actively involved in the response. Point 4 exhibited the highest peak value in Figure 5.7, and Point 3 in Figure 5.8.

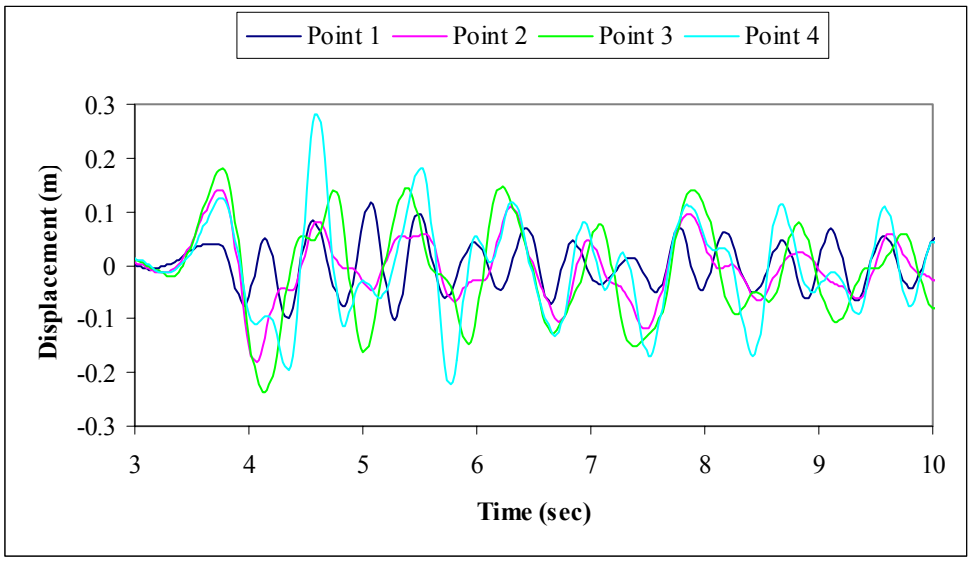

Figure 5.7 Displacement 1 for N-3-25

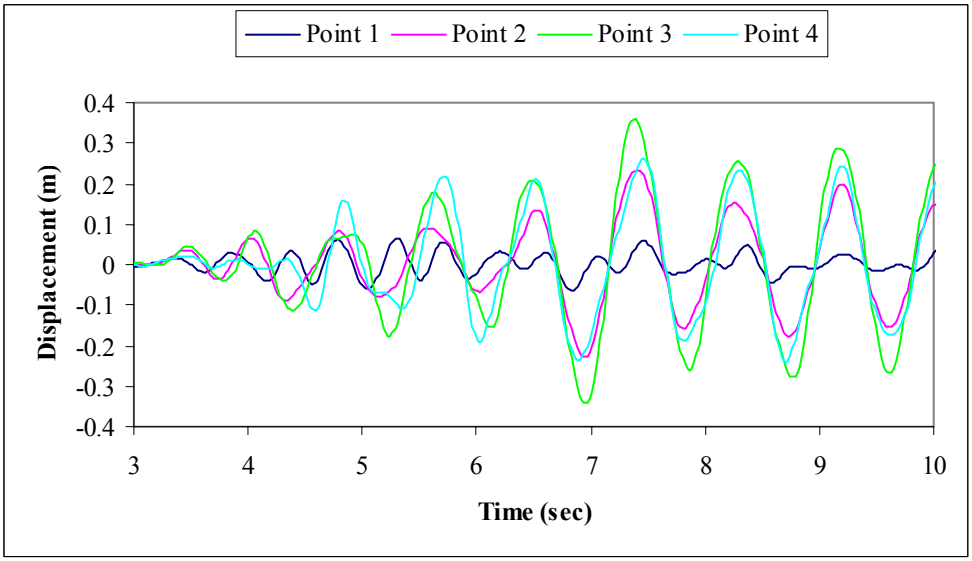

Figure 5.8 Displacement 3 for N-3-25

The bending moments at the guy levels are shown in Figures 5.9 and 5.10 for the period of strongest motion. The bending moments relating to motion in DOF1 showed significant variability and no particular trends. However, large moments at the first guy level relating to motion in DOF3 appeared after 6.5 seconds, possibly signaling a drastic change in the response of the mast in that direction.

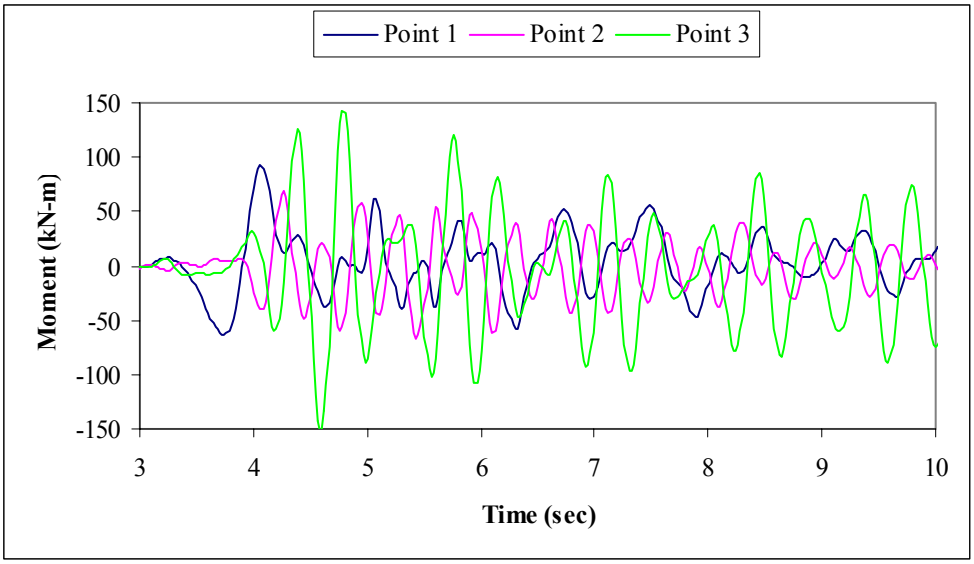

Figure 5.9 Bending Moment 1 for N-3-25

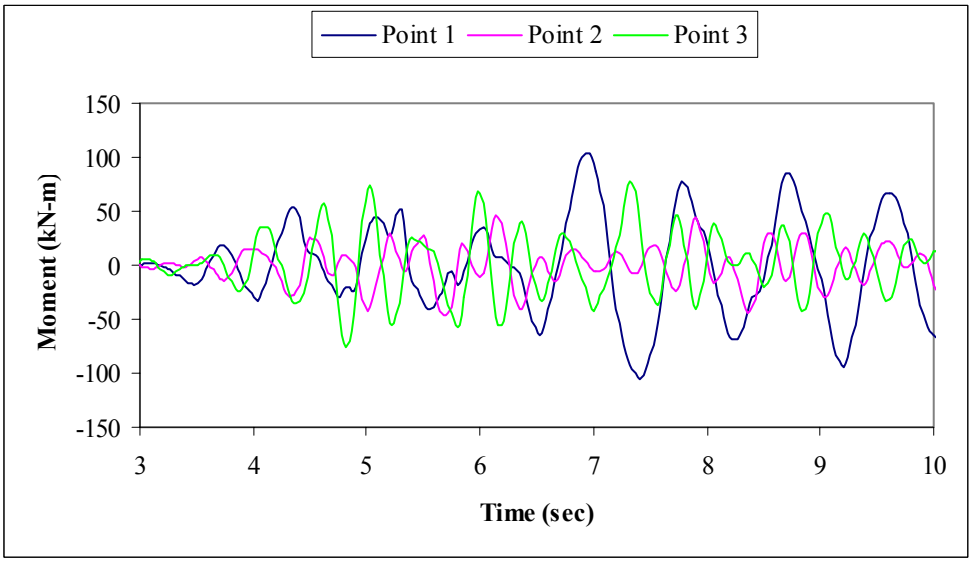

Figure 5.10 Bending Moment 3 for N-3-25

One of the main goals of this research was to look at the effect of snap loads, that is, when the guys become slack and then taut. It is of interest to this investigation to note that the distinct change in structural behavior in DOF3, as noted in Figures 5.8 and 5.10, coincided with a change in the guy behavior. Figure 5.11 shows the tension in one of the guys attached at Point 3. The tension in that guy went slack starting at about 6.5 seconds, the same time when the response changed. Thus, it appears that snap loads associated with slack-taut guy behavior can significantly alter the structural behavior.

Figures 5.12 and 5.13 show the response of all three guys at two different levels on the mast. It can be seen that guy tensions at the first guy level fluctuate at a higher frequency than at the other guy levels. In Figure 5.13, the specific guy presented in Figure 5.11 is shown in blue and another guy is shown in pink. These represent the two guys with components in DOF3 and both experience snap loads after about 6.5 seconds.

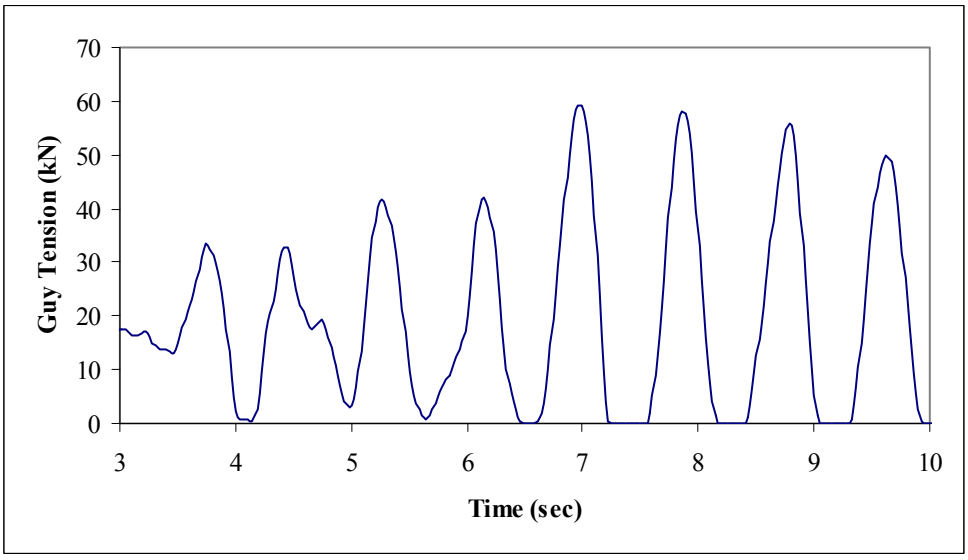

Figure 5.11 Guy Tension at Point 3 for N-3-25

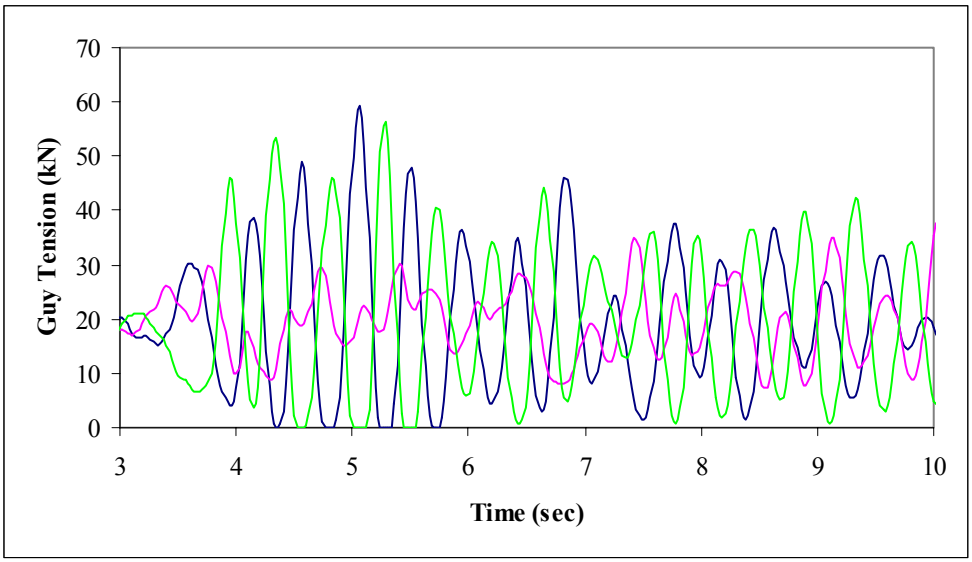

Figure 5.12 Guy Tensions at Point 1 for N-3-25

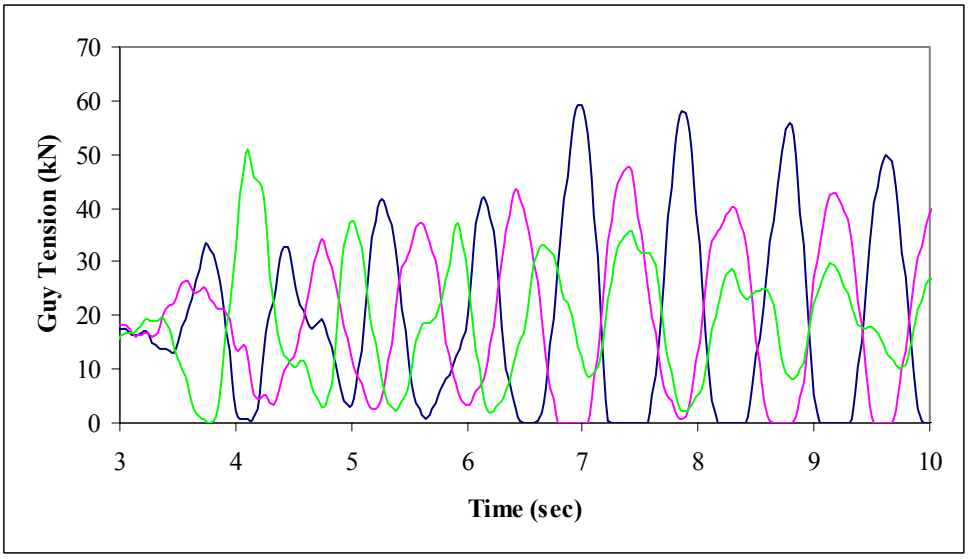

Figure 5.13 Guy Tensions at Point 3 for N-3-25

The dynamic response was highly nonlinear, so plots were created that show the displacement shapes of the mast as a progression over time. The numbers at the top of the graph correspond to the chronological sequence. Figures 5.14 and 5.15 show the bending shapes for both horizontal degrees of freedom in 0.25-second time increments running from 3.5 seconds to 6 seconds in the record. This corresponds to when the strong ground motion started. It can be seen that larger base displacements and higher bending modes were present in DOF1.

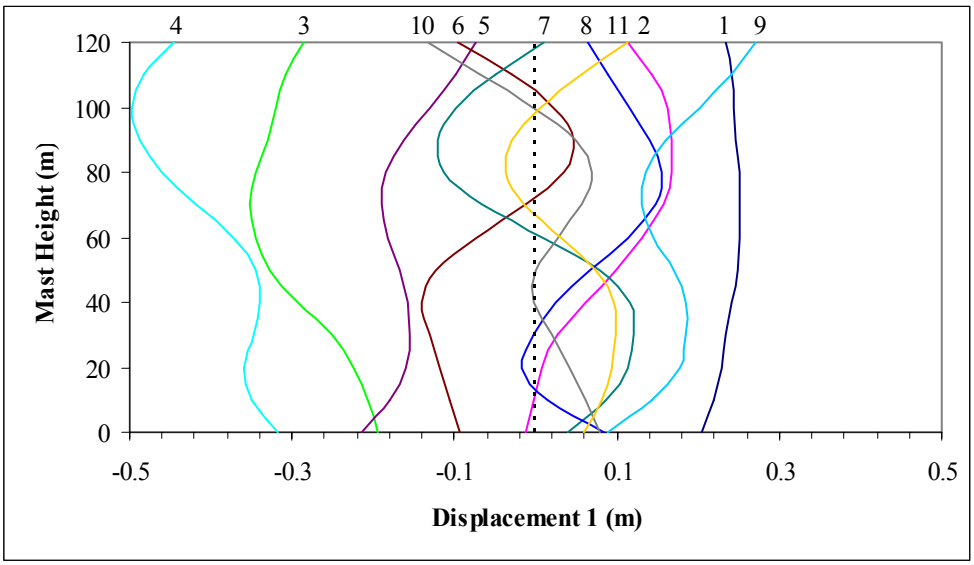

Figure 5.14 First Set of Displacement Shapes in DOF1 for N-3-25

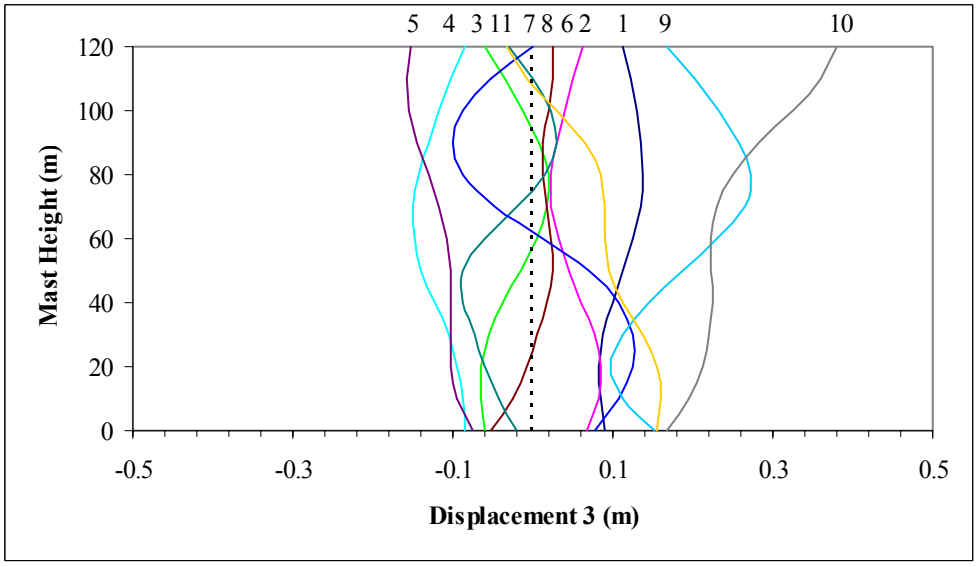

Figure 5.15 First Set of Displacement Shapes in DOF3 for N-3-25

Figures 5.16 and 5.17 show the displacement shapes of the mast starting at 7 seconds when the structural behavior started to change. These plots provide a look at the behavior for a duration of 1 second at smaller time increments of 0.1 seconds. There were obvious differences in the bending modes relating to each direction, and the displacements in DOF3 had a much more consistent shape.

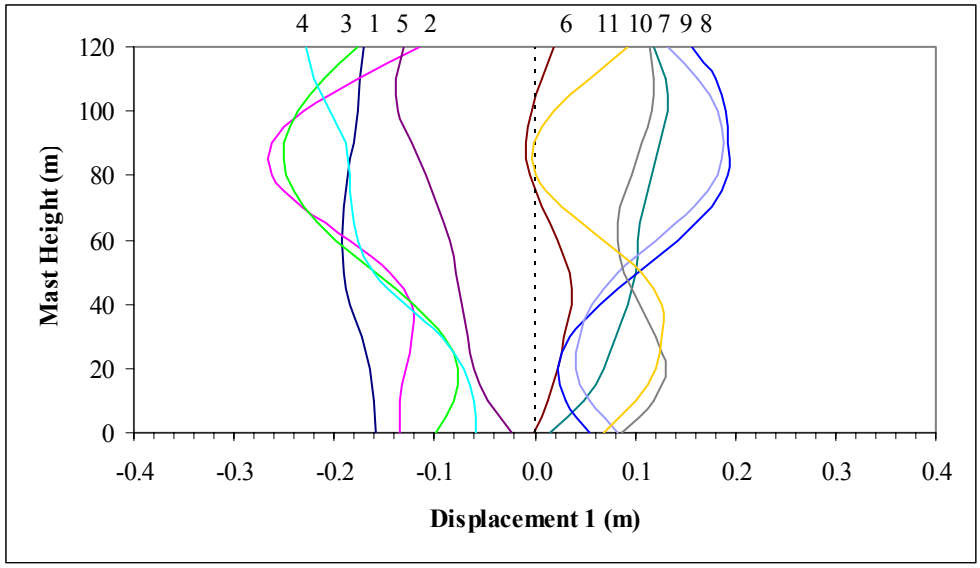

Figure 5.16 Second Set of Displacement Shapes in DOF1 for N-3-25

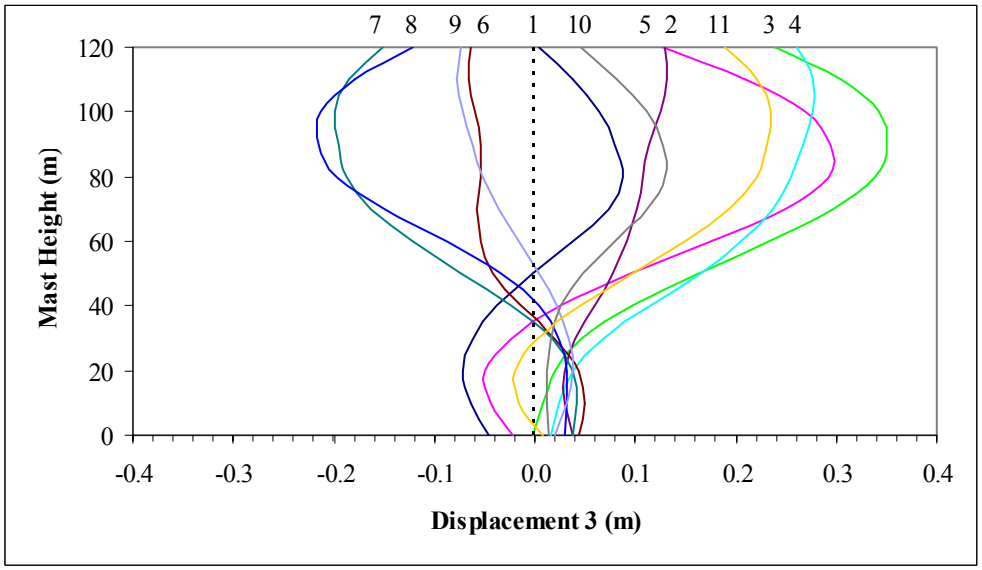

Figure 5.17 Second Set of Displacement Shapes in DOF3 for N-3-25

For a different comparison, the relative displacements of the mast are shown in Figures 5.18 and 5.19. These are presented for the same duration between 7 and 8 seconds in the record, with even smaller time increments to fully capture the displacement shapes during that time period. The displacements in DOF1 seemed to be a combination of the first three bending modes, while displacements in DOF3 were very similar to the first bending mode shown in Figure 4.16

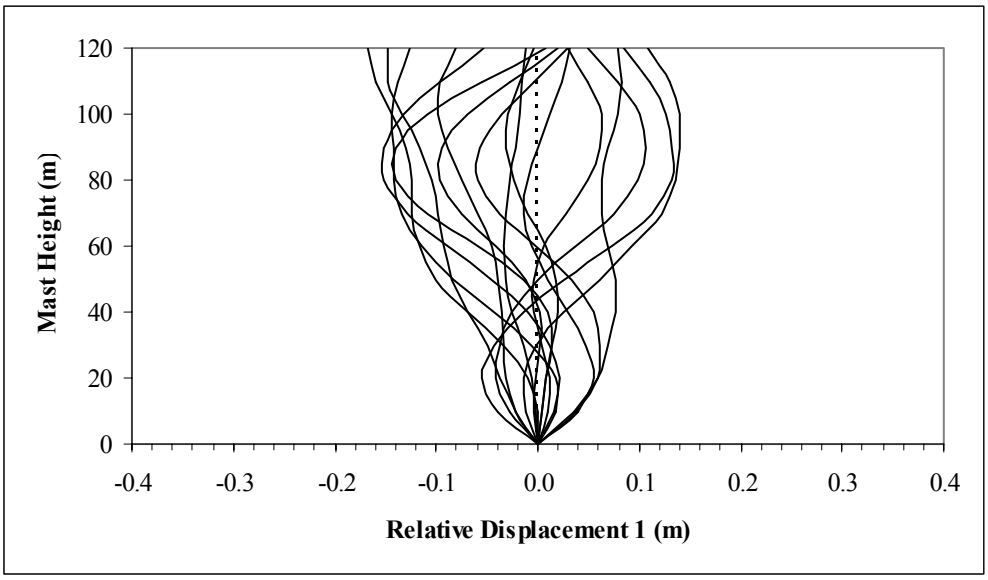

Figure 5.18 Relative Displacement Shapes in DOF1 for N-3-25

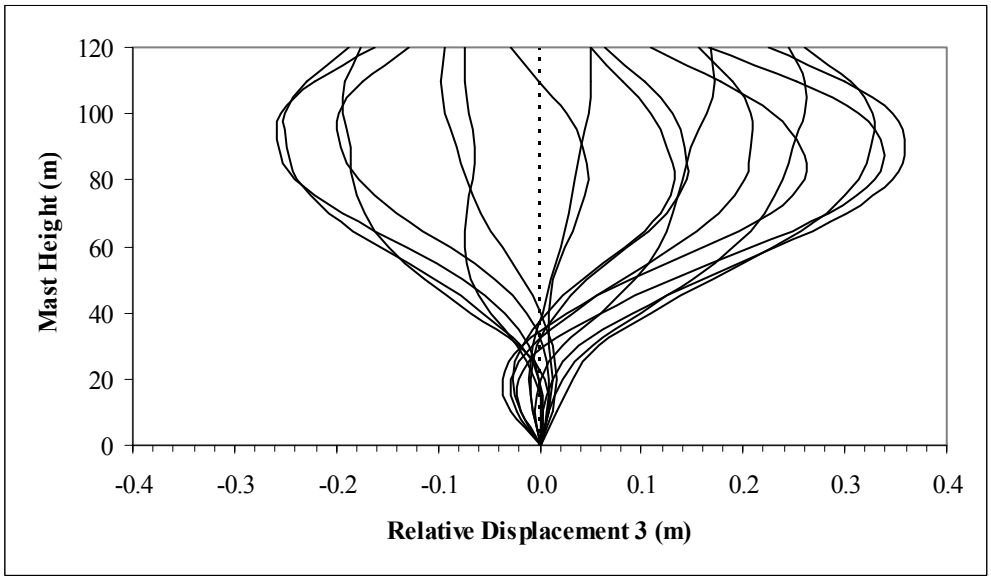

Figure 5.19 Relative Displacement Shapes in DOF3 for N-3-25

The response of the guyed mast in the vertical direction yielded some important results. Figure 5.20 shows the vertical displacement at Point 2 (this oscillated about a negative position due to compression of the tower from its original position due to self-weight and guy tension). Figure 5.21 shows the axial compressive force in the mast associated with that displacement. Thus, it can be seen that the dynamic component of axial force in the mast can be very significant, as was noted in Amiri (2002).

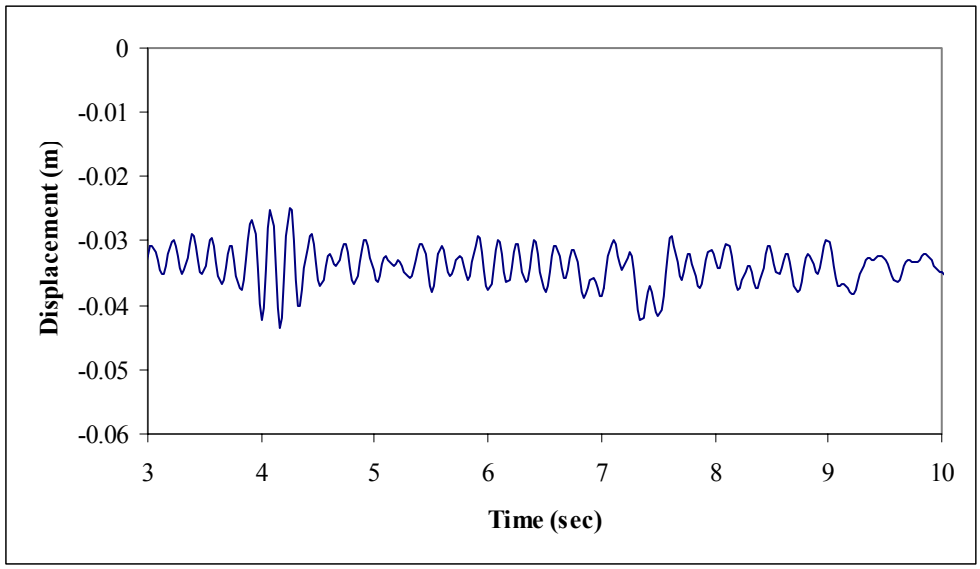

Figure 5.20 Displacement 2 at Point 2 for N-3-25

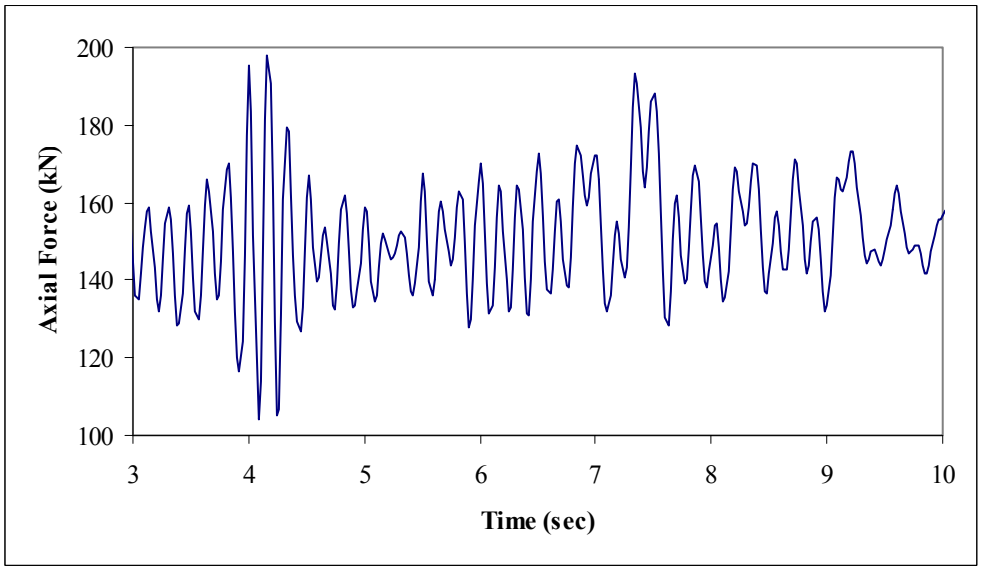

Figure 5.21 Axial Force in Mast at Point 2 for N-3-25

A graph of the base shear in DOF1 during the Northridge event can be seen in Figure 5.22. The total weight of the structure was about 70 kN, so the maximum base shear experienced was slightly larger than 20% of the structural weight. For towers taller than the one in this current investigation (150- to 350-m-tall), Amiri (2002) reported this value to be in the range of 40 to 80%.

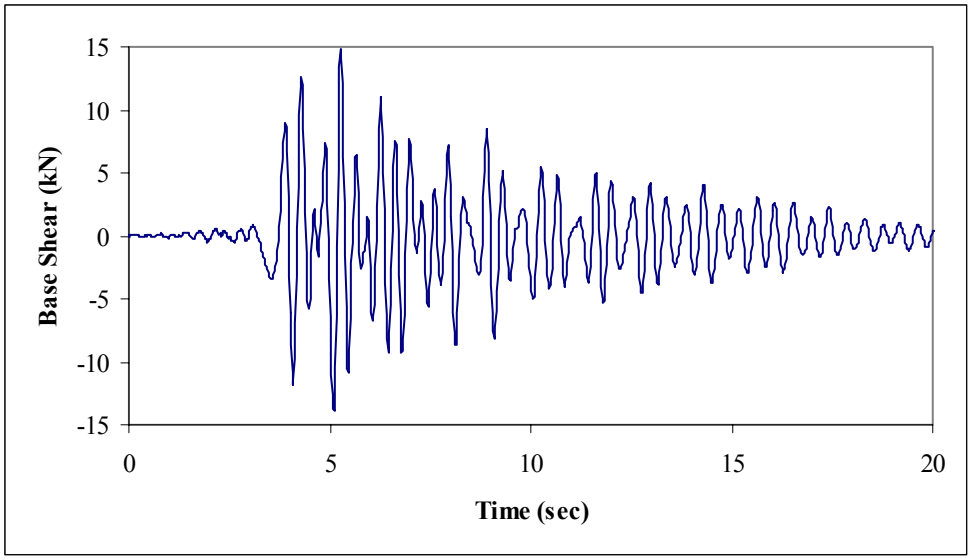

Figure 5.22 Base Shear 1 for N-3-25

5.2.2 Behavior in Amplified El Centro Earthquake

The trials involving the amplified El Centro earthquake experienced significant shaking for the majority of the 40 seconds of the record. The strongest shaking occurred in the first 20 seconds, and only the response during that period is presented to maintain clarity. Input displacements at the base, and displacements relative to the ground motion at Points 2 and 4, can be seen in Figures 5.23 through 5.28. The input motion was significantly different for the two horizontal degrees of freedom, and this resulted in much larger displacements in DOF1. As seen in the Northridge event, displacements at Point 4 were generally larger than the corresponding displacements at Point 2. Overall, the horizontal displacement of the mast was characterized by motions of a fairly consistent magnitude over the first 20 seconds of the response.

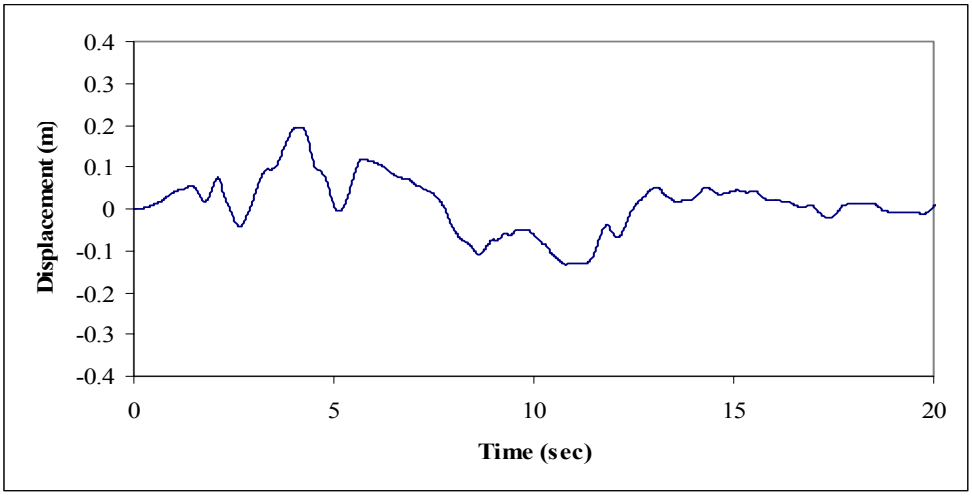

Figure 5.23 Displacement 1 at Base for E-3-25

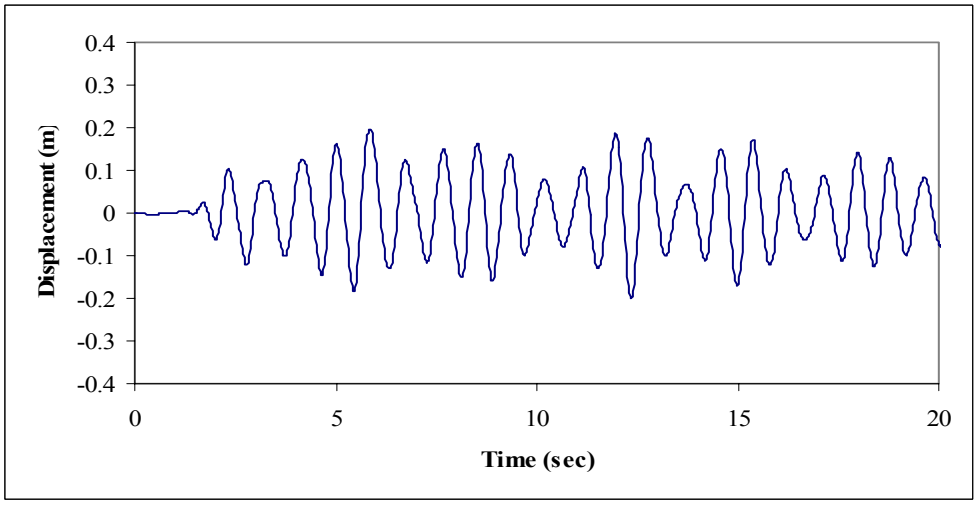

Figure 5.24 Displacement 1 at Point 2 for E-3-25

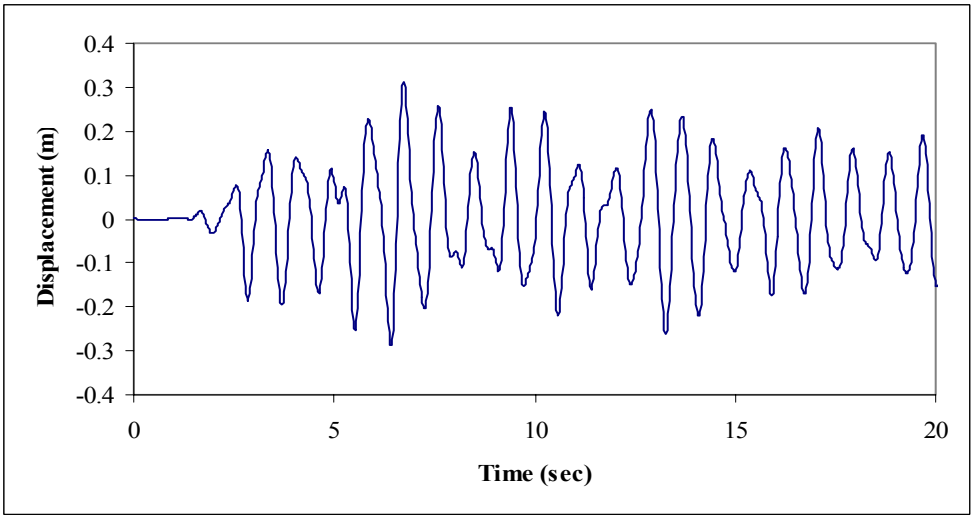

Figure 5.25 Displacement 1 at Point 4 for E-3-25

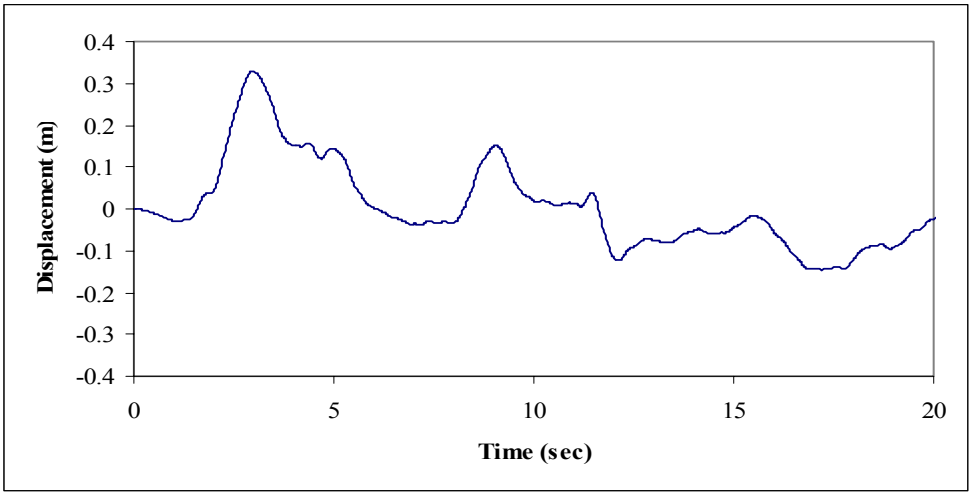

Figure 5.26 Displacement 3 at Base for E-3-25

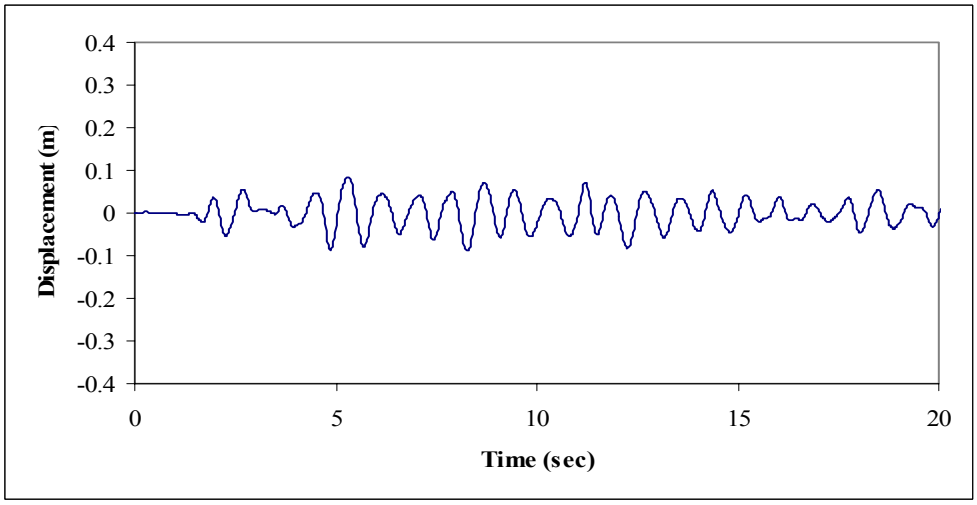

Figure 5.27 Displacement 3 at Point 2 for E-3-25

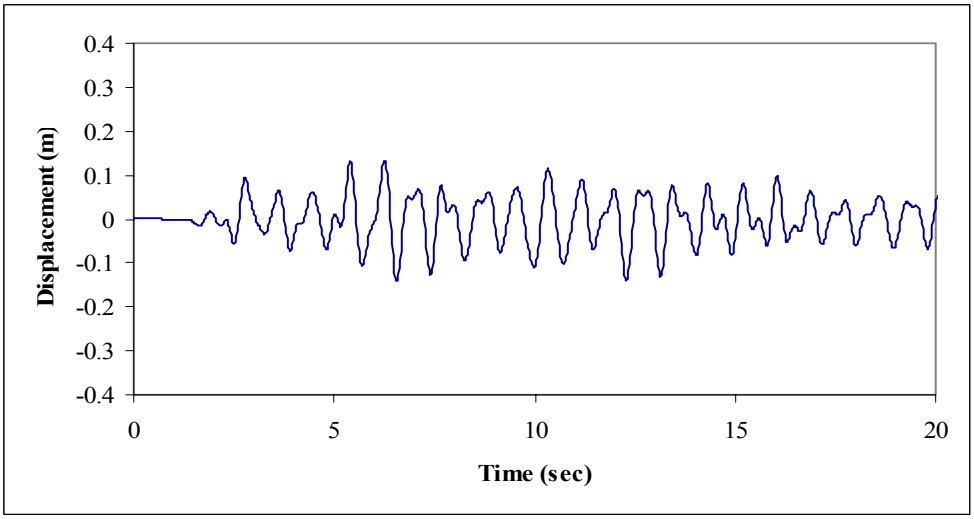

Figure 5.28 Displacement 3 at Point 4 for E-3-25

The displacement behavior at each guy level as a function of time is shown in Figures 5.29 and 5.30 for the first 10 seconds of motion. As seen in the previous plots, the displacements in DOF1 were much larger than those in DOF3. Neither direction exhibited any strong trends in behavior, and displacements at both Points 3 and 4 were comparable in magnitude and experienced peak values.

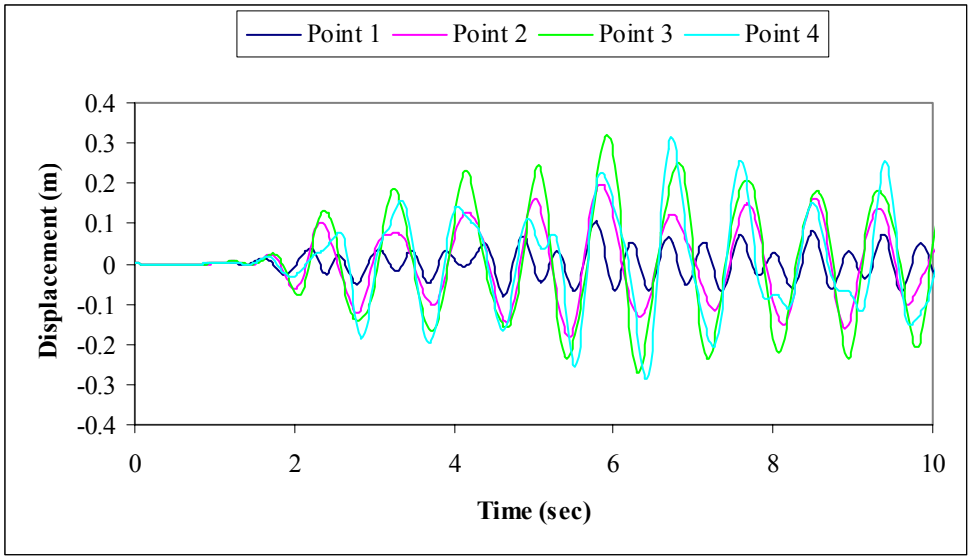

Figure 5.29 Displacement 1 for E-3-25

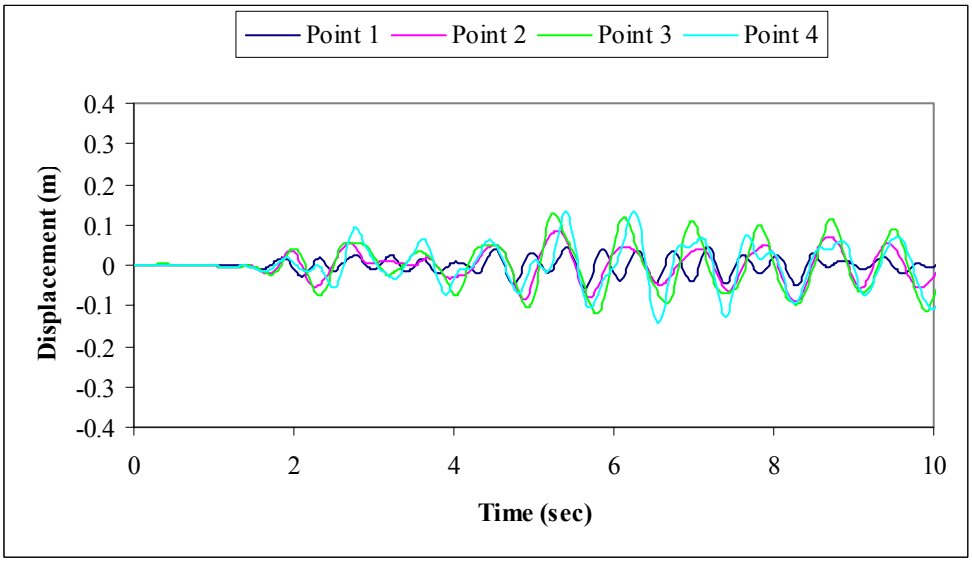

Figure 5.30 Displacement 3 for E-3-25

Figures 5.31 and 5.32 show the bending moments at the guy levels for the first 10 seconds of the earthquake record. The bending moments relating to motion in DOF1 were much larger than those in DOF3, as would be expected due to the larger displacements associated with DOF1. Additionally, the bending moments at each of the guy levels seemed to oscillate at different frequencies.

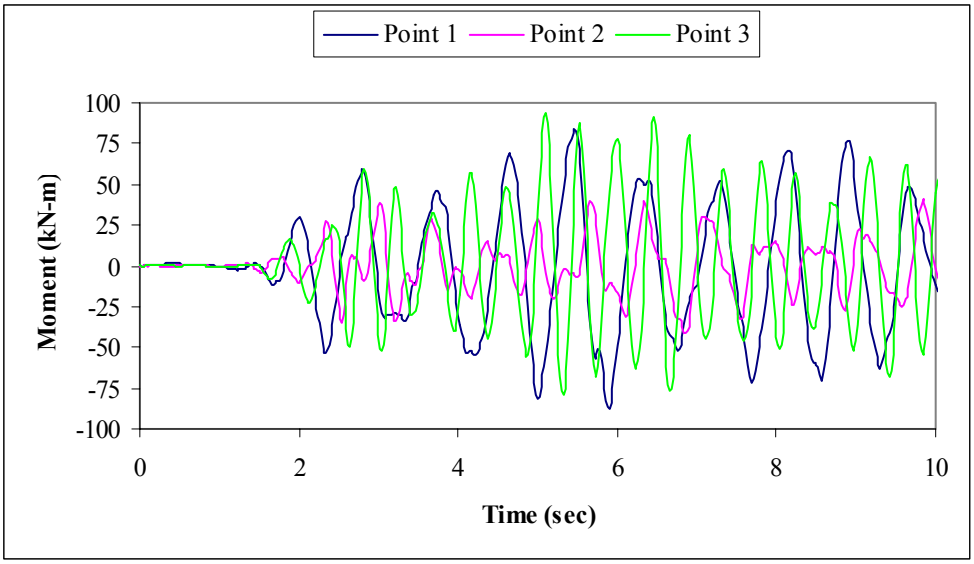

Figure 5.31 Bending Moment 1 for E-3-25

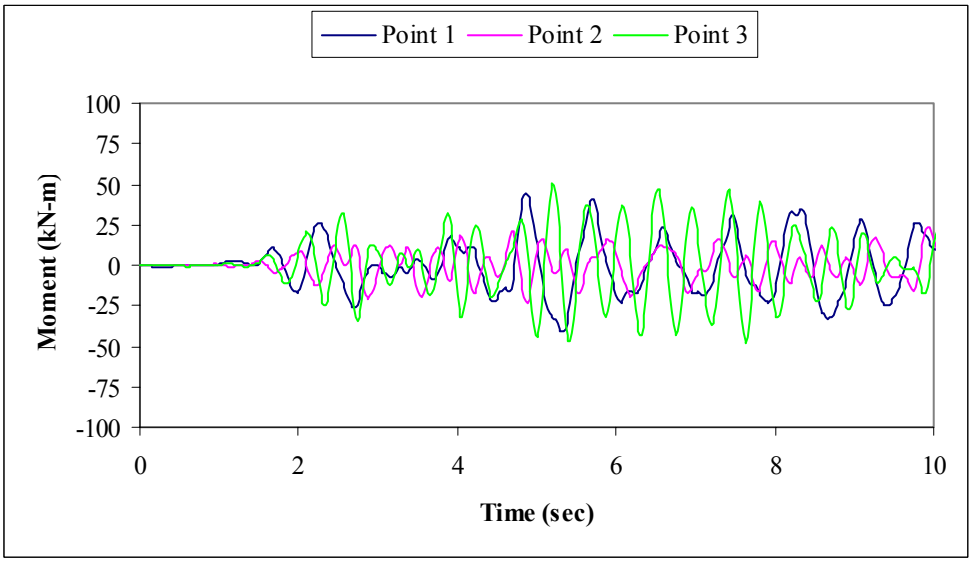

Figure 5.32 Bending Moment 3 for E-3-25

Figures 5.33 and 5.34 show the response of all three guys at two different levels on the mast. The guy tensions at the first level fluctuated at a higher frequency than at the other guy levels, as was seen in the Northridge earthquake. While there were some instances of slack guys at the first level, more slack-taut behavior occurred at the third guy level where there were much larger displacements.

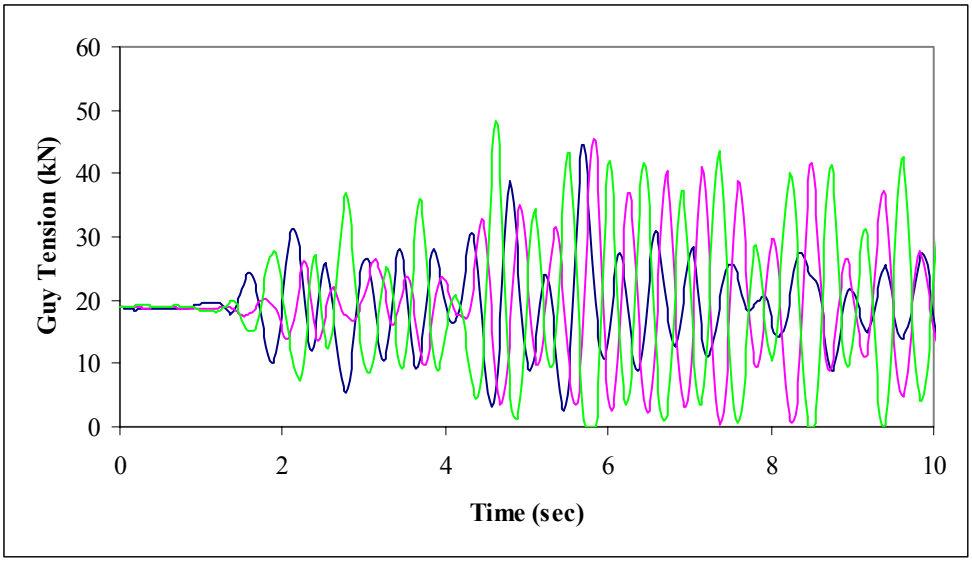

Figure 5.33 Guy Tensions at Point 1 for E-3-25

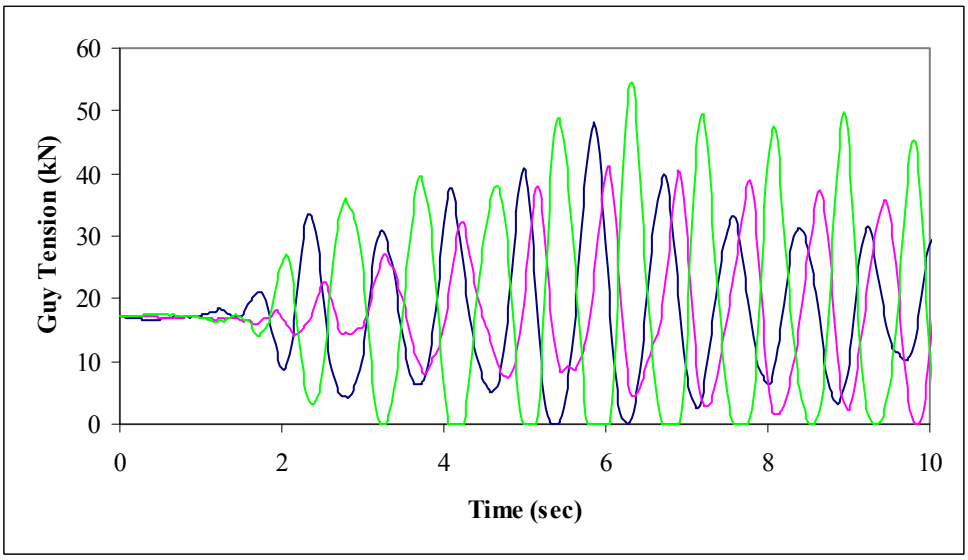

Figure 5.34 Guy Tensions at Point 3 for E-3-25

The response of the guyed mast in the vertical direction during the El Centro earthquake was not as severe as the response associated with the large vertical component in the Northridge earthquake. Figure 5.35 shows the vertical displacement at Point 2 and Figure 5.36 shows the axial compressive force in the mast associated with that displacement. While the dynamic component of axial force in the mast was not as large as that seen in Northridge event, it was still significant.

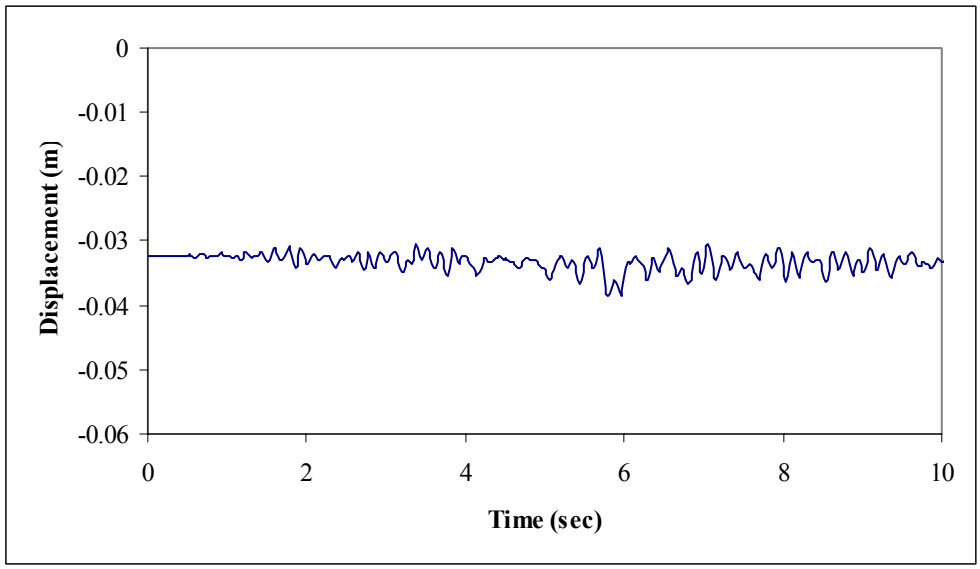

Figure 5.35 Displacement 2 at Point 2 for E-3-25

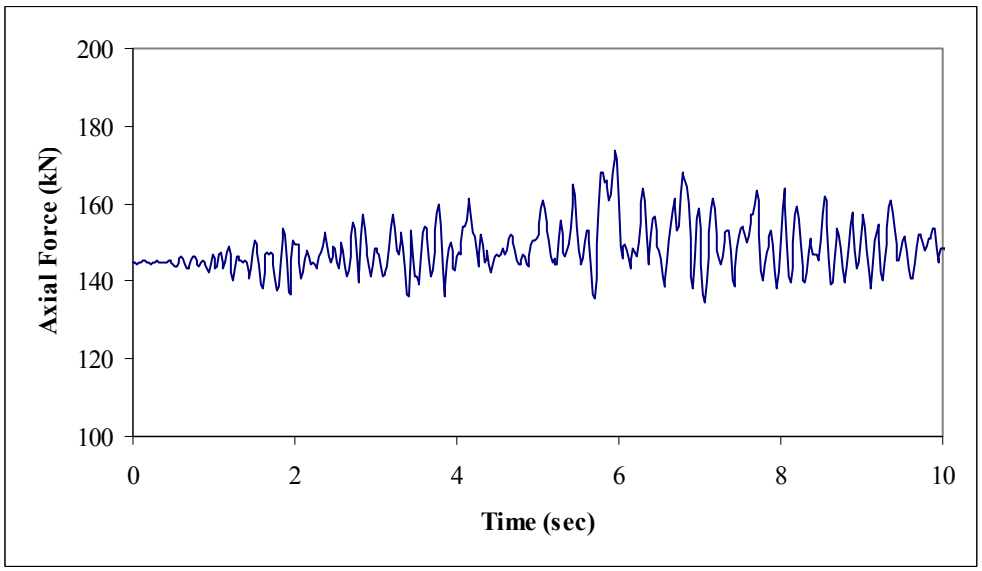

Figure 5.36 Axial Force in Mast at Point 2 for E-3-25

Figure 5.37 shows the base shear in DOF1 during the El Centro event. The maximum base shear experienced was slightly smaller than that recorded in the Northridge event, and corresponded to about 15% of the weight of the structure.

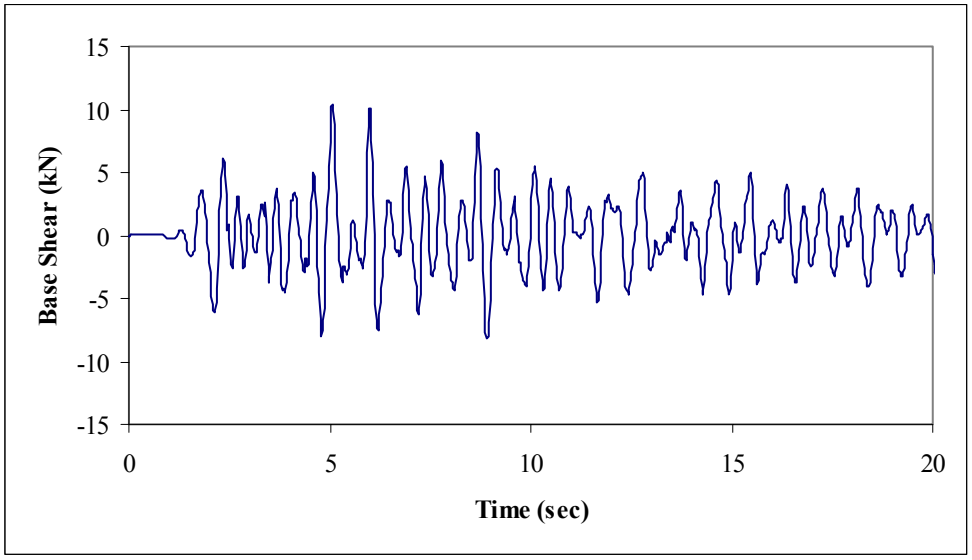

Figure 5.37 Base Shear 1 for E-3-25

5.3 Study 1: Trends Regarding Pretension

The main focus of this investigation was to examine the behavior of guyed towers and the influence of snap loads due to slack-taut action in the guys. This section attempts to cover the trends that were seen in this behavior, and the results are graphed as a function of pretension, which is directly related to slackness. Three guy stiffnesses were examined, and these are each graphed as a series. All of the response values calculated were the absolute values of the peak response. Similar behavior was seen in both horizontal directions, therefore results are presented mainly involving the response in DOF1.

Displacements were generally reduced with increased guy pretensions and increased guy stiffnesses. Figures 5.38 through 5.41 show the absolute values of maximum relative displacement of DOF1 at each of the guy levels for the three values of *EA* in both earthquakes: 2 x 10^7 N, 3 x 10^7 N, and 4 x 10^7 N. The trend of decreasing displacements was more noticeable in the upper guy levels.

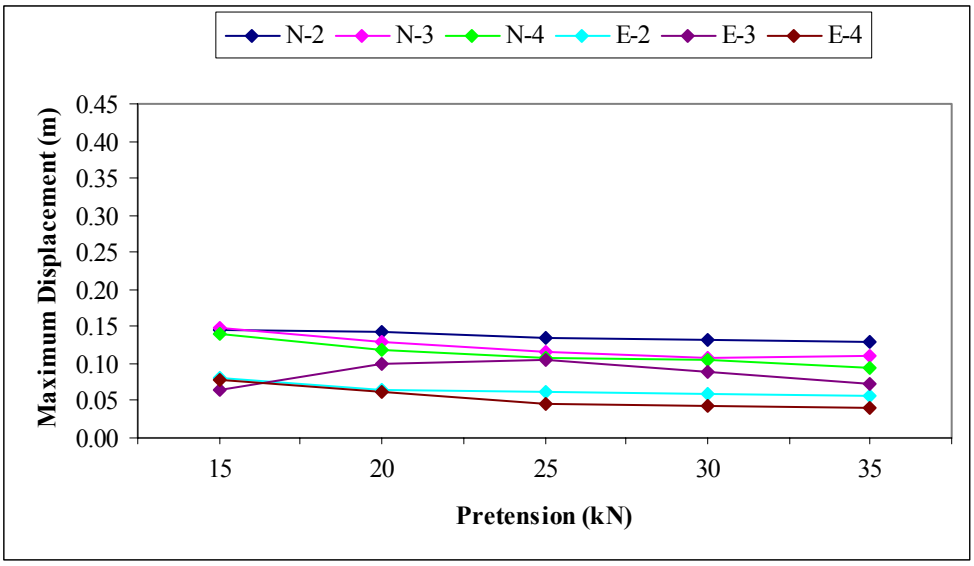

Figure 5.38 Displacement 1 at Point 1 for Study 1

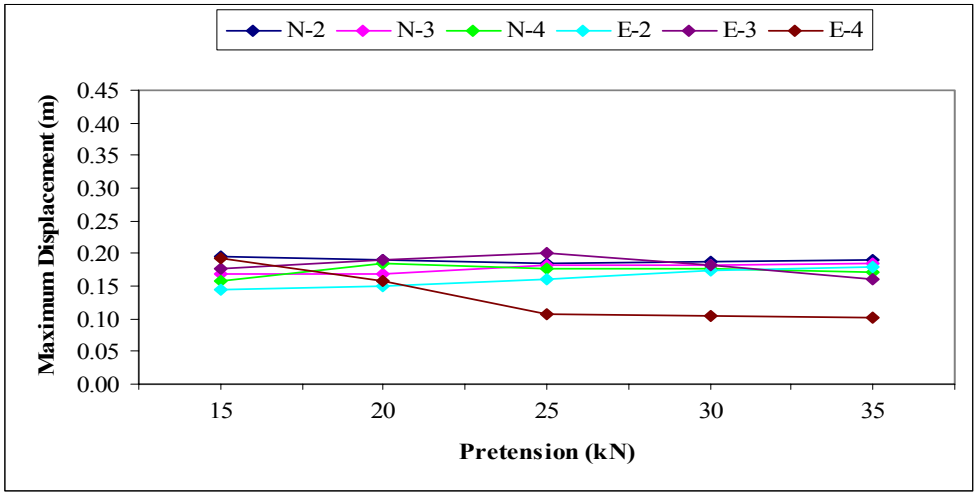

Figure 5.39 Displacement 1 at Point 2 for Study 1

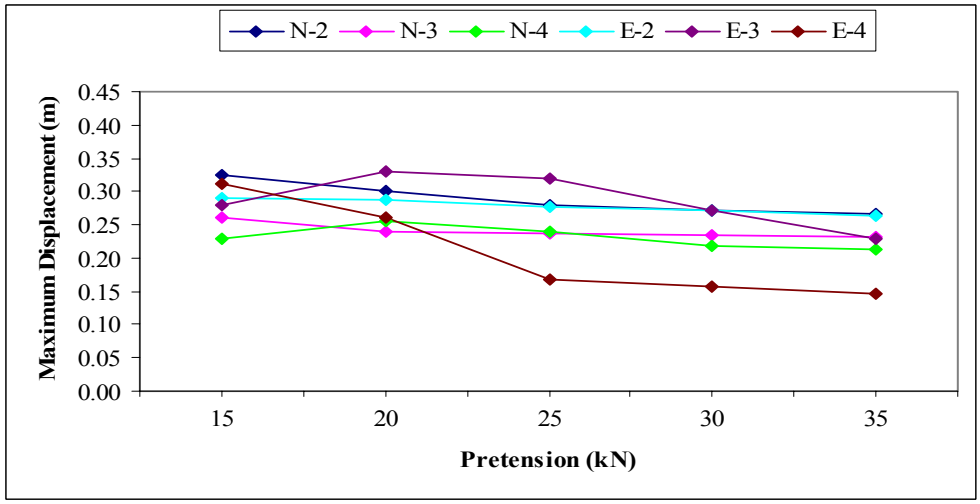

Figure 5.40 Displacement 1 at Point 3 for Study 1

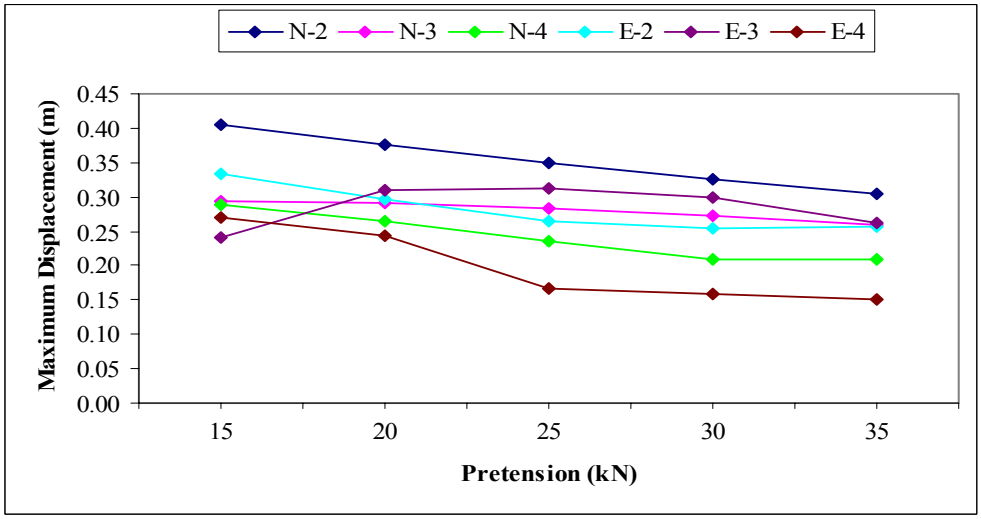

Figure 5.41 Displacement 1 at Point 4 for Study 1

The displacements in DOF3 showed the same general trend of decreasing with pretension. However, the displacements at mid-level on the mast did not entirely follow that same trend. This can be seen in Figures 5.42 and 5.43, which show the maximum displacements at Point 2 and Point 4. This also suggests that different behaviors dominate response in the two horizontal directions.

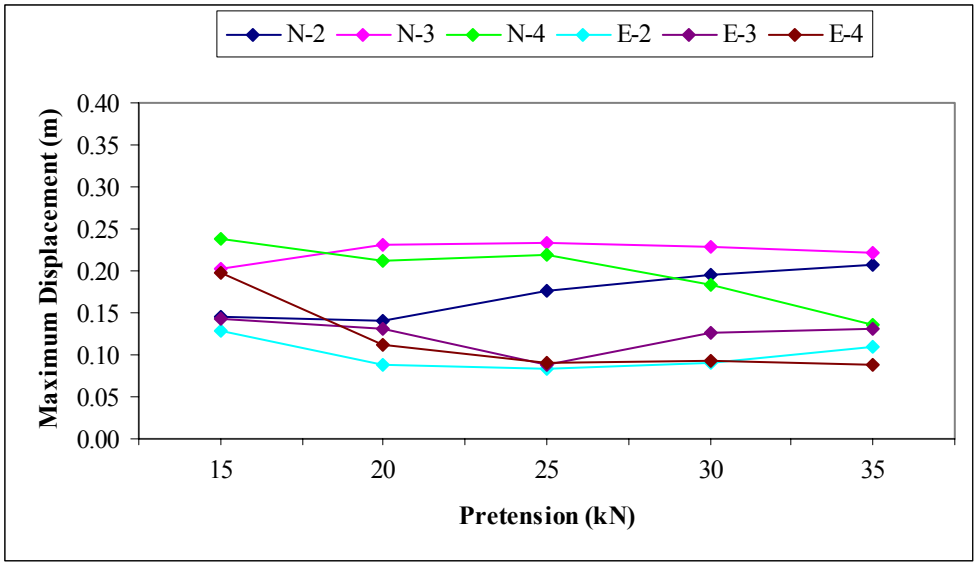

Figure 5.42 Displacement 3 at Point 2 for Study 1

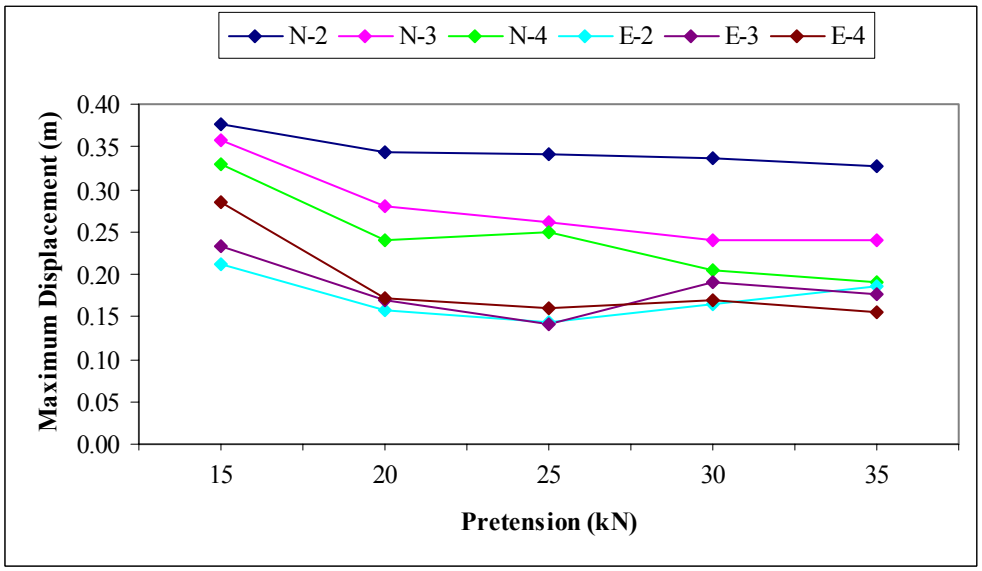

Figure 5.43 Displacement 3 at Point 4 for Study 1

The maximum vertical displacement at Point 2 increased in magnitude almost linearly with increased pretension, as can be seen in Figure 5.44. This behavior occurred at all levels of the mast, and is most likely a direct result of higher pretensions inducing larger compressive forces in the mast.

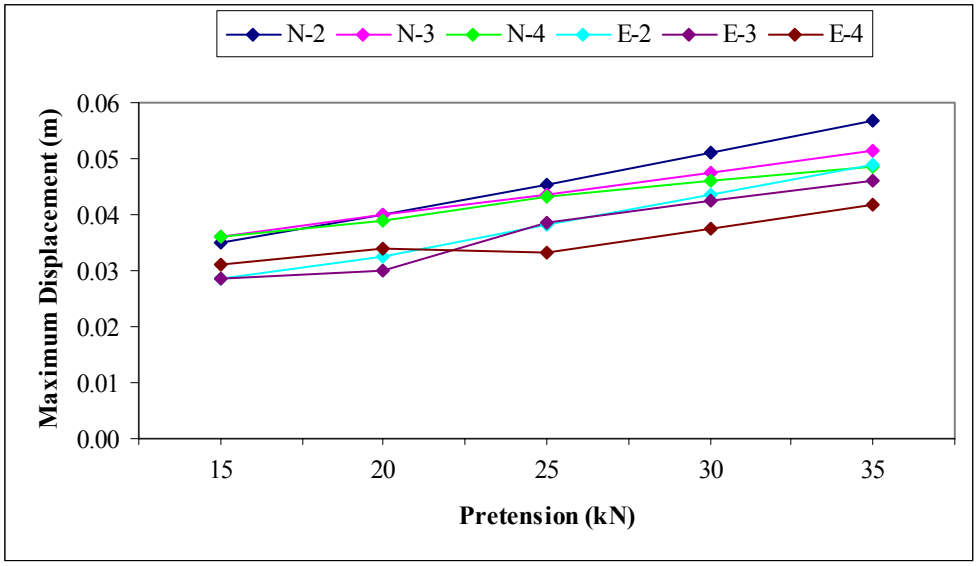

Figure 5.44 Displacement 2 at Point 2 for Study 1

Bending moments at the lowest guy level are shown in Figures 5.45 and 5.46. Both directions of bending exhibited some slight downward trends. Additionally, the bending moments at the other two internal points along the length of the mast were examined. On the whole, the bending moments seemed to decrease with increased pretension, but this was not an overly strong trend at any of the guy levels.

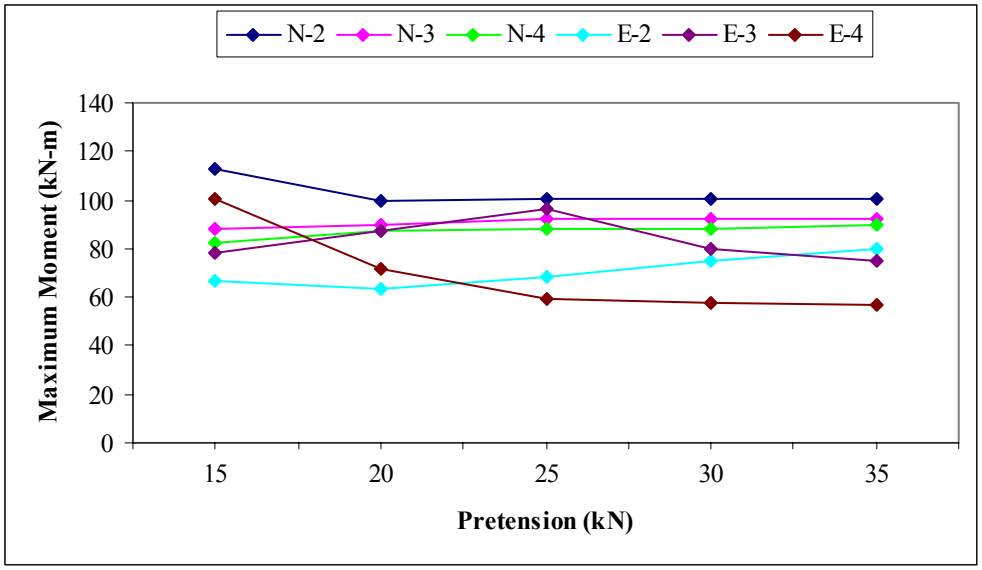

Figure 5.45 Bending Moment 1 at Point 1 for Study 1

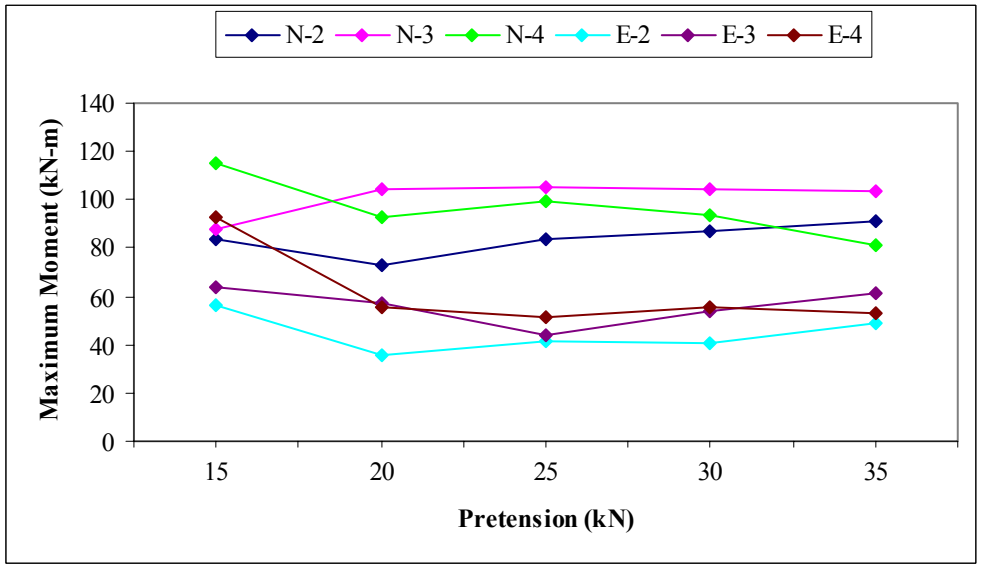

Figure 5.46 Bending Moment 3 at Point 1 for Study 1

Figure 5.47 shows the maximum guy tensions in all 12 guys for the N-3 series. They are grouped according to guy level, where the first number represents the point at which they are connected to the mast. The behavior regarding maximum guy tensions varied significantly between the different trials. There was an overall trend that maximum guy force increased with pretension, but this was not always true. Specifically, two of the guys at the first level had approximately the same maximum tension even when the pretension force was doubled. Similar trends in guy tension were also seen when the mast was subjected to the El Centro earthquake. Additionally, maximum guy force were recorded up to 400% of the initial pretension, verifying the results presented in Amiri (2002).

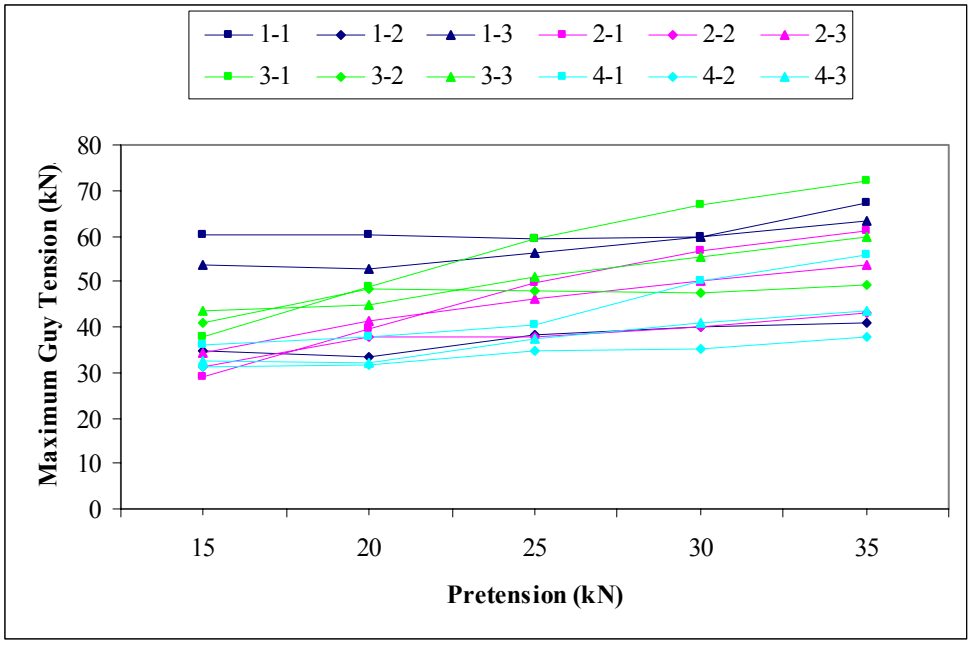

Figure 5.47 Guy Tensions for N-3 Study 1

The results showed that base shears in the guyed mast were not greatly affected by the amount of pretension present in the guys. While there was no noticeable trend for DOF1, there was a slight decrease in base shear associated with DOF3. These results are shown in Figures 5.48 and 5.49.

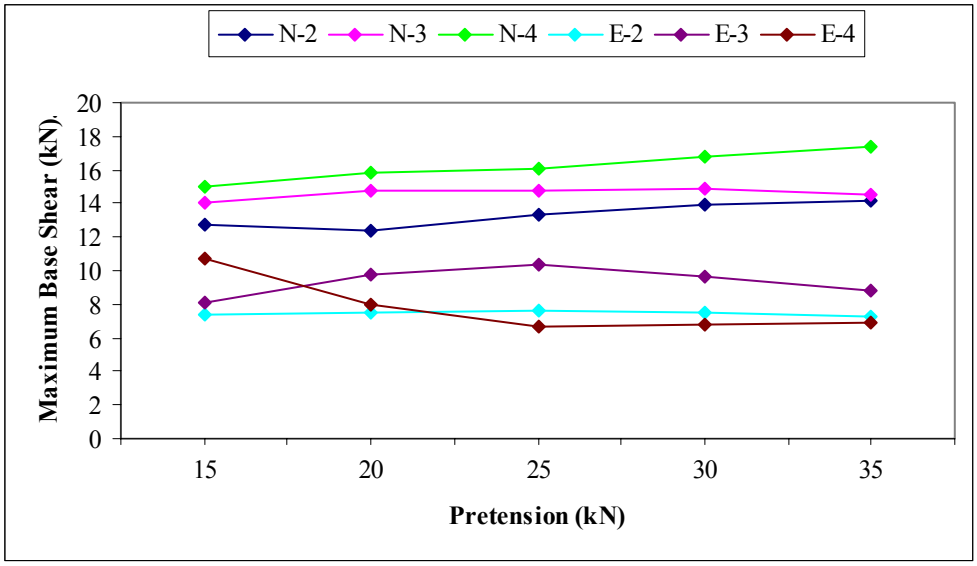

Figure 5.48 Base Shear 1 for Study 1

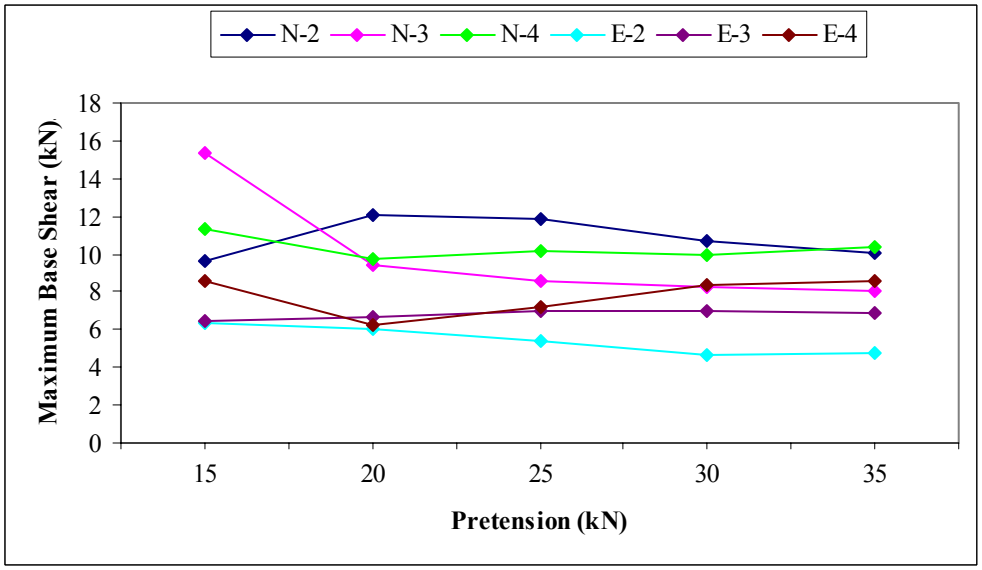

Figure 5.49 Base Shear 3 for Study 1

5.4 Study 2: Trends Regarding Mast Properties

Several additional trials examined the effect of different mast properties on the behavior of the structure. Stiffness and mass were varied together, as noted in Section 4.4. It was seen that the response seemed to be dominated by the increased mass as opposed to the increased stiffness. Figures 5.50 and 5.51 show the maximum displacements in DOF1 for both of the input motions. These trials usually exhibited increased displacements with increased mass, as would normally be associated with the larger inertial forces. However, the El Centro trials showed a decrease in displacements with the heaviest mast.

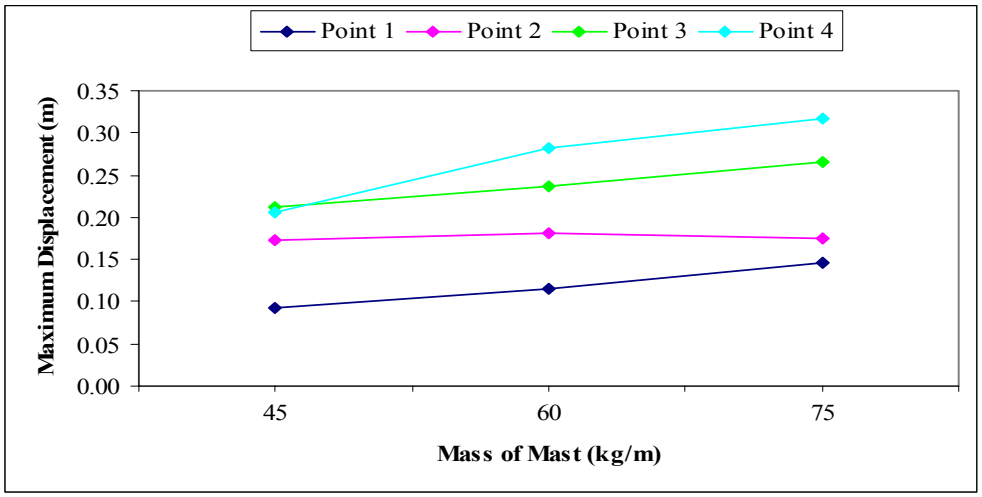

Figure 5.50 Displacement 1 for Northridge Study 2

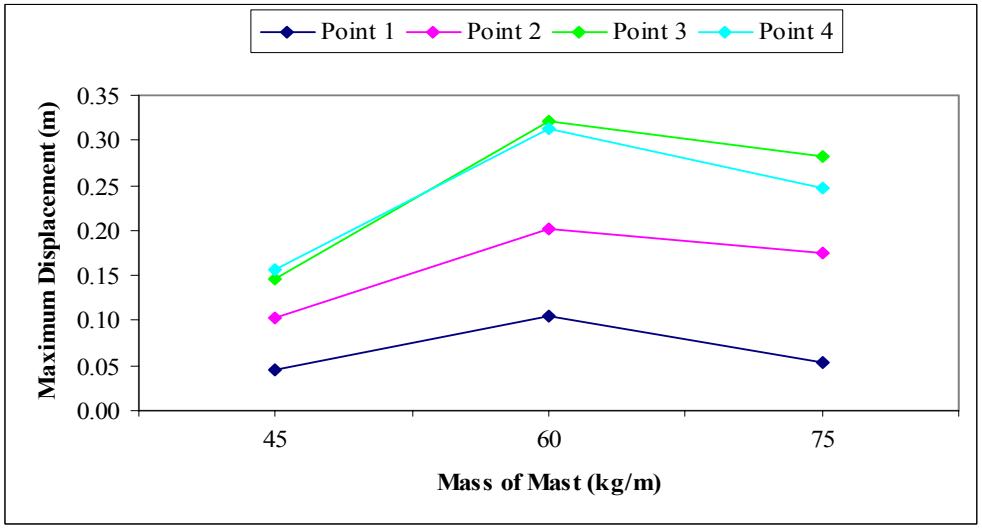

Figure 5.51 Displacement 1 for El Centro Study 2

Overall, the bending moments and base shears also exhibited increased values due to the larger inertial forces associated with increased mass. Figure 5.52 shows the maximum bending moments at Points 1, 2, and 3, and Figure 5.30 shows the two components of base shear.

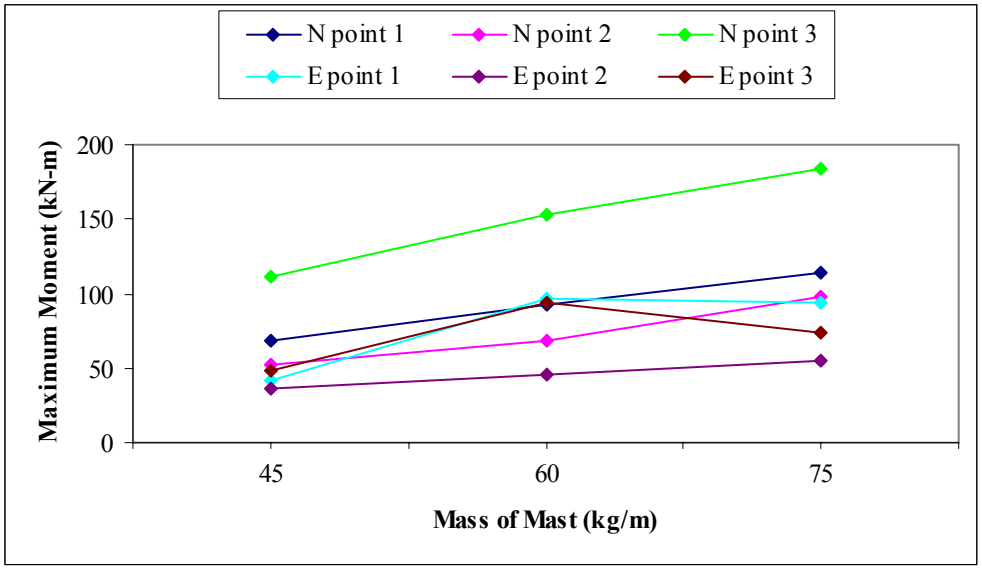

Figure 5.52 Bending Moment 1 for Study 2

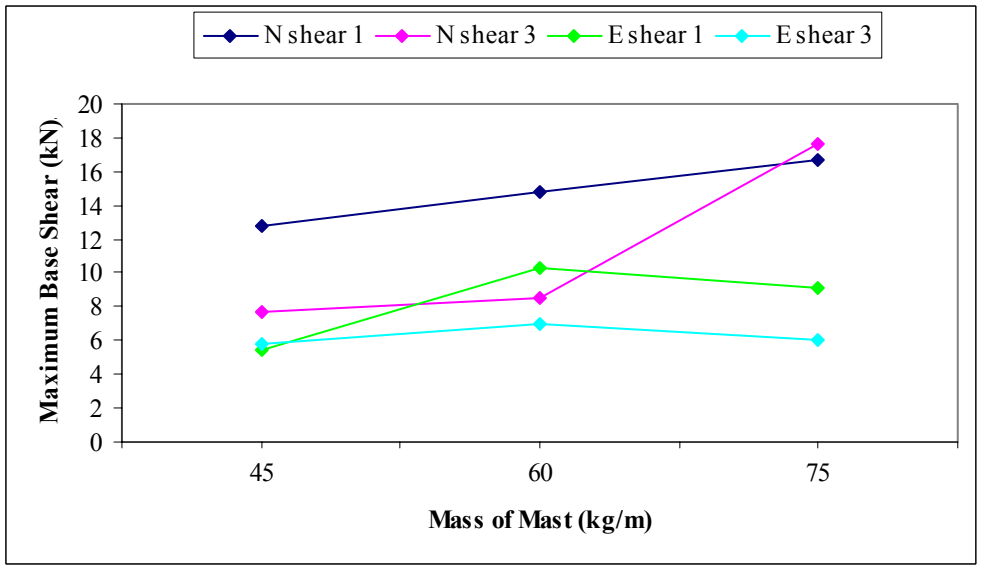

Figure 5.53 Base Shears 1 and 3 for Study 2

5.5 Study 3: Trends Regarding Earthquake Direction

It is rare that real, three-dimensional ground motion input is used in the analysis of structures. This investigation attempted to see the effects of three-dimensional motion and varied the horizontal direction of input in order to examine this. Section 4.2 addresses the different orientations that were used, and a copy of the figure presented there is shown in Figure 5.54. The degrees of freedom always remained coordinated with the two components of ground motion, and the structure itself rotated in the model space. As can be seen in the following representative graphs, the direction of loading (or angle of incidence) had a negligible effect on the behavior of the structure in most instances. All of the response values examined showed no strong trends. Figures 5.55 through 5.58 show the maximum horizontal displacements as a function of input direction. The bending moments at the different guy levels can be seen in Figure 5.59, and the base shears can be seen in Figure 5.60.

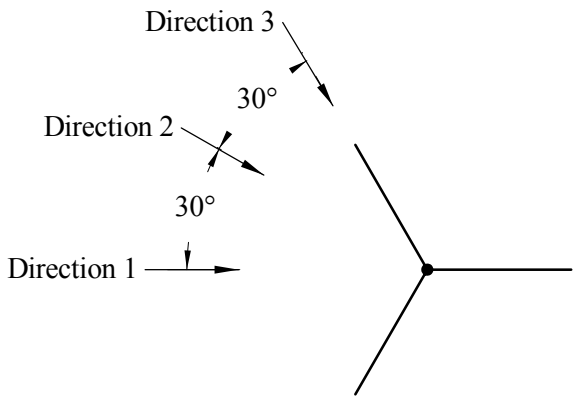

Figure 5.54 Plan View of Directions of Strongest Earthquake Input

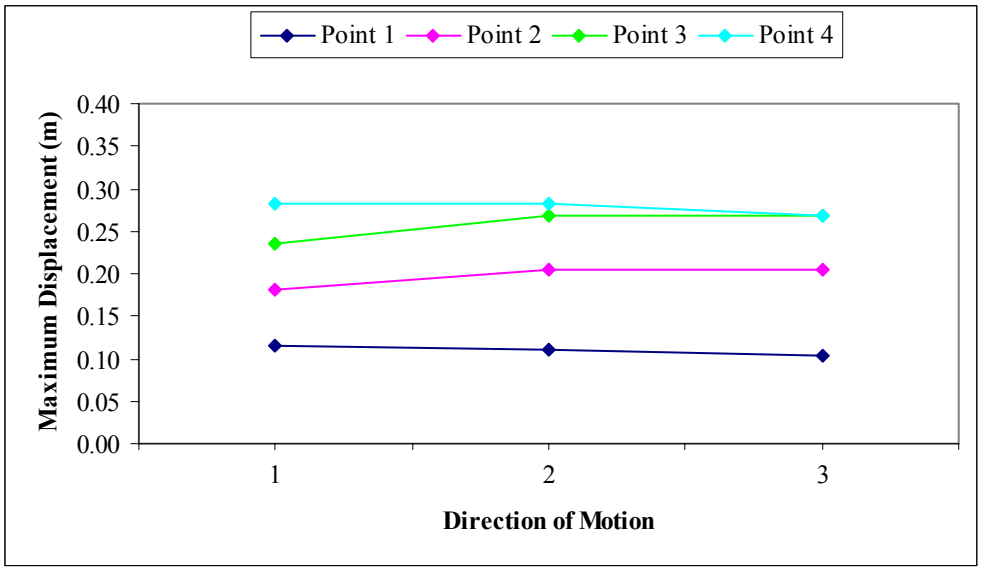

Figure 5.55 Displacement 1 for Northridge Study 3

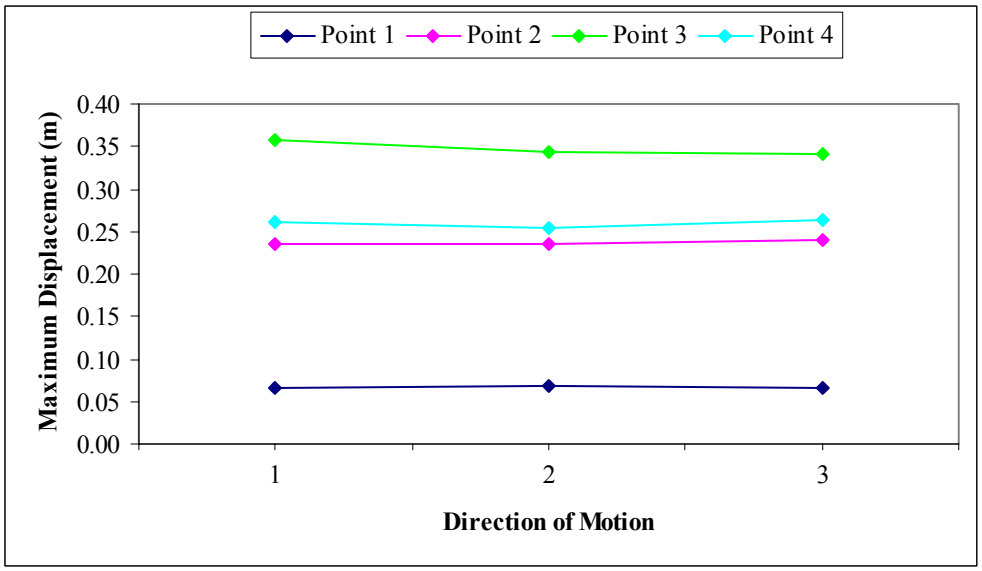

Figure 5.56 Displacement 3 for Northridge Study 3

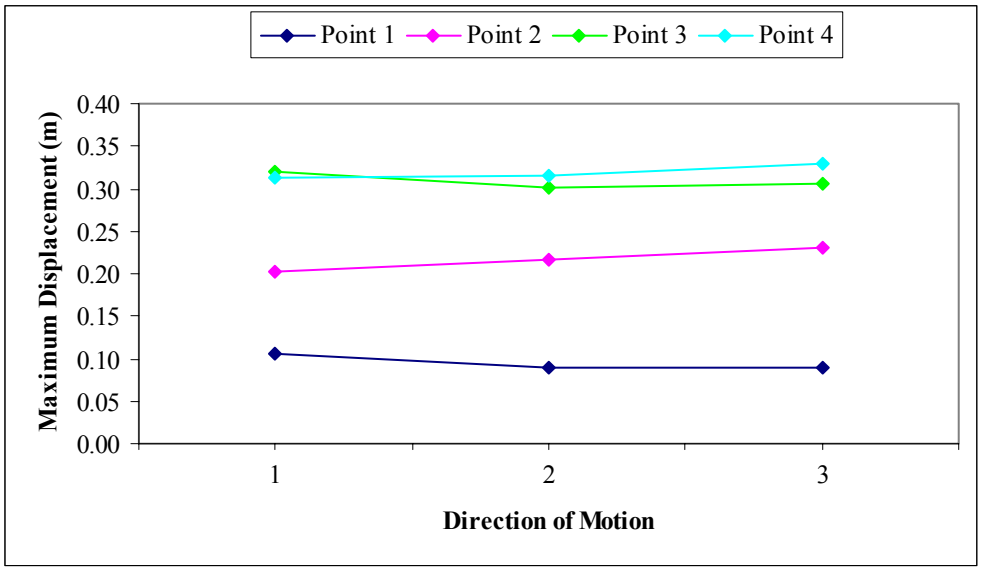

Figure 5.57 Displacement 1 for El Centro Study 3

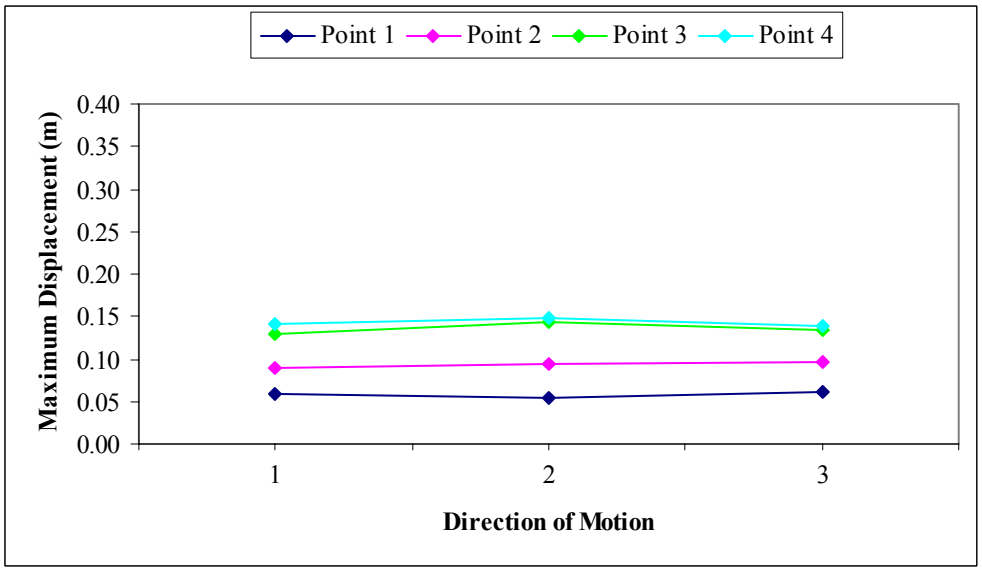

Figure 5.58 Displacement 3 for El Centro Study 3

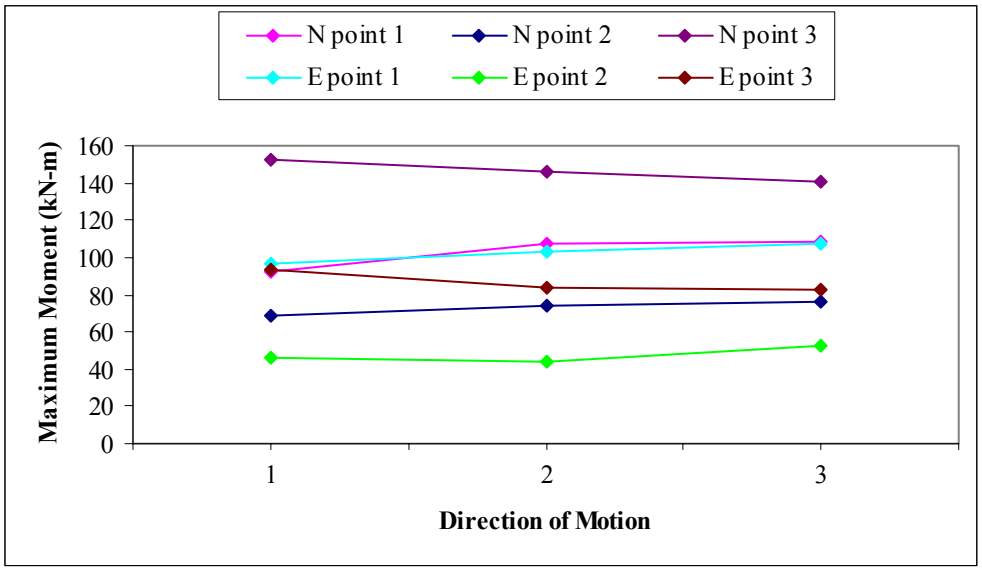

Figure 5.59 Bending Moment 1 for Study 3

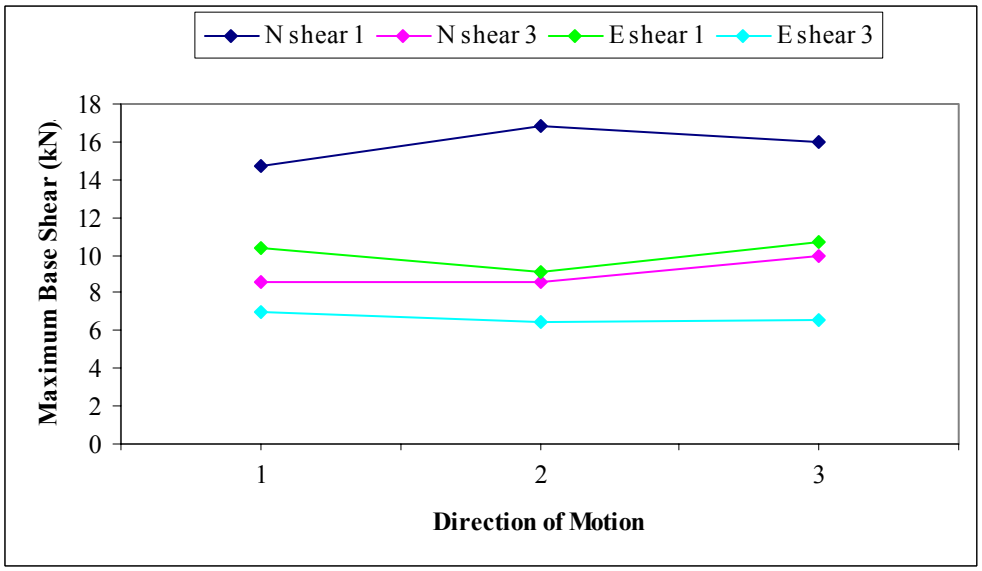

Figure 5.60 Base Shears 1 and 3 for Study 3

Chapter 6
Summary and Conclusions

6.1 Summary and Conclusions

This research analytically examined the seismic behavior of guyed masts that incorporate synthetic ropes as guys. Much research has been performed on the behavior of guyed masts under wind loads, as this generally controls the design. There are no seismic codes expressly for the design of guyed masts in the United States, but it has been shown that seismic forces can sometimes control the design. However, very little research has been reported on the behavior of guyed towers under earthquake loads. This investigation attempted to examine the seismic behavior of guyed towers while specifically looking at two issues: snap loads and three-dimensional loading.

The nonlinear behavior of cables can cause large snap loads when the cable transitions from a slack to taut state. This particular behavior is usually modeled in guyed masts, but not much research has specifically examined its effect on structural behavior. Additionally, many analytical studies use just one horizontal component of ground motion. While this may be sufficient in certain cases, the three-dimensional behavior is significantly different than simple rectilinear motion. In order to examine these questions, numerical trials were used to perform a parametric study on the seismic behavior of guyed masts.

This study is part of a multi-stage research project designed to investigate the potential use of synthetic ropes to dissipate energy and provide an added means of lateral resistance in structures. Previous and current students have physically tested and characterized the dynamic behavior of synthetic ropes in an effort to identify synthetic ropes with suitable properties. This particular investigation attempted to take the known dynamic rope properties and incorporate these synthetic ropes as guys in guyed masts, common to the broadcasting and telecommunication industries. A nonlinear hardening constitutive law, based on the previous research, was used to model the stiffness of the

synthetic ropes. However, this research used general values for the product *EA*, which makes the results also applicable to other cable materials like steel, the most frequently used material for guys (which generally experiences strain hardening as well). It should be noted that with the additional weight associated with steel cables, it may be advisable to generate a more complex cable model for the analysis. However, the slack-taut effects of guys examined here should be somewhat representative of all guyed mast behavior.

Three-dimensional modeling of the guyed mast structures was accomplished with the finite element analysis program ABAQUS. A significant amount of preliminary research was spent on the validation of modeling methods and examination of possible spring and dashpot models to simulate the dynamic behavior observed in the synthetic ropes. The main portion of research consisted of 38 numerical trials involving slight variations on the general design of a 120-m-tall guyed mast. The guyed mast used for the analytical trials was based on one that had been analyzed in previous studies, and thus provided a benchmark for validation and a realistically designed structure from which to vary parameters for the studies. The mast consisted of a triangular cross-section with four evenly spaced guy levels. All of the guys had the same properties (except for length) and were initially loaded to the same pretension. Twelve beam-column elements were used along the length of the mast, and nonlinear springs were used for the guys. Time histories of two characteristic strong ground motions, the 1940 El Centro Earthquake (scaled up) and the 1994 Northridge Earthquake, were used as the input motions at the base of the structure.

Most of the trials were aimed at examining the effect of pretension on the structural behavior. A smaller level of pretension in the guys is directly related to the possibility of slack behavior; it requires less displacement of the mast for the guy to go slack. These trials consisted of combinations of five guy pretensions and three guy stiffnesses under both earthquake inputs, resulting in a total of 30 trials. Additionally, the mass and stiffness of the mast were varied for additional trials under both earthquake inputs. In order to examine the potential for spatial variations in response resulting from three-dimensional input motions, the horizontal direction of the earthquake (angle of incidence)

was varied from the standard case for both earthquakes. The main study looking at pretensions was the focus of this research, and two additional studies were supplementary. Also, a shorter mast, 40 m in height with two guy levels, was examined, but this particular structure did not exhibit slack motion in the guys when subjected to the seismic motion, and consequently was not further addressed in this thesis.

Output data from the numerical trials consisted of displacements, bending moments, axial forces, guy tensions, and base shears. There were all used as measures of structural response. Two different types of response were examined in the analysis of the results from the numerical trials. First, the behavior of the standard case of the guyed mast was examined in depth to describe the time-dependent response of the guyed mast to both of the earthquakes. Examining these two trials characterized the general response that would be seen for all of the trials. Second, peak values in the response parameters were calculated and used to establish trends in the behavior for all of the trials.

The detailed behavior of the guyed mast under the Northridge loading was characterized by somewhat different behavior in the two horizontal directions. In the strong direction of motion, there was a fairly random displacement response with several seconds of large motion and then smaller oscillations that damped out. In the perpendicular horizontal direction, larger displacements occurred even though there was less input energy. Also, the response was much more periodic and slower to damp out, suggesting that the behavior was dominated by one of the bending modes.

The response of the structure in the vertical direction of motion did not exhibit the same dependencies on guy behavior as seen in the two horizontal directions of motion. A main point of interest was that the dynamic components of axial force can be significant, and thus should be modeled when looking at the design of guyed masts.

When the guys started to exhibit slack behavior, the bending response of the structure drastically changed and increased moments at certain locations on the mast were observed to coincide with the snap loads in the guys. This demonstrates the direct

influence of slack guy behavior on the structure and the fact that snap loads in the guys have the possibility of increasing structural response. Additionally, dynamic guy tensions were seen to become significantly larger than the initial guy tensions.

The base shear was observed to have a fairly random response. The magnitudes of shear force relating to the strong direction of the earthquake were larger than in the other direction by about the same factor as the relationship between the PGA of each of the components of input motion. Additionally, the maximum base shear was seen to be about 20% of the mast weight, slightly less than that seen with taller masts in a previous study.

The detailed behavior of the guyed mast during the El Centro loading was fairly similar to the Northridge behavior in most aspects. One of the few differences in behavior was that the larger horizontal component dominated the response in the El Centro trial. The dynamic behavior, especially involving bending moments, changed when guys exhibited slack behavior, but the change was not as drastic as that seen in the Northridge event. However, once again the vertical response was not greatly influenced by guy behavior. Additionally, the maximum base shear experienced during this earthquake was slightly smaller.

Peak response values were calculated for the different parametric studies, and used to analyze trends in the behavior. Study 1, involving pretensions, showed some indication of fairly strong trends for some of the response values, although there were also some random instances of peak values that did not follow the trends and are not attributed to any particular cause. The maximum horizontal displacements were observed to generally remain constant or decrease as a function of guy pretension. This behavior was distinctly different at the various guy levels for both degrees of freedom. This suggests that different bending modes influence the response of the mast due to the two different components of motion. Vertical displacements were observed to be an almost linear function of guy tension, most likely due to the increased guy tensions directly relating to compression of the mast.

The bending moments in the mast showed a slight trend of decreasing moment with the additional pretension. However, this correlation was not consistent for the bending moments at all of the locations and was stronger at the middle guy level. Maximum guy tensions were strongly related to the level of pretension. The maximum values were generally 200 to 300% of the initial tensions, which is in accordance with the ranges seen in a previous study. The base shear had very negligible trends for both horizontal directions.

The dynamic behavior of the guyed mast in Study 2, when both mass and mast stiffness were varied, was dominated by the change in mass. It seemed that the increased stiffness was not enough to resist the larger inertial forces, and consequently all of the response values increased with the addition of mass to the mast, especially the bending moments present at the different guy levels.

In Study 3, varying the input direction of the ground motion was observed to have very little effect on the dynamic behavior of the guyed mast. Although the tension in each of the guys is dependent on the orientation of the seismic base input, the orientation seems to have a negligible effect. Nonetheless, this does not by any means take away from the importance of using three-dimensional ground motions in dynamic analyses of guyed masts. The additional effects of three-dimensional input motions can cause increases in displacements, moments, and stresses in the mast. Also, the response in each horizontal direction can be different, as was observed for the Northridge input motion where the smaller component of ground motion produced larger displacements. Finally, the vertical accelerations associated with seismic events can produce significant dynamic components of axial force in the mast.

6.2 Need for Further Research

The analytical modeling of guyed towers incorporating synthetic ropes is part of a multi-stage research project aimed at determining the energy dissipation associated with SCED's and their application to new and existing structures for additional stiffness

during large instances of lateral displacement such as earthquakes and blast loads. The analyses and data associated with this investigation into the dynamic behavior of guyed masts and the influence of snap loads on structural response should provide a better understanding for the behavior of structures that incorporate these ropes.

This investigation determined that a more detailed model to represent the constitutive properties of the synthetic ropes could be useful for numerical analysis. One possible option for the development of this model is the addition of a user-defined function to retrieve information on displacement and velocities at each time step and update the tension in the rope accordingly. Also, it might be possible to develop or define more complex elements to arrive at a better approximation of the highly nonlinear behavior, including internal friction in the ropes. Regardless of how it is accomplished, a more detailed look at numerical rope models is warranted for the continuing analytical research.

Several other investigations concerning the application of synthetic ropes in structures are currently ongoing, such as experimental trials on cross-bracing in a building frame, and numerical analysis using the ropes as bridge deck restrainers to prevent unseating of spans. The transition from analyzing theoretical behavior to experimental results has already started, but this should continue and further expand to look at realistic design of structures incorporating the synthetic ropes.

References

ABAQUS (2005). *Abaqus: Superior Finite Element Solutions*. ABAQUS, Incorporated, Providence, Rhode Island (http://www.hks.com).

Ajrab, J. J., Pekcan, G., and Mander, J. B. (2004). "Rocking wall-frame structures with supplemental tendon systems." *Journal of Structural Engineering*, 130, 895-903.

Amiri, G. G. (2002). "Seismic sensitivity indicators for tall guyed telecommunication towers." *Computers and Structures*, 80, 349-364.

Amiri, G. G., Zahedi, M., and Jalali, R. S. (2004). "Multiple-support seismic excitation of tall guyed telecommunication towers." *13th World Conference on Earthquake Engineering*, Vancouver, British Columbia, Canada, August 1-6, 2004, Paper No. 212.

ASCE (1988). *ASCE Manuals and Reports on Engineering Practice No. 52: Guide for Design of Steel Transmission Towers*. American Society of Civil Engineers, New York, New York.

ASCE (1990). *ASCE Manuals and Reports on Engineering Practice No. 72: Design of Steel Transmission Pole Structures*. American Society of Civil Engineers, New York, New York.

ASCE (1991). *ASCE Manuals and Reports on Engineering Practice No. 74: Guidelines for Electrical Transmission Line Structural Loading*. American Society of Civil Engineers, New York, New York.

ASCE (1997). *ASCE Manuals and Reports on Engineering Practice No. 91: Design of Guyed Electrical Transmission Structures*. American Society of Civil Engineers, New York, New York.

Borri, C., and Zahlten, W. (1991). "Fully simulated nonlinear analysis of large structures subjected to turbulent artificial wind." *Mechanics of Structures and Machines*, 19, 213-250.

Chen, W., and Scawthorn, C., eds. (2003). *Earthquake Engineering Handbook*. CRC Press, Boca Raton, Florida.

Chopra, A. K. (2001). *Dynamics of Structures: Theory and Applications to Earthquake Engineering, Second Edition*. Prentice Hall, Upper Saddle River, New Jersey.

Desai, Y. M., and Punde, S. (2001). "Simple model for dynamic analysis of cable supported structures." *Engineering Structures*, 23, 271-279.

Filiatrault, A., and Stearns, C. (2004). "Seismic response of electrical substation equipment interconnected by flexible conductors." *Journal of Structural Engineering*, 130, 769-778.

Guevara, E., and McClure, G. (1993). "Nonlinear seismic response of antenna-supporting structures." *Computers and Structures*, 47, 711-724.

Harikrishna, P., Annadurai, A., Gomathinayagam, S., and Lakshmanan, N. (2003). "Full scale measurements of the structural response of a 50 m guyed mast under wind loading." *Engineering Structures*, 25, 859-867.

Hennessey, C. M. (2003). "Analysis and modeling of snap loads on synthetic fiber ropes." MS thesis, Virginia Polytechnic Institute and State University, Blacksburg, Virginia (http://scholar.lib.vt.edu/theses/available/etd-11092003-135228).

Hennessey, C. M., Pearson, N. J., and Plaut, R. H. (2005). "Experimental snap loading of synthetic ropes." *Shock and Vibration*, 12, 163-175.

Irvine, H. M. (1981). *Cable Structures*. The MIT Press, Cambridge, Massachusetts.

Kahla, N. B. (1994). "Dynamic analysis of guyed towers." *Engineering Structures*, 16, 293-301.

Madugula, M. K. S., ed. (2002). *Dynamic Response of Lattice Towers and Guyed Masts*. American Society of Civil Engineers, Reston, Virginia.

Moossavi Nejad, S. E. (1996). "Dynamic response of guyed masts to strong motion earthquake." *Proceedings of the 11th World Conference on Earthquake Engineering*, Acapulco, Mexico, Paper No. 289.

Motley, M. R. (2004). "Finite element analysis of the application of synthetic fiber ropes to reduce blast response of frames." MS thesis, Virginia Polytechnic Institute and State University, Blacksburg, Virginia (http://scholar.lib.vt.edu/theses/available/etd-12152004-102556).

Mulherin, N. D. (1998). "Atmospheric icing and communication tower failure in the United States." *Cold Regions Science and Technology*, 27, 91-104.

Pearson, N. J. (2002). "Experimental snap loading of synthetic fiber ropes." MS thesis, Virginia Polytechnic Institute and State University, Blacksburg, Virginia (http://scholar.lib.vt.edu/theses/available/etd-01132003-105300).

PEER (2005). *PEER Strong Motion Database*. Pacific Earthquake Engineering Research Center, Berkeley, California (http://peer.berkeley.edu/smcat/index.html).

Plaut, R. H., Archilla, J. C., and Mays, T. W. (2000). "Snap loads in mooring lines during large three-dimensional motions of a cylinder." *Nonlinear Dynamics*, 23, 271-284.

Preumont, A., Achkire, Y., and Bossens, F. (2000). "Active tendon control of large trusses." *AIAA Journal*, 38, 493-498.

Samson (2005). *Rigging: Double Braid: Amsteel II*. Samson Rope Technologies, Ferndale, Washington (http://www.samsonrope.com/home/industrial/rigging-doublebraids-amsteelii.cfm?ProdNum=180).

Shome, N., Cornell, C. A., Bazzurro, P., and Carballo, J. E. (1998). "Earthquakes, records, and nonlinear responses." *Earthquake Spectra*, 14, 469-500.

TIA (1996). *TIA-222-F: Structural Standards for Steel Antenna Towers and Antenna Supporting Structures*. Telecommunications Industry Association, Arlington, Virginia.

Virgin, L. N., and Plaut, R. H. (1993). "Effect of axial load on forced vibrations of beams." *Journal of Sound and Vibration*, 168, 395-405.

Appendix A

Supporting Information on Second Preliminary Model

A.1 Theoretical Beam Motion for Second Preliminary Model

For Second Preliminary Model Case A:

$$Y_1(x) = A\cosh\alpha x + A_1(\cos\alpha x - \cosh\alpha x) + B_1(\sin\alpha x - \sinh\alpha x)$$

and

$$Y_1(L) = \frac{A(\cos\delta + \cosh\delta)}{(1 + \cos\delta\cosh\delta)}$$

where $Y_1(x)$ = displacement amplitude along beam

$Y_1(L)$ = displacement amplitude at tip

$$A_1 = \frac{(1 + \cos\delta\cosh\delta - \sin\delta\sinh\delta)A}{2(1 + \cos\delta\cosh\delta)}$$

$$B_1 = \frac{(\cos\delta\sinh\delta - \sin\delta\cosh\delta)A}{2(1 + \cos\delta\cosh\delta)}$$

$$\alpha = \left(\frac{\Omega^2\mu}{EI}\right)^{1/4}$$

$$\delta = \alpha L$$

For Second Preliminary Model Cases B and C:

$$Y_2(L) = A_2 \cos\delta + B_2 \sin\delta + C_2 \cosh\delta + D_2 \sinh\delta$$

where $Y_2(L)$ = displacement amplitude at tip

and the coefficients are obtained by solving the following matrix:

$$\begin{bmatrix} \cos(\varepsilon) - \cosh(\varepsilon) & \sin(\varepsilon) - \sinh(\varepsilon) & -\cos(\varepsilon) & -\sin(\varepsilon) & -\cosh(\varepsilon) & -\sinh(\varepsilon) \\ -\sin(\varepsilon) - \sinh(\varepsilon) & \cos(\varepsilon) - \cosh(\varepsilon) & \sin(\varepsilon) & -\cos(\varepsilon) & -\sinh(\varepsilon) & -\cosh(\varepsilon) \\ -\cos(\varepsilon) - \cosh(\varepsilon) & -\sin(\varepsilon) - \sinh(\varepsilon) & \cos(\varepsilon) & \sin(\varepsilon) & -\cosh(\varepsilon) & -\sinh(\varepsilon) \\ (-\sin(\varepsilon) + \sinh(\varepsilon) + k\cdot\cos(\varepsilon) - k\cdot\cosh(\varepsilon)) & (\cos(\varepsilon) + \cosh(\varepsilon) + k\cdot\sin(\varepsilon) - k\cdot\sinh(\varepsilon)) & \sin(\varepsilon) & -\cos(\varepsilon) & \sinh(\varepsilon) & \cosh(\varepsilon) \\ 0 & 0 & -\cos(\delta) & -\sin(\delta) & \cosh(\delta) & \sinh(\delta) \\ 0 & 0 & \sin(\delta) & -\cos(\delta) & \sinh(\delta) & \cosh(\delta) \end{bmatrix} \cdot \begin{pmatrix} A_1 \\ B_1 \\ A_2 \\ B_2 \\ C_2 \\ D_2 \end{pmatrix} = \begin{pmatrix} -\cosh(\varepsilon) \\ -\sinh(\varepsilon) \\ -\cosh(\varepsilon) \\ \sinh(\varepsilon) - k\cdot\cosh(\varepsilon) \\ 0 \\ 0 \end{pmatrix} \cdot A$$

where $\alpha = \left(\frac{\Omega^2 \mu}{EI}\right)^{1/4}$

$\delta = \alpha L$

$\varepsilon = \alpha B$

$k = \frac{2K}{\alpha^3 EI}$

K = spring stiffness

A factor $\frac{c^2}{(1+c^2)}$ is applied to the spring stiffness K to account for the angle in Case C

where $c = \frac{C}{B}$

A.2 Parameter Values for Second Preliminary Model

Table A.1 Parameter Values for Second Preliminary Model

Case	Trial	E (Gpa)	μ (kg/m)	a_0 (sec^{-1})	a_1 (sec)	L (m)	I (m^4)	ω (rad/sec)	A (m)	k (kN/m)	B (m)	C (m)
A	1	209	1570	0.25	0.0005	10	0.004	2π	0.2	-	-	-
	2	"	"	"	"	10	0.004	2π	0.5	-	-	-
	3	"	"	"	"	10	0.004	6π	0.02	-	-	-
	4	"	"	"	"	10	0.004	6π	0.05	-	-	-
	5	"	"	"	"	5	0.001	2π	0.2	-	-	-
	6	"	"	"	"	5	0.001	2π	0.5	-	-	-
	7	"	"	"	"	5	0.001	6π	0.02	-	-	-
	8	"	"	"	"	5	0.001	6π	0.05	-	-	-
B	1	209	1570	0.25	0.0005	10	0.002	2π	0.2	525	5	-
	2	"	"	"	"	"	"	4π	0.05	525	5	-
	3	"	"	"	"	"	"	2π	0.2	263	5	-
	4	"	"	"	"	"	"	4π	0.05	263	5	-
	5	"	"	"	"	"	"	2π	0.2	525	7	-
	6	"	"	"	"	"	"	4π	0.05	525	7	-
	7	"	"	"	"	"	"	2π	0.2	263	7	-
	8	"	"	"	"	"	"	4π	0.05	263	7	-
C	1	209	1570	0.25	0.0005	10	0.002	2π	0.2	263	7	5
	2	"	"	"	"	"	"	4π	0.05	263	7	5
	3	"	"	"	"	"	"	2π	0.2	525	7	5
	4	"	"	"	"	"	"	4π	0.05	525	7	5
	5	"	"	"	"	"	"	2π	0.2	263	7	10
	6	"	"	"	"	"	"	4π	0.05	263	7	10
	7	"	"	"	"	"	"	2π	0.2	525	7	10
	8	"	"	"	"	"	"	4π	0.05	525	7	10

Appendix B

Supporting Information on Analytical Model

B.1 Ground Motion Plots

The following figures show the spatial variation in accelerations and displacements during ground motion. The accelerations are plotted for two seconds of strong motion so as not to become too cluttered, and the displacements are plotted for the first 15 seconds of motion.

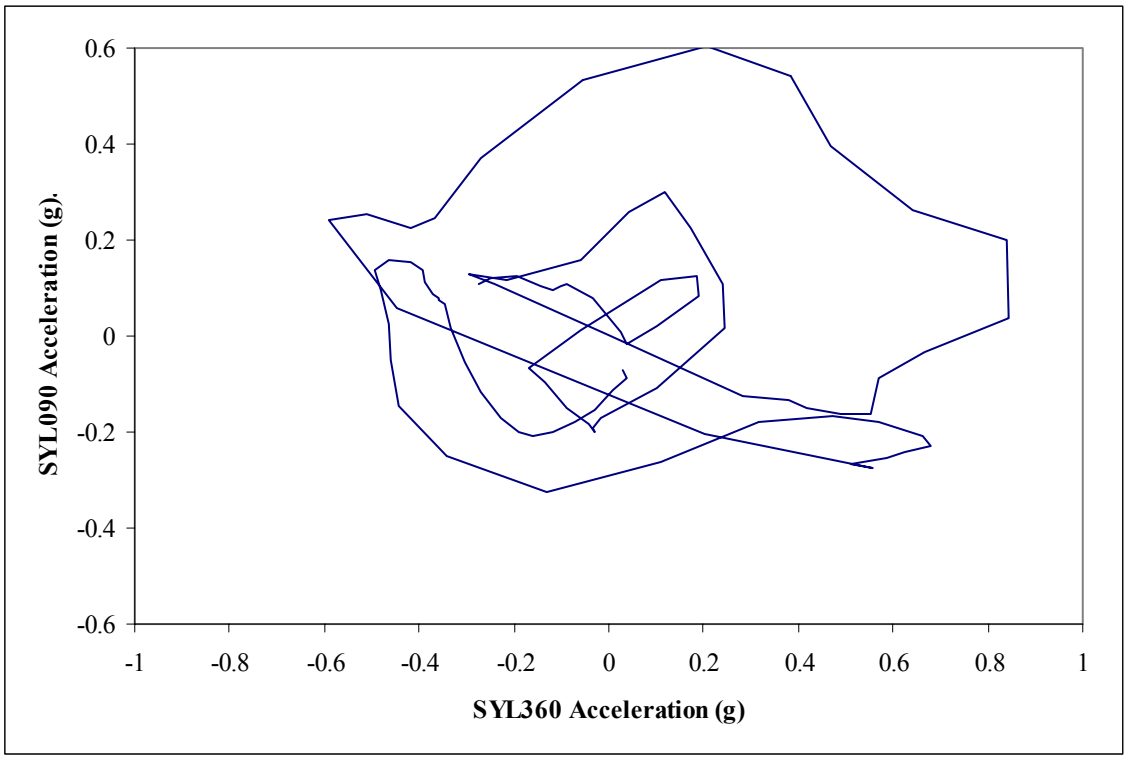

Figure B.1 Accelerations in Horizontal Plane for Northridge

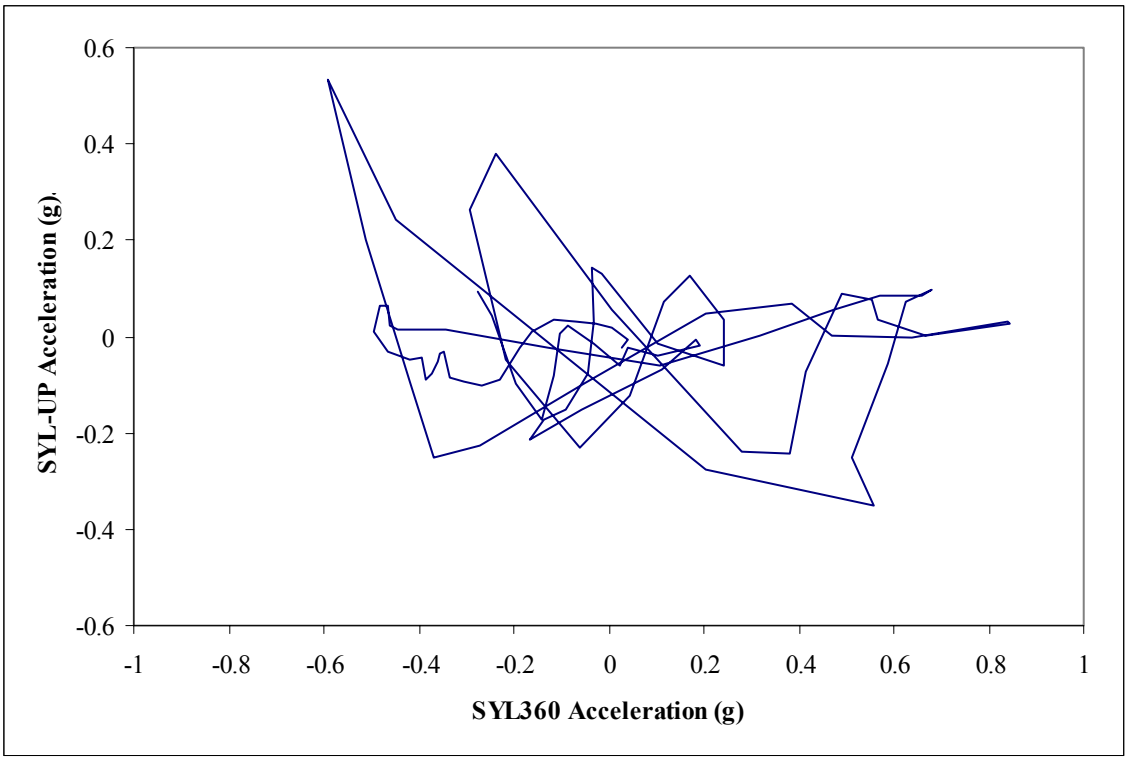

Figure B.2 Accelerations in Vertical Plane 1 for Northridge

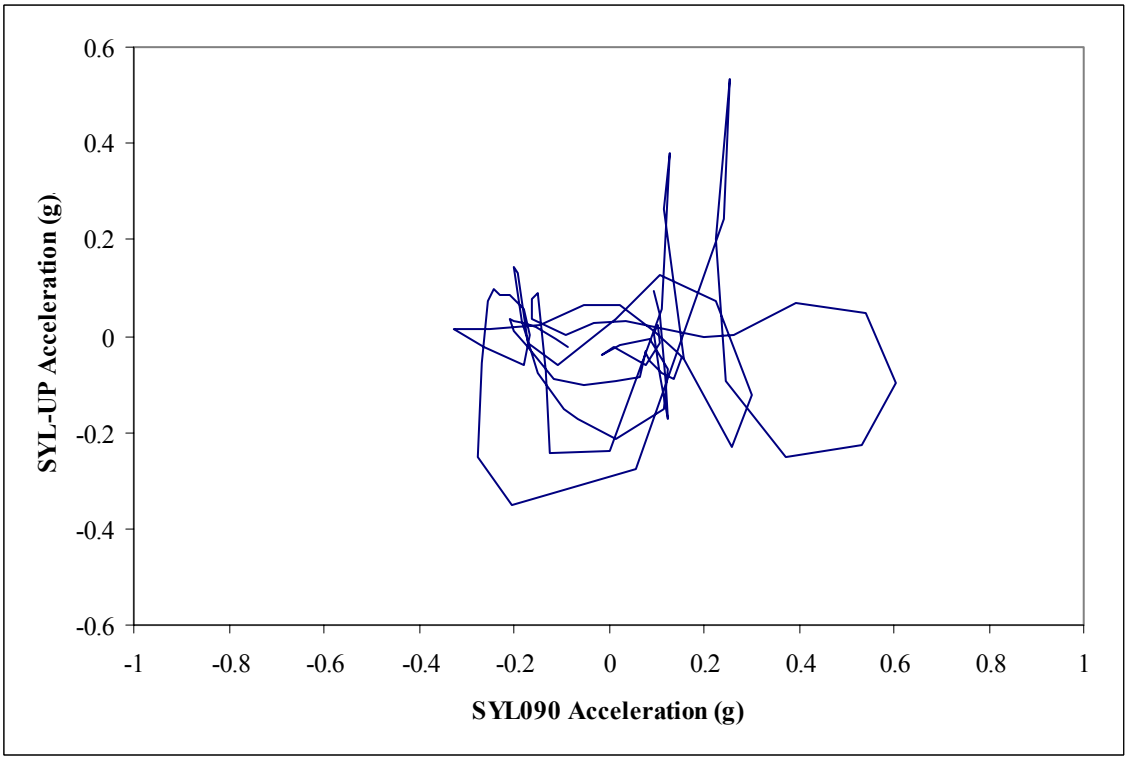

Figure B.3 Accelerations in Vertical Plane 2 for Northridge

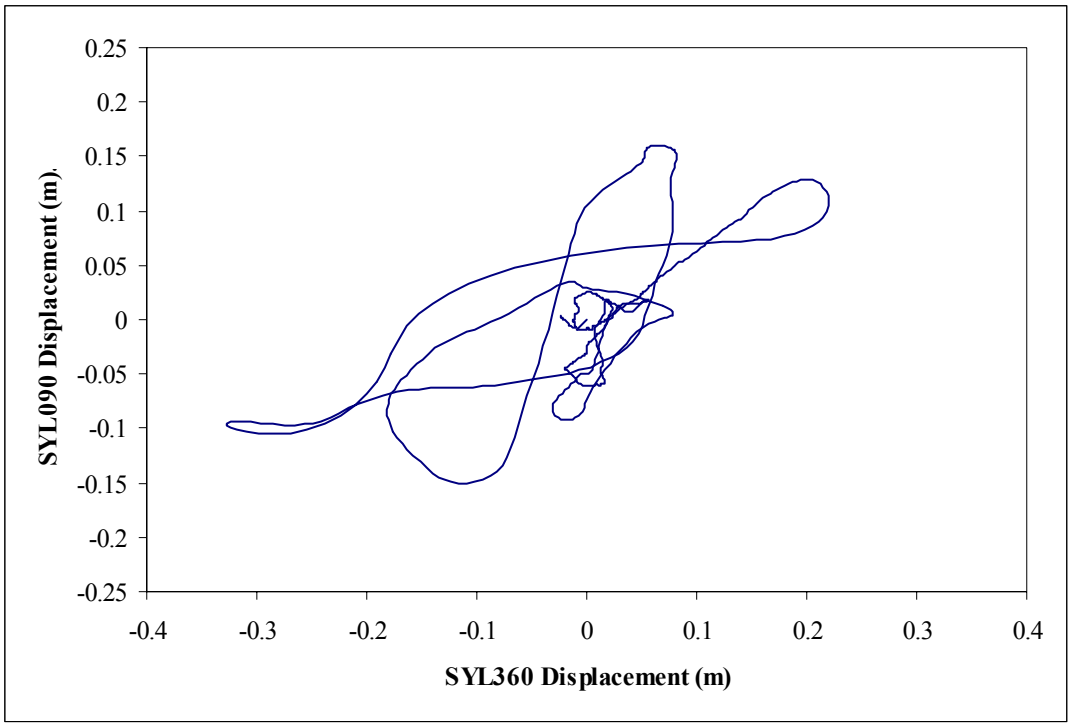

Figure B.4 Displacements in Horizontal Plane for Northridge

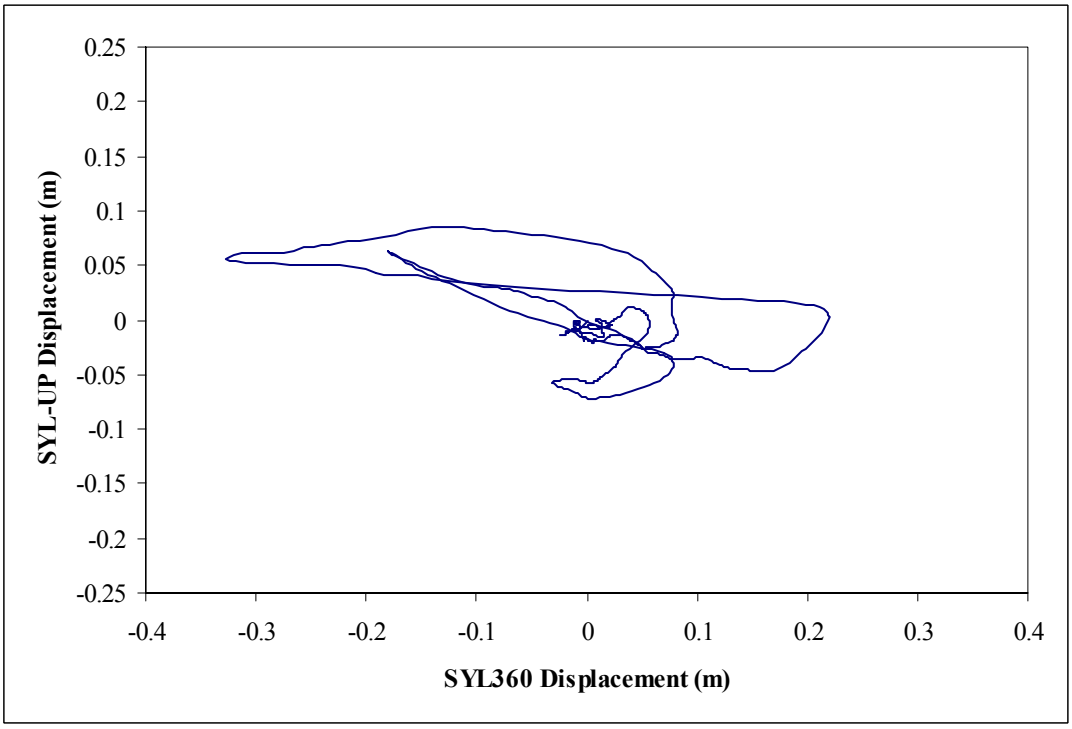

Figure B.5 Displacements in Vertical Plane 1 for Northridge

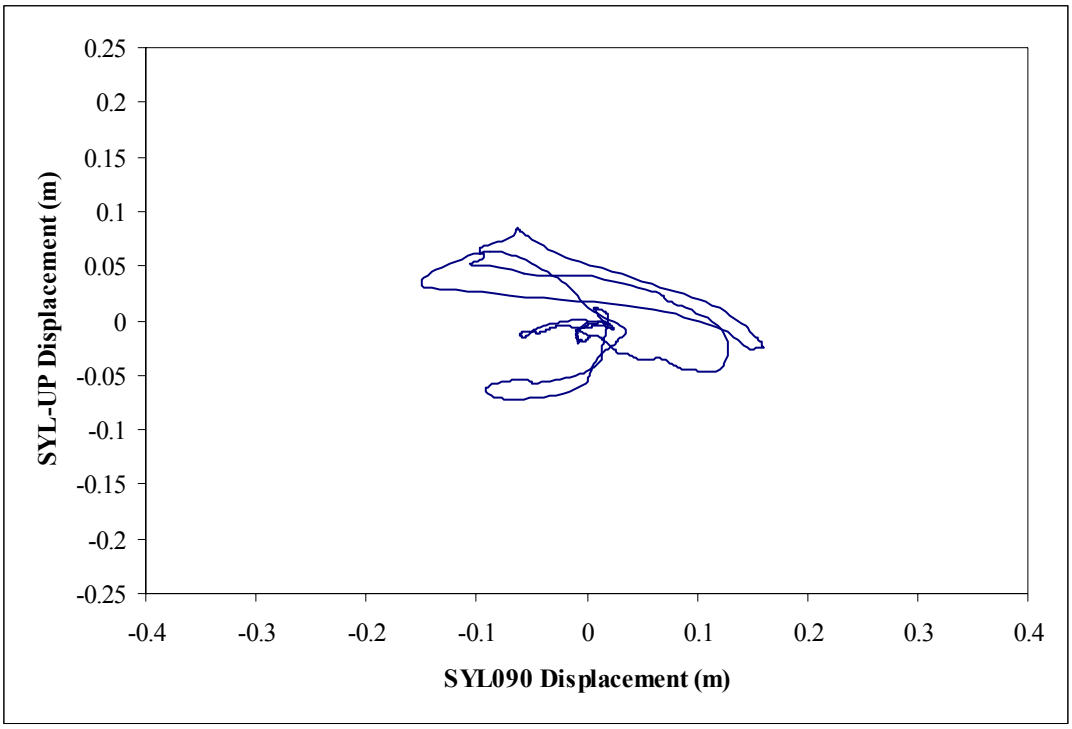

Figure B.6 Displacements in Vertical Plane 2 for Northridge

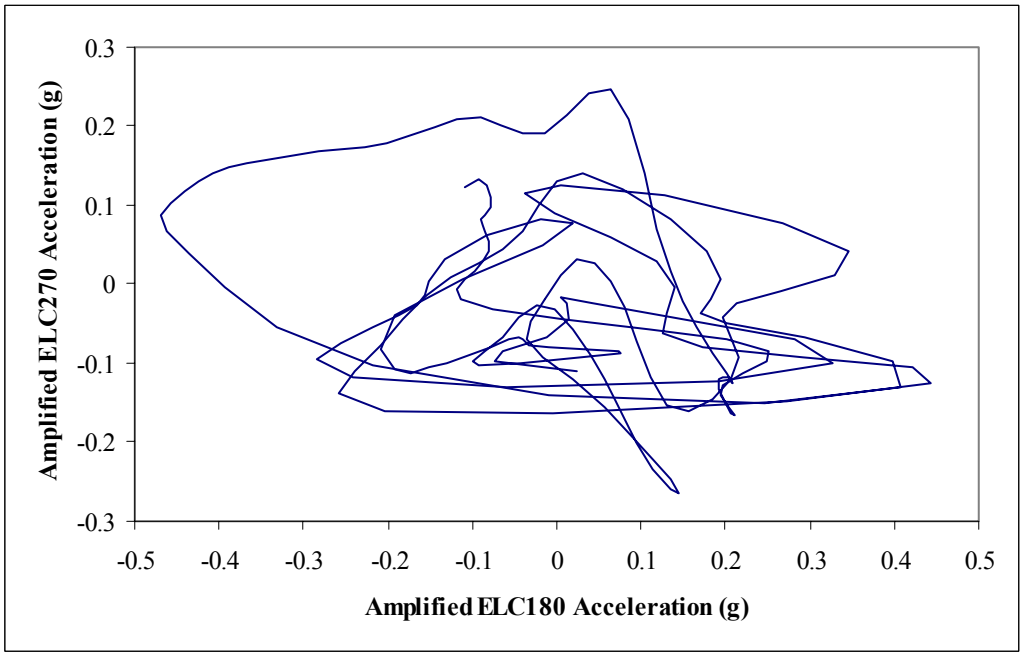

Figure B.7 Accelerations in Horizontal Plane for Amplified El Centro

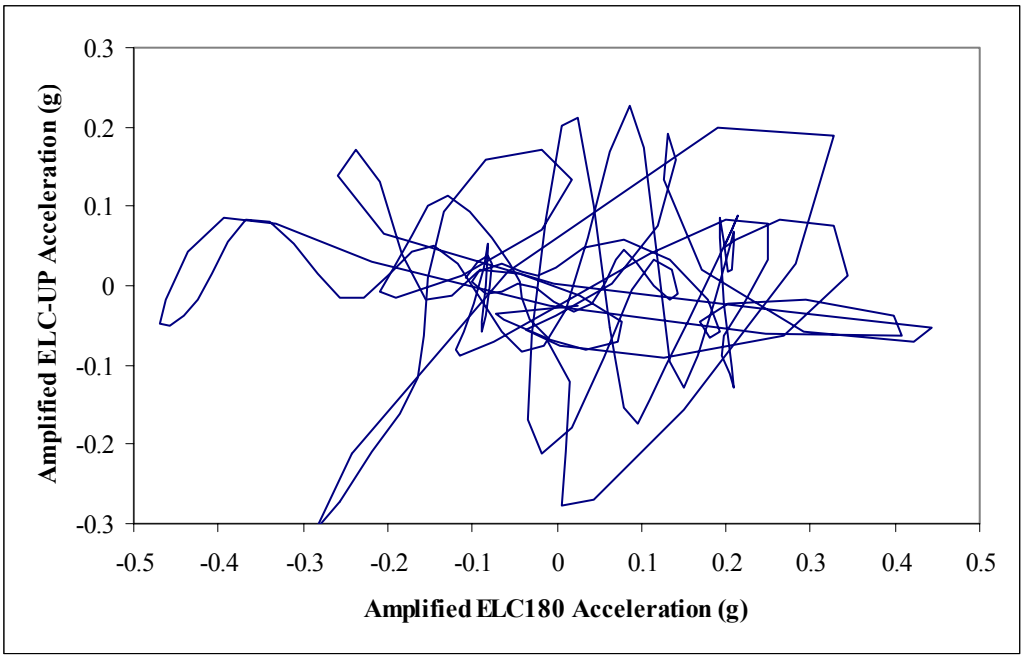

Figure B.8 Accelerations in Vertical Plane 1 for Amplified El Centro

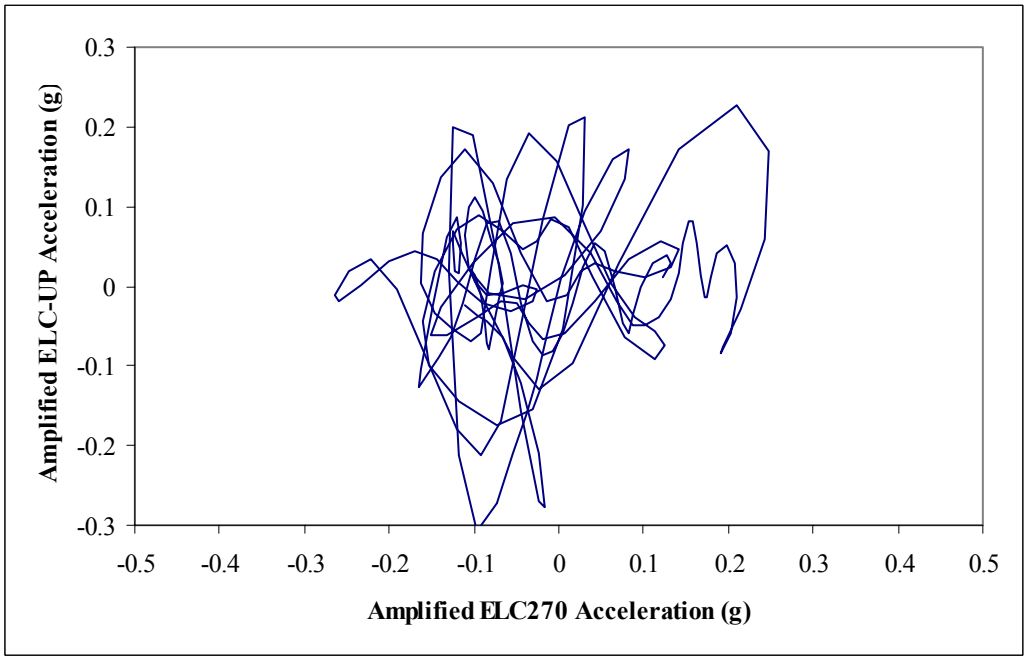

Figure B.9 Accelerations in Vertical Plane 2 for Amplified El Centro

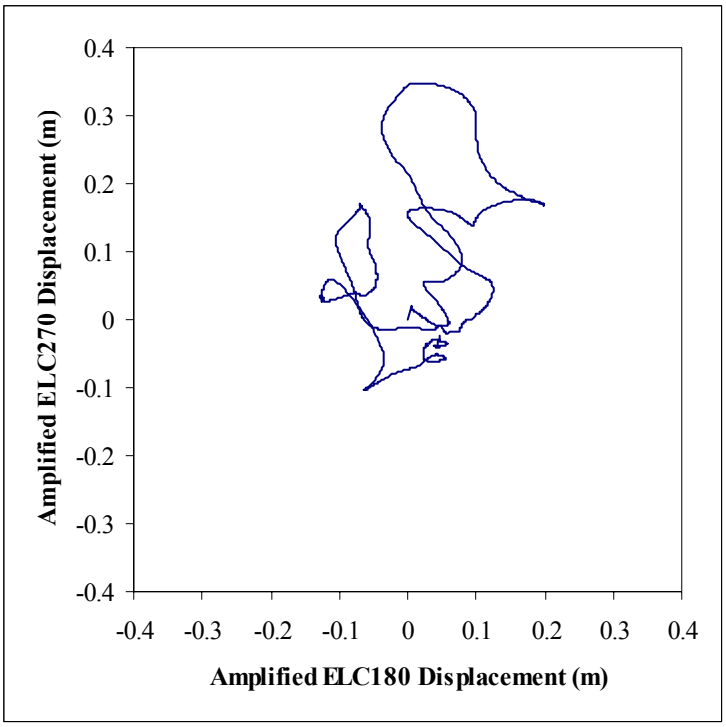

Figure B.10 Displacements in Horizontal Plane for Amplified El Centro

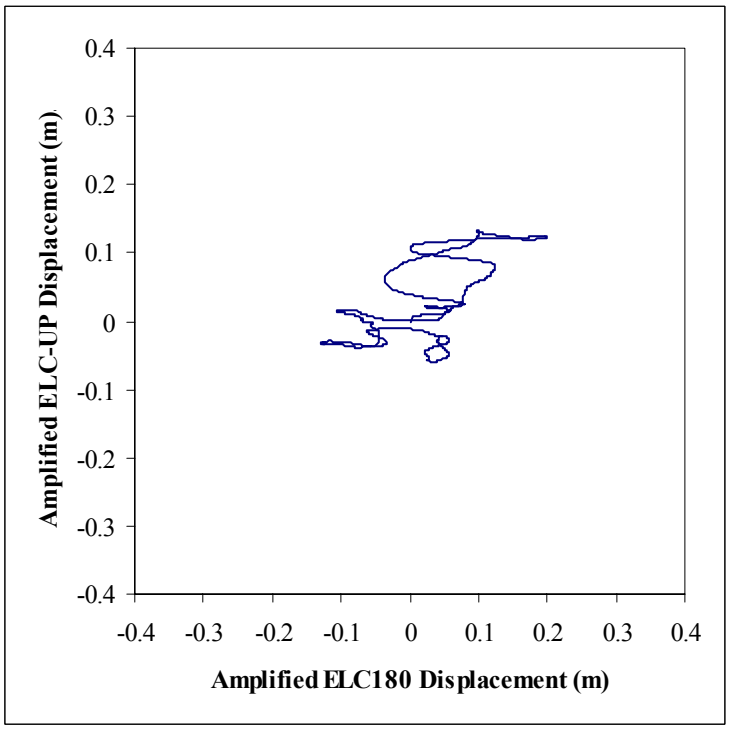

Figure B.11 Displacements in Vertical Plane 1 for Amplified El Centro

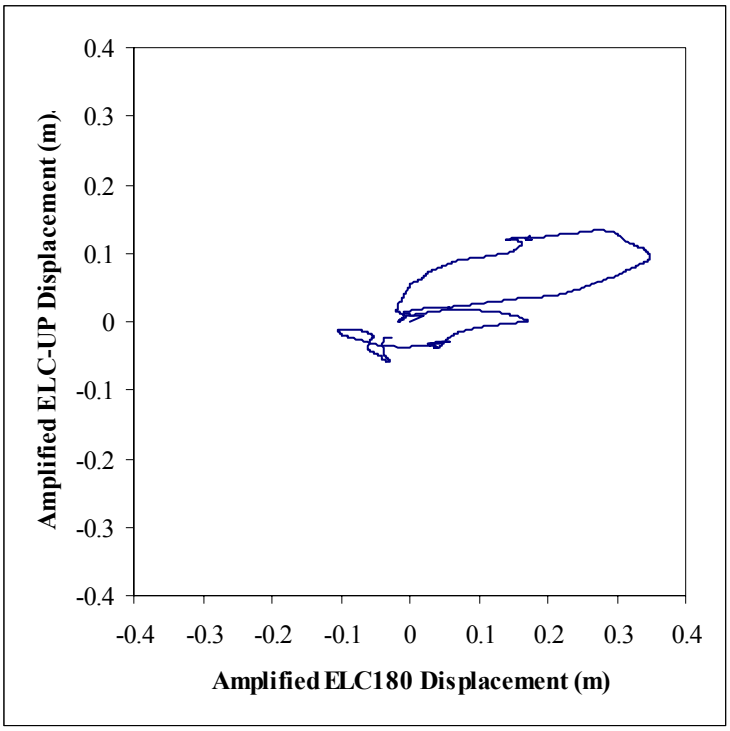

Figure B.12 Displacements in Vertical Plane 2 for Amplified El Centro

B.2 Example Input File, N-3-25

```
*HEADING
TALL MAST, 3D MODEL
** Date: 052805
** SYL eq input
** EA=3, pre=25
** mass=2, dir=1
**-----------------------------------
*NODE
**
1,        0,        0,        0,        0,0,1
2,        0,        10,       0,        0,0,1
3,        0,        20,       0,        0,0,1
4,        0,        30,       0,        0,0,1
5,        0,        40,       0,        0,0,1
6,        0,        50,       0,        0,0,1
7,        0,        60,       0,        0,0,1
8,        0,        70,       0,        0,0,1
9,        0,        80,       0,        0,0,1
10,       0,        90,       0,        0,0,1
11,       0,        100,      0,        0,0,1
12,       0,        110,      0,        0,0,1
13,       0,        120,      0,        0,0,1
14,       -15,      0,        26,       0,0,1
15,       -15,      0,        -26,      0,0,1
16,       30,       0,        0,        0,0,1
17,       -30,      0,        52,       0,0,1
18,       -30,      0,        -52,      0,0,1
19,       60,       0,        0,        0,0,1
**
*NSET, NSET=base
1
*NSET, NSET=pt1
4
*NSET, NSET=pt2
7
*NSET, NSET=pt3
10
*NSET, NSET=pt4
13
*NSET, NSET=all, GENERATE
2, 13
*NSET, NSET=motion
1, 14, 15, 16, 17, 18, 19
**-------------------------------------------
*ELEMENT, TYPE=B33, ELSET=mast
**
1, 1, 2
2, 2, 3
3, 3, 4
4, 4, 5
5, 5, 6
6, 6, 7
```

```
7, 7, 8
8, 8, 9
9, 9, 10
10, 10, 11
11, 11, 12
12, 12, 13
**
*ELEMENT, TYPE=springa, ELSET=rope1
13, 14, 4
14, 15, 4
15, 16, 4
*ELEMENT, TYPE=springa, ELSET=rope2
16, 14, 7
17, 15, 7
18, 16, 7
*ELEMENT, TYPE=springa, ELSET=rope3
19, 17, 10
20, 18, 10
21, 19, 10
*ELEMENT, TYPE=springa, ELSET=rope4
22, 17, 13
23, 18, 13
24, 19, 13
**----------------------------------------------------------------
*BEAM GENERAL SECTION, ELSET=mast, DENSITY=33333, SECTION=general
0.0018, 0.0015, 0, 0.0015, 0.00001
0, 0, -1
210000000000, 80000000000
*DAMPING, ALPHA=0.237, BETA=0.00140
**----------------------------------------------------------------
*SPRING, ELSET=rope1, NONLINEAR

0,-0.066453564
2131.406315,-0.056453564
5248.137955,-0.046453564
8890.452774,-0.036453564
12922.43145,-0.026453564
.
.
.
2035162.731,1.893546436
2048671.577,1.903546436
2062201.012,1.913546436
2075750.96,1.923546436
2089321.352,1.933546436
**----------------------------------------------------------------
*SPRING, ELSET=rope2, NONLINEAR

0,-0.094530537
1348.019715,-0.084530537
3319.213882,-0.074530537
5622.816039,-0.064530537
8172.863256,-0.054530537
.
.
.
```

```
1287149.928,1.865469463
1295693.672,1.875469463
1304250.438,1.885469463
1312820.178,1.895469463
1321402.847,1.905469463
**----------------------------------------------------------------------
*SPRING, ELSET=rope3, NONLINEAR

0,-0.136514022
836.0063379,-0.126514022
2058.489065,-0.116514022
3487.122475,-0.106514022
5068.594624,-0.096514022
.
.
.
798256.4983,1.823485978
803555.1039,1.833485978
808861.7845,1.843485978
814176.5118,1.853485978
819499.2572,1.863485978
**----------------------------------------------------------------------
*SPRING, ELSET=rope4, NONLINEAR

0,-0.161114142
674.0098575,-0.151114142
1659.606941,-0.141114142
2811.40802,-0.131114142
4086.431628,-0.121114142
.
.
.
643574.9639,1.798885858
647846.8362,1.808885858
652125.219,1.818885858
656410.089,1.828885858
660701.4236,1.838885858
**----------------------------------------------------------------
*Step, NAME=eqinput, NLGEOM=yes, INC=10000
**
*DYNAMIC, HAFTOL=10000
0.01, 20,  , 0.01
**
*Boundary, Type=displacement, Amplitude=SYL360
motion, 1, 1, 1
*Boundary, Type=displacement, Amplitude=SYL090
motion, 3, 3, 1
*Boundary, Type=displacement, Amplitude=SYLUP
motion, 2, 2, 1
**
*DLOAD
mast, GRAV, 9.81, 0, -2, 0
**
*OUTPUT, FIELD, VARIABLE=preselect, FREQUENCY=2
*ELEMENT OUTPUT, ELSET=mast, VARIABLE=preselect
```

```
SF
*OUTPUT, HISTORY, VARIABLE=preselect
**
*END STEP
**----------------------------------------------------------------
*AMPLITUDE, NAME=SYL360, DEFINITION=tabular
0,0.000000,0.02,0.000017,0.04,0.000053,0.06,0.000105
0.08,0.000166,0.1,0.000241,0.12,0.000349,0.14,0.000511
0.16,0.000726,0.18,0.000972,0.2,0.001212,0.22,0.001418
0.24,0.001596,0.26,0.001778,0.28,0.001961,0.3,0.002142
0.32,0.002337,0.34,0.002548,0.36,0.002763,0.38,0.003000
.
.
.
19.68,0.025877,19.7,0.026120,19.72,0.026356,19.74,0.026579
19.76,0.026780,19.78,0.026940,19.8,0.027031,19.82,0.027026
19.84,0.026908,19.86,0.026669,19.88,0.026320,19.9,0.025883
19.92,0.025371,19.94,0.024802,19.96,0.024209,19.98,0.023623
20,0.023075
**----------------------------------------------------------------
*AMPLITUDE, NAME=SYL090, DEFINITION=tabular
0.00,0.000000,0.02,0.000017,0.04,0.000047,0.06,0.000082
0.08,0.000120,0.10,0.000159,0.12,0.000196,0.14,0.000230
0.16,0.000256,0.18,0.000275,0.20,0.000296,0.22,0.000313
0.24,0.000338,0.26,0.000404,0.28,0.000511,0.30,0.000613
0.32,0.000654,0.34,0.000647,0.36,0.000617,0.38,0.000544
.
.
.
19.68,0.004934,19.70,0.004725,19.72,0.004637,19.74,0.004653
19.76,0.004762,19.78,0.004970,19.80,0.005276,19.82,0.005670
19.84,0.006133,19.86,0.006643,19.88,0.007184,19.90,0.007749
19.92,0.008329,19.94,0.008915,19.96,0.009501,19.98,0.010082
20.00,0.010651
**----------------------------------------------------------------
*AMPLITUDE, NAME=SYLUP, DEFINITION=tabular
0,0.000000,0.02,0.000024,0.04,0.000108,0.06,0.000271
0.08,0.000505,0.1,0.000748,0.12,0.000918,0.14,0.000951
0.16,0.000806,0.18,0.000502,0.2,0.000135,0.22,-0.000256
0.24,-0.000739,0.26,-0.001350,0.28,-0.001888,0.3,-0.002107
0.32,-0.002121,0.34,-0.002114,0.36,-0.002062,0.38,-0.002047
.
.
.
19.68,0.025751,19.7,0.026227,19.72,0.026675,19.74,0.027099
19.76,0.027490,19.78,0.027844,19.8,0.028160,19.82,0.028447
19.84,0.028722,19.86,0.028987,19.88,0.029223,19.9,0.029410
19.92,0.029548,19.94,0.029649,19.96,0.029721,19.98,0.029769
20,0.029792
```

Appendix C

Data and Figures from Dynamic Test Results

C.1 Results from Parametric Study 1

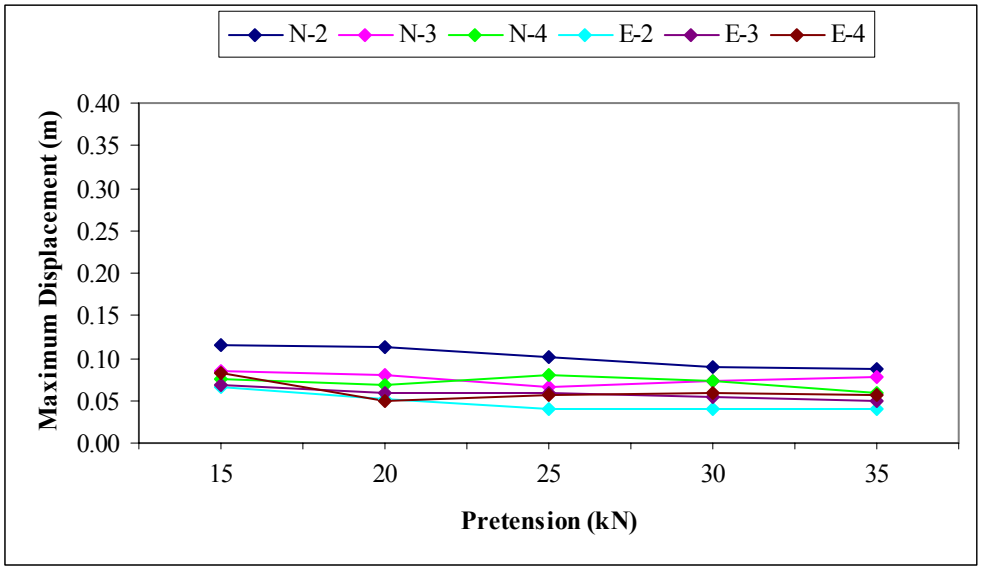

Figure C.1 Displacement 3 at Point 1 for Study 1

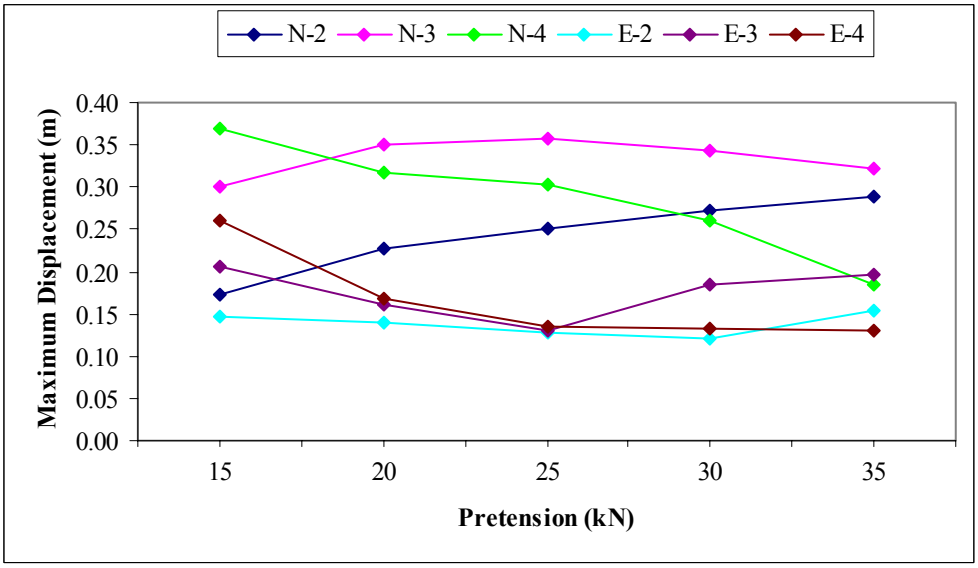

Figure C.2 Displacement 3 at Point 3 for Study 1

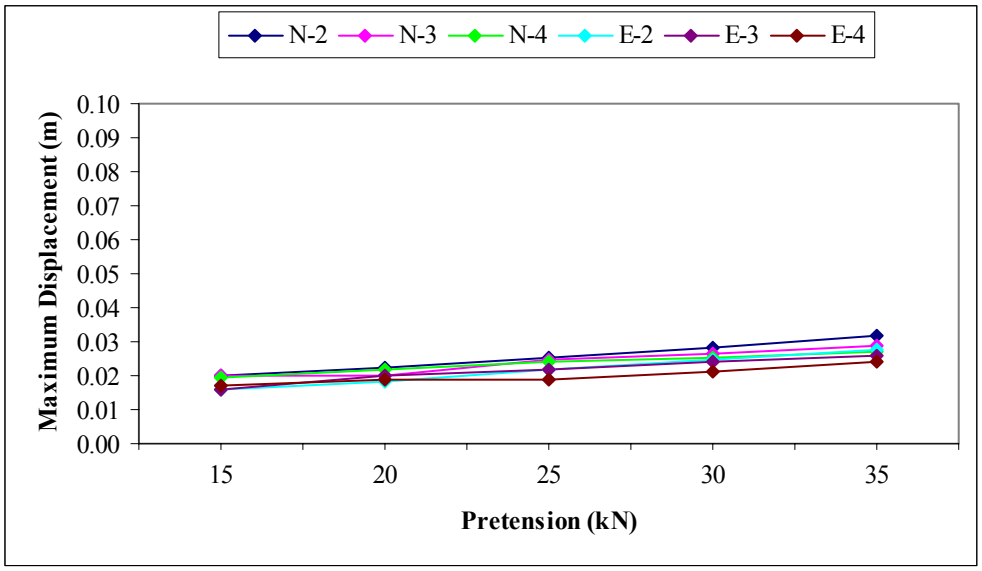

Figure C.3 Displacement 2 at Point 1 for Study 1

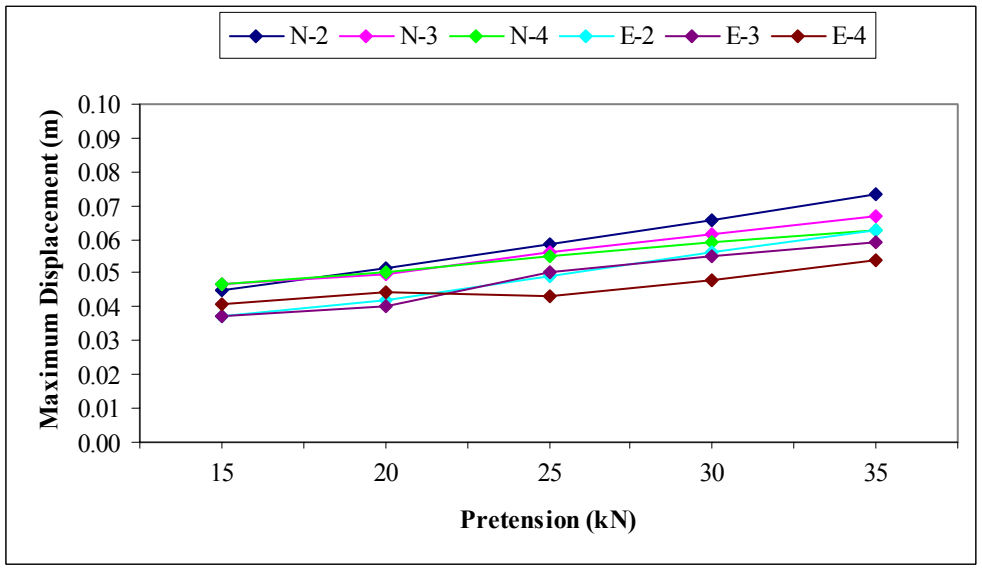

Figure C.4 Displacement 2 at Point 3 for Study 1

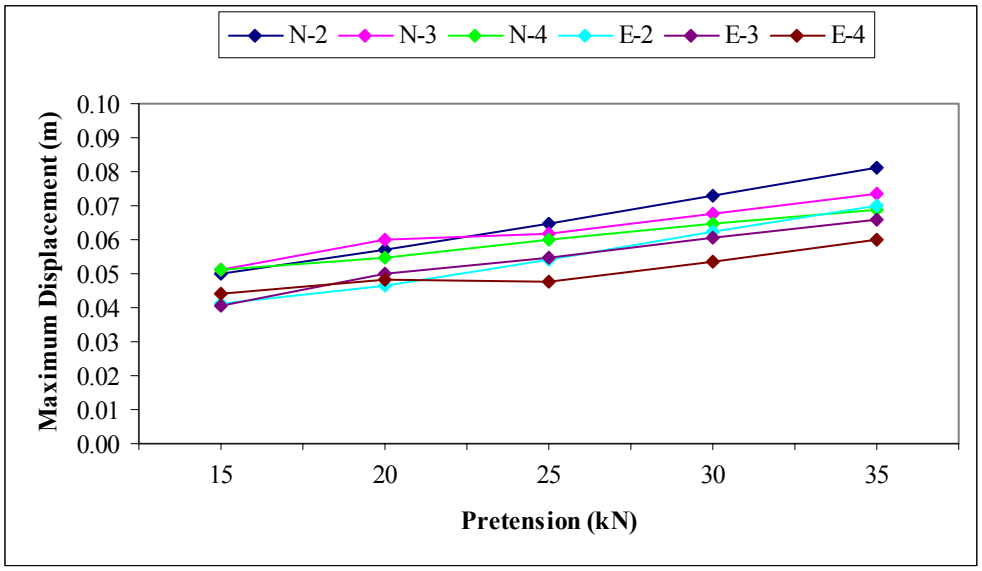

Figure C.5 Displacement 2 at Point 4 for Study 1

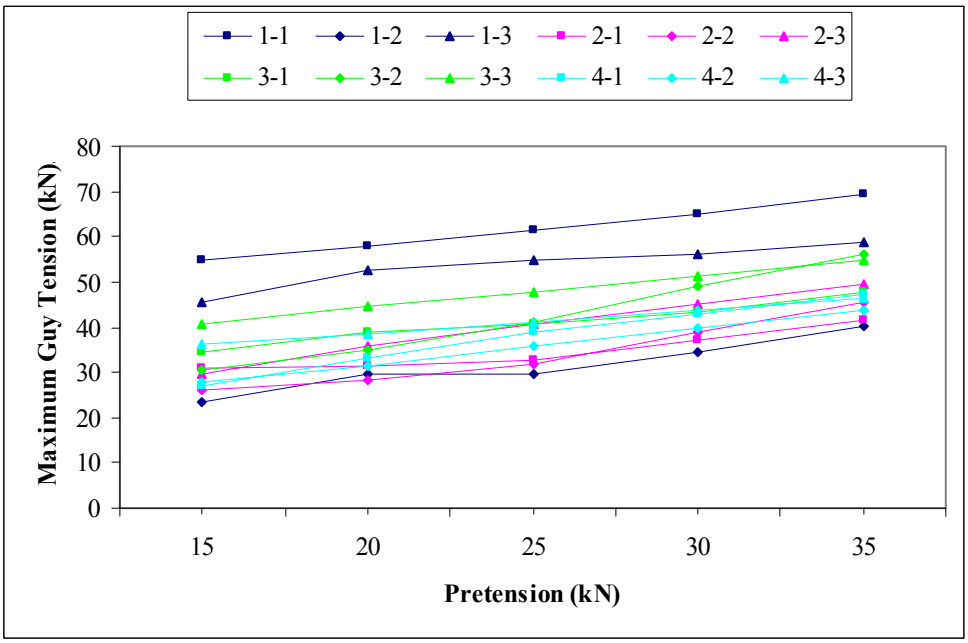

Figure C.6 Guy Tensions for N-2 Study 1

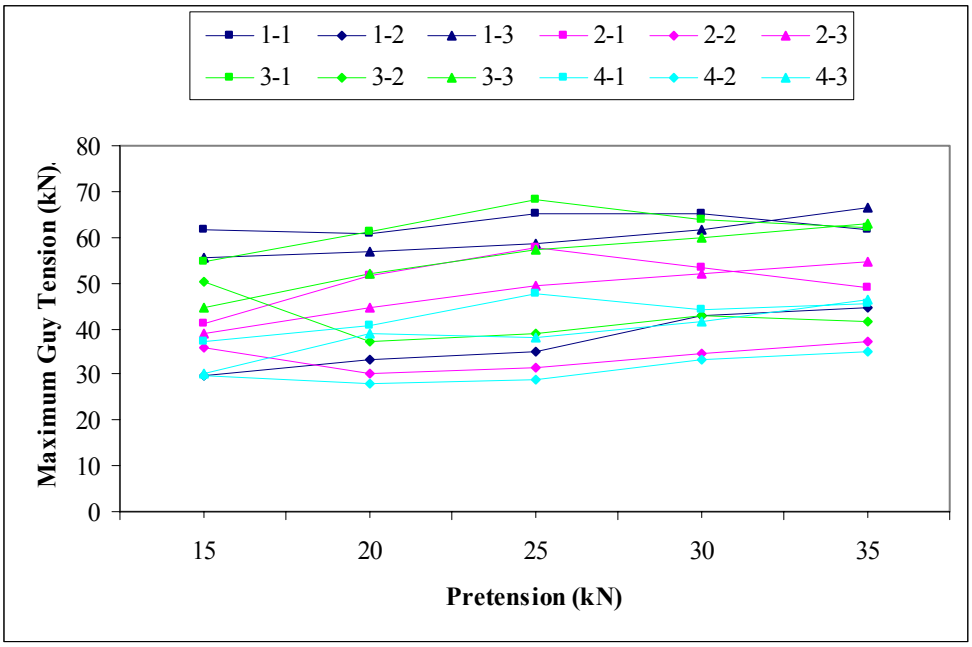

Figure C.7 Guy Tensions for N-4 Study 1

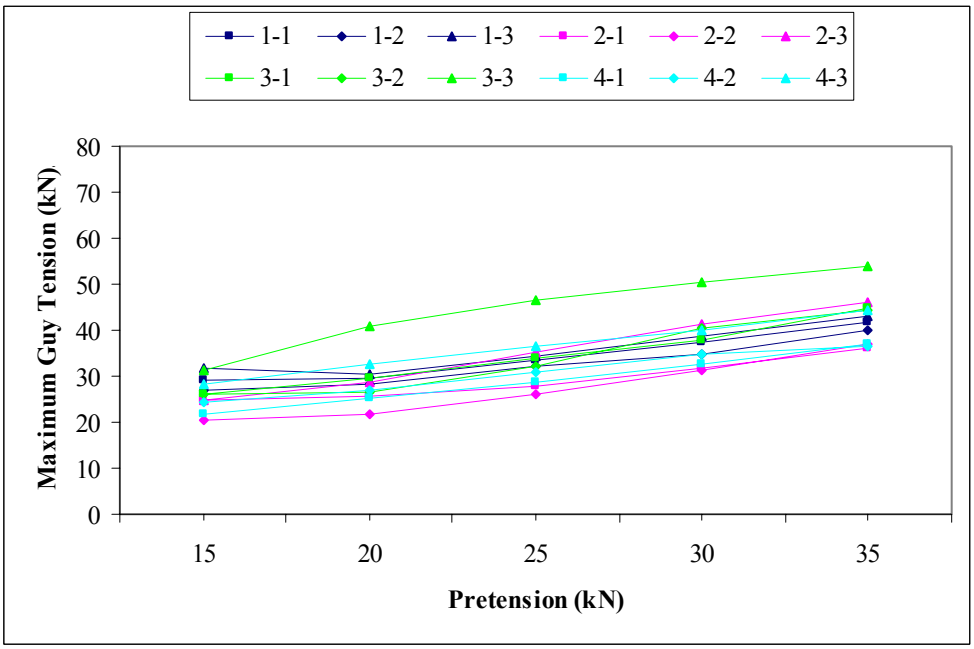

Figure C.8 Guy Tensions for E-2 Study 1

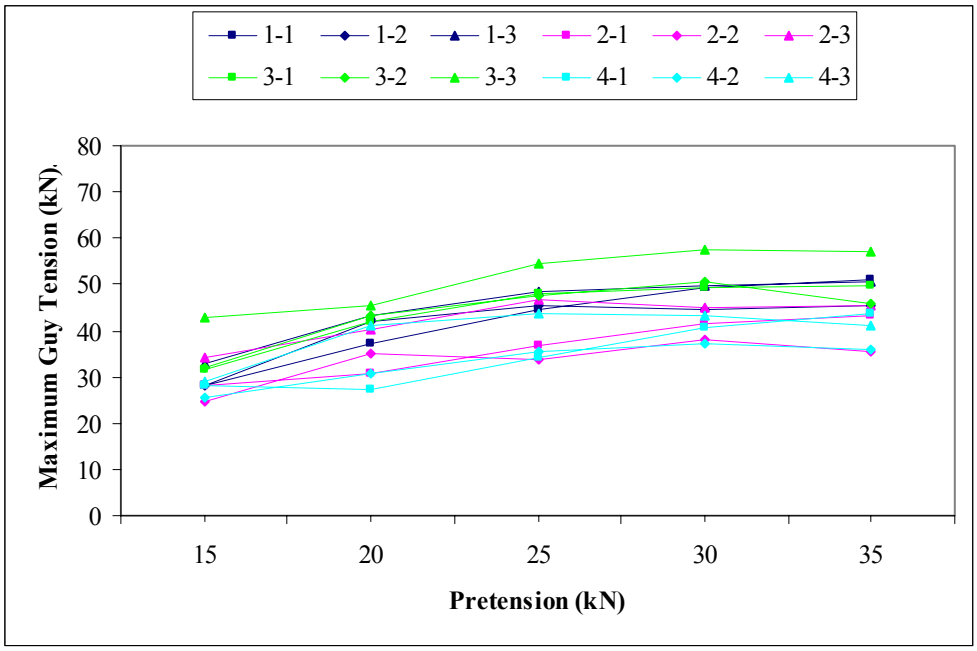

Figure C.9 Guy Tensions for E-3 Study 1

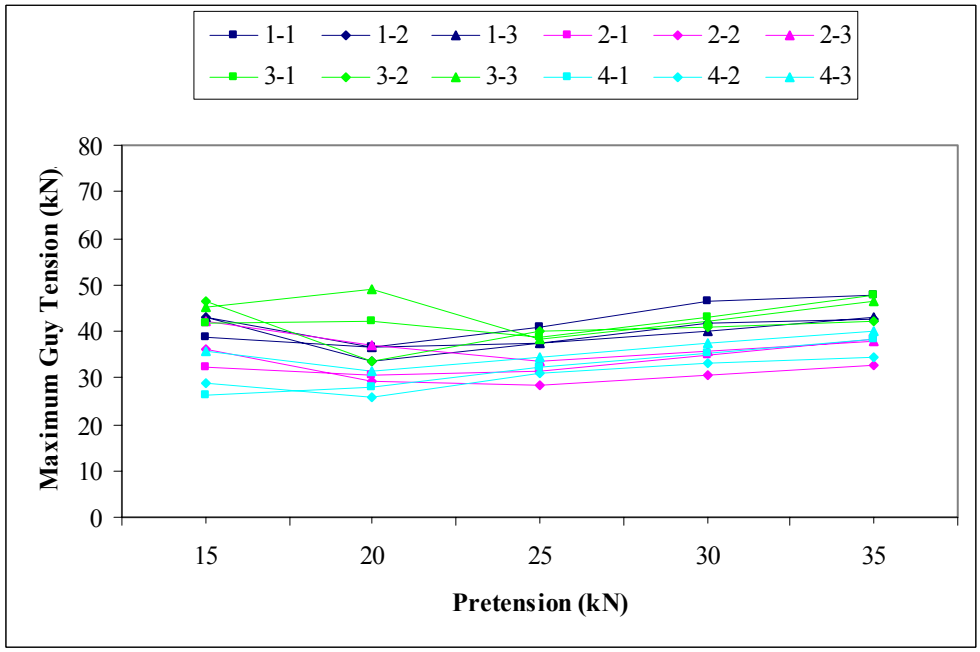

Figure C.10 Guy Tensions for E-4 Study 1

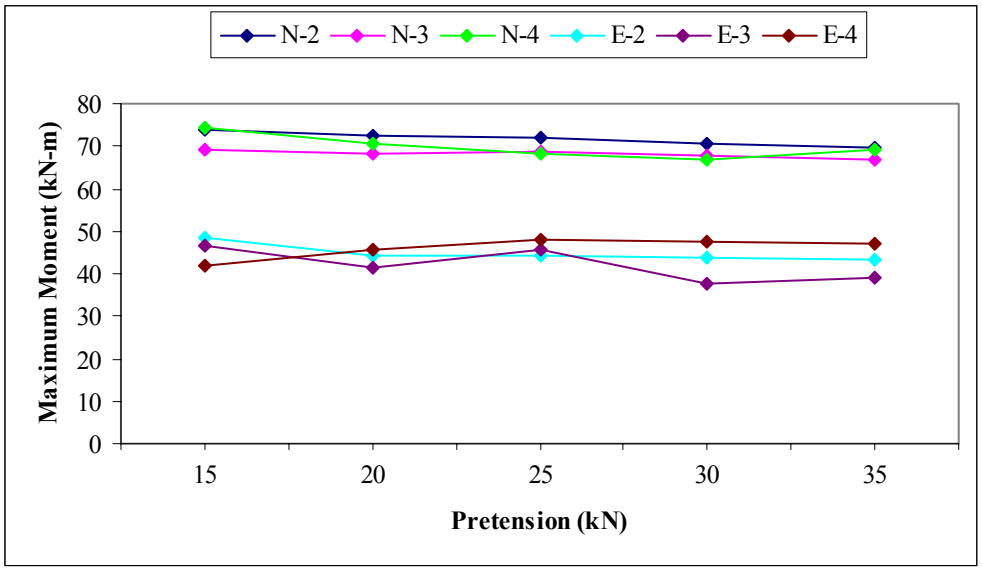

Figure C.11 Bending Moment 1 at Point 2 for Study 1

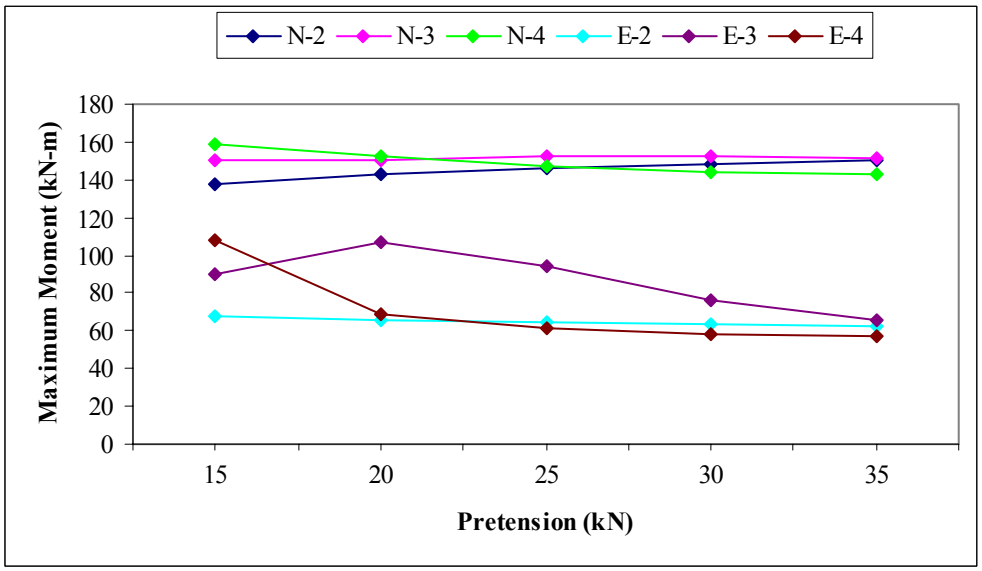

Figure C.12 Bending Moment 1 at Point 3 for Study 1

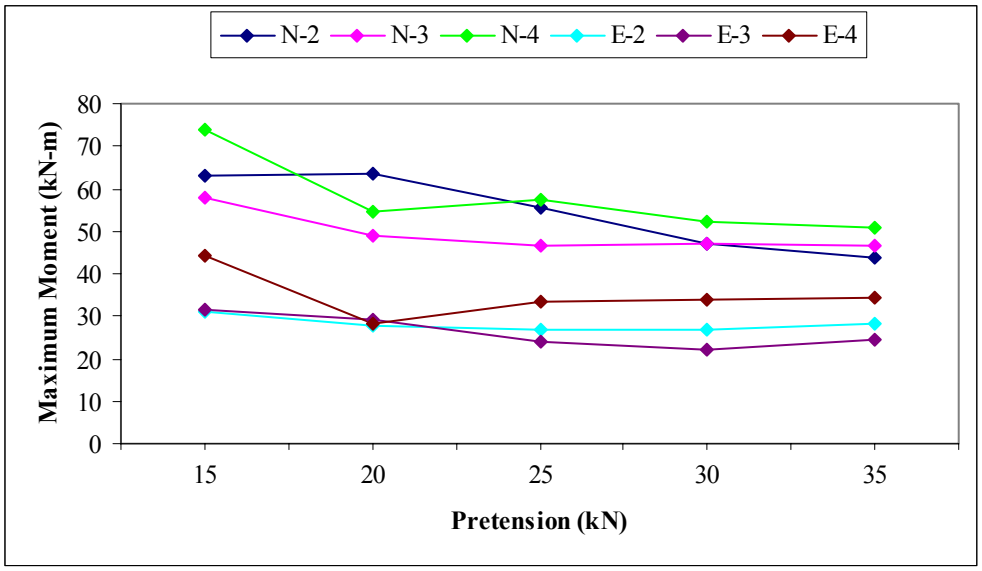

Figure C.13 Bending Moment 3 at Point 2 for Study 1

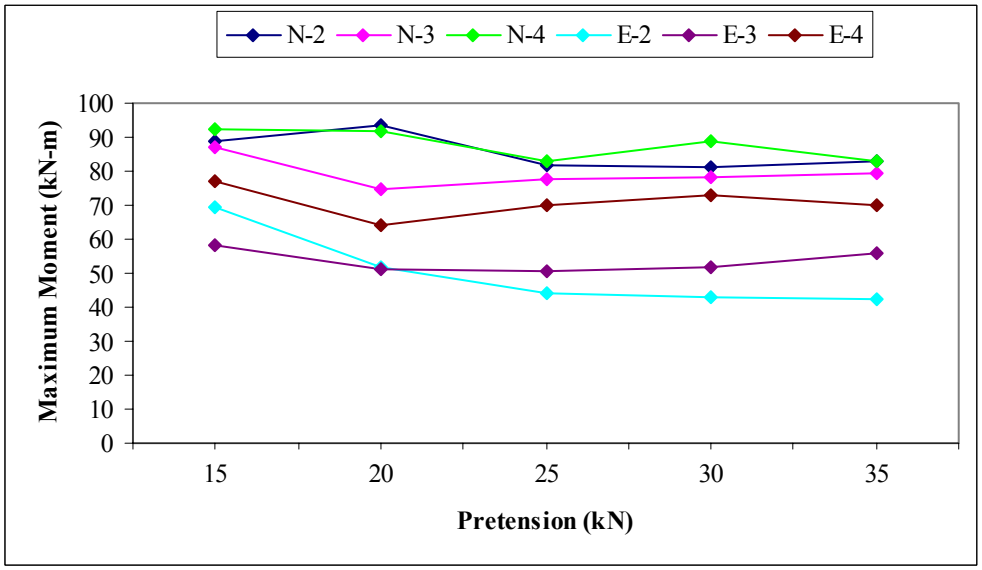

Figure C.14 Bending Moment 3 at Point 3 for Study 1

Vita

Greg Hensley was born on March 22, 1983 in Statesville, North Carolina to Larry and Faye Hensley. After several moves, his family returned home to Midlothian, Virginia where he lived for the duration of his primary and secondary schooling. Greg attended the Chesterfield County Mathematics and Science High School at Clover Hill, graduating in 2001. Following high school, he attended Virginia Polytechnic Institute and State University where he earned his Bachelor of Science degree in Civil Engineering in May of 2004. He continued his studies there, and upon completion of his Master of Science degree he will be gainfully employed at Pinnacle Engineering in central Virginia.